An examination of age-related differences in lower extremity joint torques and strains in the proximal femur during gait

Dennis Earl Anderson

Dissertation submitted to the faculty of the Virginia Polytechnic Institute and State University in partial fulfillment of the requirements for the degree of

Doctor of Philosophy
In
Engineering Mechanics

Michael L. Madigan, Chair
J. Wallace Grant
Scott L. Hendricks
Maury A. Nussbaum
Robert L. West
Kevin P. Granata

March 26, 2010
Blacksburg, Virginia

Keywords:
aging, hip fractures, walking, joint torque, femur, finite element modeling

An examination of age-related differences in lower extremity joint torques and strains in the proximal femur during gait

by

Dennis Earl Anderson

Abstract

Hip fractures are serious injuries that are associated with high rates of morbidity and mortality in older adults. While much of the increased risk of hip fracture with age can be explained by age-related decreases in bone mineral density, muscles and motor control are altered by aging as well. Muscles forces *in vivo* are thought to have a prophylactic effect that can reduce shear and bending in the femur. This is beneficial because bone is stronger in compression than in shear or tension, and shear plays an important role in fatiguing bone. Understanding how aging and muscular loads affect strains in the proximal femur could lead to improvements in clinical screening and preventative measures for hip fracture.

Three studies were performed to investigate age-related changes in neuromuscular function during gait and how these changes affect strains in the proximal femur. Study 1 examined age differences in peak lower extremity joint torques during walking with controlled speed and step length. Studies 2 and 3 applied muscle forces estimated during gait to finite element models of the femur. Study 2 examined age differences in femoral strains, and Study 3 examined the sensitivity of strains to individual muscle forces.

The results support the idea that older adults walk with reduced contributions from the ankle plantar flexors and increased contributions from the hip extensors. Interactions between age and speed indicate that older adults utilized a different neuromuscular strategy than young adults to vary the speed of their gait. No age differences were found for the largest magnitude strains in the proximal femur. However, young adults were able to apply larger loads to the femur without corresponding increases in femoral strains. Strains in the femoral neck were found to be sensitive to muscle forces, particularly hip abductor forces. Strains in the sub-trochanteric region tended to be larger than those in the femoral neck, and less sensitive to muscle forces. These results increase our understanding of neuromuscular changes that occur with age, and the effects of these changes on the femur.

Acknowledgements

This work may have my name on it, but it would not have happened without the help and support of many others. My thanks and appreciation to all of them:

A special thanks to my advisor, Dr. Michael Madigan. Taking his class in Musculoskeletal Biomechanics sparked the idea that, many years later, has become this dissertation. He has been there to push me forward when I needed it, and just as importantly has allowed me to find my own way. His support has gone far above and beyond that of mere faculty advisor, and I value his friendship tremendously.

To my committee members, who have all made important contributions to my education and accomplishments at Virginia Tech. Dr. West co-sponsored my NIH fellowship application and gave much guidance on finite element modeling. Dr. Hendricks demonstrated what excellent teaching looks like and gave me something to aspire to in my own teaching career. Dr. Grant was a model of good humor and friendliness, and was always willing to help. Dr. Nussbaum provided much advice and support, especially in terms of statistics and preparing manuscripts for publication.

To Dr. Kevin P. Granata, who had a contagious enthusiasm for life and his work that I have rarely seen. In the short time that I knew him I learned a lot from him; I can only imagine how much more I could have learned. He is greatly missed.

To those who helped directly with this work. Kellen Shain, Sara Matrangola and Katie Bieryla for assistance with data collection in our lab. Dr. Kevin Davy and Elaina Marinik in the Department of Human Nutrition, Foods and Exercise for being kind enough to provide DEXA scans for all my participants. The participants themselves, who submitted themselves to being poked, prodded, measured, scanned and ordered around in the name of science. Also to the Department of Engineering Science and Mechanics at Virginia Tech and to the National Institutes of Health for funding support. This work was supported by Award Number F31AG030904 from the National Institute on Aging. The content is solely the responsibility of the author and does not necessarily represent the official views of the National Institute on Aging or the National Institutes of Health.

To many friends and colleagues who have helped me enjoy life and stay sane throughout the years of this program. Julian Davis, who is always willing to talk, even when we both probably have more “important” things to be doing. Bradley Davidson, for good times in the lab and out, and for freely sharing the wisdom of a man from the hills of Tennessee (and now Colorado). Tanya Henry, for keeping in touch all these years, for prayers and for always being excited to hear from me. Katie Bieryla, for making the lab more fun and interesting. Sara Matrangola, for making the lab more fun and interesting, and also for being a really nice person. Also Noel Carson, Kerry Costello, Mike Diersing, Pranitha Gottipati, Emily Miller, Lisa, Matt and David Moore, Kellen Shain, Corrie Spoon, and many others.

Finally, to my family, who have always been and continue to be a mighty source of love and encouragement. My parents, James and Darla, for always caring, for lots of advice, for encouraging me to go for the PhD now instead of waiting, for setting good examples in so many ways, and of course for the genes. My sister, Janet, and brother-in-law, Jeremiah, for staying close even though they’re far away, for their senses of humor and for carefully choosing their professions so we sound like the start of a bad joke: A doctor, a lawyer and an engineer walk into a bar…

Attribution

Dr. Michael Madigan made significant contributions in reviewing and editing the three manuscripts presented in Chapters 3, 5 and 6 of this dissertation. He will be listed as second author when they are submitted for publication.

Table of Contents

Abstract ii

Acknowledgements iv

Attribution vi

Table of Contents vii

List of Figures ix

List of Tables xii

Chapter 1 – Introduction 1

Motivation 1
Project Overview 2
Document Organization 2
References 3

Chapter 2 – Hip Fractures and Femoral Loading 5

Prevalence and impact of hip fractures 5
Risk factors and etiology of hip fractures 7
In vivo loading of the femur 12
Age-related changes in neuromuscular function 13
References 15

Chapter 3 – Age differences in lower extremity joint torques during walking with controlled speed and step length 23

Abstract 23
Introduction 24
Methods 26
Results 29
Discussion 33
Acknowledgement 37
References 37

Chapter 4 – Finite element modeling of the femur 42

Introduction 42
Femoral geometry in finite element models 44
Modeling of material properties 46
Loading applied to femur models 50
Summary of finite element modeling of the femur 51
References 52

Chapter 5 – The effect of age differences in femoral loading during controlled walking on strains in the proximal femur 58

Abstract 58
Introduction 59

Methods ... 61
Results ... 66
Discussion ... 70
Acknowledgement ... 73
References ... 74

Chapter 6 – Sensitivity of strains in the proximal femur to variations in muscle forces ... 80

Abstract ... 80
Introduction ... 81
Methods ... 82
Results ... 86
Discussion ... 92
Acknowledgement ... 95
References ... 95

Chapter 7 – Conclusions and Future Work ... 99

Conclusions ... 99
Future Work ... 101
References ... 104

Appendix A – IRB Approval ... 105

Appendix B – Informed Consent Form ... 106

Appendix C – Data Collection Sheets ... 109

Gait Data Collection Sheet ... 109
DXA and Strength Data Collection Sheet ... 115

Appendix D - Additional Model Information ... 122

Musculoskeletal Models ... 122
Maximum Isometric Muscle Force Estimates ... 124
Convergence Check ... 127
Finite Element Model Loading and Boundary Conditions ... 128
References ... 130

Appendix E – Permissions and Fair Use ... 132

List of Figures

Figure 2.1: Example showing increase in hip fracture incidence with age, based on data for Medicare beneficiaries aged 65 and older in Washington State (data from Sugarman et al. 2002). 6

Figure 2.2: Anatomical regions for classification of hip fractures. (Reprinted from Ageing Research Reviews, 2, Marks, R., Allegrante, J. P., Ronald MacKenzie, C., and Lane, J. M., Hip fractures among the elderly: causes, consequences and control, Page 59, Copyright 2003, with permission from Elsevier). 8

Figure 3.1: Mean joint torques normalized by body mass for young and older age groups throughout a single cycle of self-selected gait. Peak torques examined for age effects are circled. [a]Significant age difference in peak torque ($p<0.05$). [t]Trend toward significant age difference ($0.05<p<0.1$).......... 31

Figure 3.2: Mean joint torques normalized by body mass for young and older age groups throughout a single cycle of controlled gait (Slow and Fast). Peak torques examined for age and speed effects are circled. [a]Significant main effect of age ($p<0.05$). [s]Significant main effect of speed ($p<0.05$). [i]Significant age × speed interaction ($p<0.05$). [t]Trend toward a significant age effect ($0.05<p<0.1$). 33

Figure 4.1: Proximal end of right femur viewed from behind and above showing femoral head and neck, greater trochanter and lesser trochanter. Image from Gray (1918), fair use. ... 44

Figure 4.2: Finite element model of the proximal femur composed of 11,604 cube elements 3 mm on a side. (Reprinted from Journal of Biomechanics 31, Keyak, J. H., Rossi, S. A., Jones, K. A., and Skinner, H. B., Prediction of femoral fracture load using automated finite element modeling. Page 128, Copyright 1998, with permission from Elsevier). ... 45

Figure 4.3: A frontal longitudinal midsection of a left femur showing cancellous bone within the proximal and distal femur, and the varying thickness of the cortical shell. Image from Gray (1918), fair use. 46

Figure 4.4: Non-linear material model of bone used by Keyak and Falkinstein. (Reprinted from Medical Engineering & Physics, 25, Keyak, J. H., and Falkinstein, Y., Comparison of in situ and in vitro CT scan-based finite element model predictions of proximal femoral fracture load, Page 783, Copyright 2003, with permission from Elsevier). 49

Figure 5.1: Musculoskeletal model used to estimate muscle forces during gait. The model included 35 muscles crossing the hip, knee and ankle joints as shown. 63

Figure 5.2: Finite element model of the femur from the VAKHUM project used in this study. In femoral coordinates, the X axis points anteriorly, Y superiorly, and Z laterally. 65

Figure 5.3: Anterior view of the proximal portion of the femur model, with heavy lines indicating sections in femoral neck and sub-trochanteric region where strains were examined. 66

Figure 5.4: Maximum principal and maximum shear strains in the femoral neck during a full gait cycle. Thick lines indicate mean values, and the thin lines indicate ±1 SD. The vertical lines denote the beginning of stance phase. Note that strain scales are not identical. *Significant age difference in peak strain. 68

Figure 5.5: Maximum principal and maximum shear strains in sub-trochanteric locations during a full gait cycle. Thick lines indicate mean values, and the thin lines indicate ±1 SD. The vertical lines denote the beginning of stance phase. Note that strain scales are not identical. 69

Figure 5.6: Average hip joint contact forces (%BW) in a femur-fixed coordinate frame during gait for young and older age groups. Thick lines indicate mean values, and the thin lines indicate ±1 SD. The X axis points anteriorly, Y up, and Z laterally. *Significant age difference in peak force. 70

Figure 6.1: Maximum principal strains in the superior femoral neck (black) and lateral sub-trochanteric region (grey) throughout the gait cycle. These locations had the largest peak strains in the femoral neck and sub-trochanteric regions, with peaks occurring at 55% and 86% of gait. 83

Figure 6.2: Illustrations of muscle lines of action in the musculoskeletal model for muscles attaching to the femur that cross the hip. Forces for these muscles were perturbed in the finite element model to examine their effect on strains. 84

Figure 6.3: Anterior and posterior views of the proximal portion of the femur finite element model. Black areas indicate locations at which strains were examined: superior, anterior, inferior and posterior femoral neck, and lateral, anterior, medial and posterior sub-trochanteric region. 86

Figure 6.4: Percent change in baseline strains in the femoral neck relative to percent change in baseline muscle forces. Results are shown for both maximum principal (MP) and maximum shear (MS) strains at 55% and 86% of the gait cycle. Muscles that produced less than 1% change in strain with 20% change in muscle force have been omitted. 88

Figure 6.5: Percent change in baseline strains in the sub-trochanteric region relative to percent change in baseline muscle forces. Results are shown for both maximum principal (MP) and maximum shear (MS) strains at 55% and 86% of the gait cycle. Muscles that produced less than 1% change in strain with 20% change in muscle force have been omitted. 89

Figure D.1: Examples of the models used for inverse dynamics in Study 1 (left) and static optimization in Study 2 (right). 123

Figure D.2: Linear least-squares best fit of maximum deflection to characteristic element size. The intercept of the best fit equation was used as true deflection for error calculations.128

Figure D.3: Finite element model for Study 2, from antero-medial (left) and postero-lateral (right) directions. Hip joint contact forces were applied as pressure loads on the acetabulum part. Light grey arrows indicate applied muscle forces, and dark grey at the distal femur indicates fixed boundary conditions. 129

Figure D.4: The finite element model for Study 3, showing the additional part added to apply loading at the distal femur.. 130

List of Tables

Table 2.1 – Factors affecting the risk of hip fracture (from Wehren & Magaziner, 2003). 9

Table 3.1: Mean (SD) values of gait speed and step length by age group for the three gait conditions tested, self-selected (SS), slow-controlled (SC) and fast-controlled (FC). 29

Table 3.2: Mean (SD) peak torque values during self-selected gait normalized by body mass (N-m/kg) compared between age groups. 30

Table 3.3: Mean (SD) peak torque values normalized by body mass (N-m/kg) for controlled gait conditions, compared by age group and speed. 32

Table 5.1: Mean (SD) values of peak strains (με) in the femoral neck during early stance and late stance.. 67

Table 5.2: Mean (SD) values of peak strains (με) in the sub-trochanteric region during early stance and late stance. N/A indicates no peak in strain was present................................ 69

Table 6.1: Baseline muscle forces (N) applied to the model, representing loading at 55% and 86% of the gait cycle.. 84

Table 6.2: Strain (με) in femoral neck (FN) and sub-trochanteric region (ST) of the femur when baseline muscle forces were applied... 87

Table 6.3: Sensitivities (με/N) of maximum principal (MP) and maximum shear (MS, shaded cells) strains to muscle forces at different locations in the proximal femur at 55% and 86% of gait cycle. The largest magnitude positive and negative sensitivities in each row are in bold. 91

Table D.1: Maximum isometric muscle forces in the musculoskeletal model. *Initial* indicates initial values for force estimation process. Mean (standard deviation) values are given for young and older adults in terms of force (N) and percent body weight (%BW). *Original* provides values from original OpenSim model for comparison. Forces that are significantly greater in young adults ($p < 0.05$) are displayed in bold. 126

Table D.2: Information on the different refinements of the femur model available from the VAKHUM project and results of convergence testing. 127

Chapter 1 – Introduction

Motivation

Hip fractures are serious injuries that are associated with high rates of morbidity and mortality in older adults (Magaziner et al. 2000; OTA 1994; Zuckerman 1996), and the incidence of these injuries increases dramatically with age (Sugarman et al. 2002). Part of this increase is due to a decrease in bone mineral density (BMD) with age (Marks et al. 2003). However, muscles and motor control are altered by aging as well (DeVita and Hortobagyi 2000; Doherty 2003; Hurley 1995), and thus age-related changes in muscular loading of the bone may be an important factor in hip fracture etiology.

Muscles contribute directly to *in vivo* loading of the femur, and are thought to have a prophylactic effect that can reduce shear and/or tensile stresses and strains in the bone (Duda et al. 1998; Polgar et al. 2003; Taylor et al. 1996). This is beneficial because bone is stronger in compression than in shear or tension, and shear plays an important role in fatiguing bone (Turner et al. 2001). Thus, age-related alterations in muscle forces may increase shear or tensile loads in the proximal femoral, and as a result accelerate bone fatigue secondary to osteoporosis. As material fatigue progressively weakens the femoral neck, the risk of hip fracture will increase, whether spontaneous or as the result of a fall.

The contribution of *in vivo* muscle loading to hip fracture etiology is not well defined, but may be important. Understanding how aging and muscular loads affect strains in the proximal femur could lead to improvements in clinical screening and preventative measures for hip fracture. The goals of this research were to investigate age-related changes in neuromuscular function during gait and how these changes affect strains in the proximal femur. Three studies were performed to address these goals.

Project Overview

Study 1 examined age differences in peak joint torques at the hip, knee and ankle during gait. The purpose of this study was to increase our understanding of age differences in gait kinetics and account for the fact that older adults tend to select gait patterns with slower speed and shorter step length than young adults. Experimental measurements of gait were collected in young and older adults walking in both self-selected and controlled conditions. Speed and step length were specified in the controlled conditions, thereby separating the effects of these spatio-temporal characteristics on joint torques during gait from the effects of age.

Study 2 examined how age-related differences in loading during gait affect strains the proximal femur. Static optimization was used to estimate individual muscle forces during gait for both young and older individuals. The resulting muscle forces were applied to finite element models of the femur throughout the gait cycle. Maximum principal and maximum shear strains in the femoral neck and sub-trochanteric region were examined for age differences.

Study 3 was a perturbation study examining the importance of various muscles to strains in the proximal femur. Using a finite element model from Study 2, muscle forces were varied systematically, and the resulting change in strains determined. This allowed the sensitivity of strains to the applied muscle forces to be determined.

Document Organization

This dissertation is composed of seven chapters, and presents three studies in manuscript form. Chapter 2 presents background information on hip fractures and femoral loading. Study 1 is presented in Chapter 3, entitled “Age differences in lower extremity joint torques during walking with controlled speed and step length.” Chapter 4 presents background information on finite element modeling of the femur. Study 2 is presented in Chapter 5, entitled “The effect of age differences in femoral loading during controlled walking on strains in the proximal femur.” Study 3 is presented in Chapter 6, entitled “Sensitivity of strains in the proximal femur to variations in muscle forces.” Conclusions are presented in Chapter 7, along with plans and possibilities for future work.

References

DeVita, P., and Hortobagyi, T., 2000. Age causes a redistribution of joint torques and powers during gait. Journal of Applied Physiology 88, 1804-1811.

Doherty, T. J., 2003. Invited review: Aging and sarcopenia. Journal of Applied Physiology 95, 1717-1727.

Duda, G. N., Heller, M., Albinger, J., Schulz, O., Schneider, E., and Claes, L., 1998. Influence of muscle forces on femoral strain distribution. Journal of Biomechanics 31, 841-846.

Hurley, B. F., 1995. Age, gender, and muscular strength. The Journals of Gerontology. Series A, Biological Sciences and Medical Sciences 50 Spec No, 41-44.

Magaziner, J., Hawkes, W., Hebel, J. R., Zimmerman, S. I., Fox, K. M., Dolan, M., Felsenthal, G., and Kenzora, J., 2000. Recovery from hip fracture in eight areas of function. The Journals of Gerontology. Series A, Biological Sciences and Medical Sciences 55, M498-507.

Marks, R., Allegrante, J. P., Ronald MacKenzie, C., and Lane, J. M., 2003. Hip fractures among the elderly: causes, consequences and control. Ageing Research Reviews 2, 57-93.

Office of Technology Assessment, 1994. Hip Fracture Outcomes in People Age 50 and Over-Background Paper. U.S. Government Printing Office, Washington, DC, OTA-BP-H- 120.

Polgar, K., Gill, H. S., Viceconti, M., Murray, D. W., and O'Connor, J. J., 2003. Strain distribution within the human femur due to physiological and simplified loading: finite element analysis using the muscle standardized femur model. Proceedings of the Institution of Mechanical Engineers. Part H, Journal of Engineering in Medicine 217, 173-189.

Sugarman, J. R., Connell, F. A., Hansen, A., Helgerson, S. D., Jessup, M. C., and Lee, H., 2002. Hip fracture incidence in nursing home residents and community-dwelling older people, Washington State, 1993-1995. Journal of the American Geriatrics Society 50, 1638-1643.

Taylor, M. E., Tanner, K. E., Freeman, M. A., and Yettram, A. L., 1996. Stress and strain distribution within the intact femur: compression or bending? Medical Engineering & Physics 18, 122-131.

Turner, C. H., Wang, T., and Burr, D. B., 2001. Shear strength and fatigue properties of human cortical bone determined from pure shear tests. Calcified Tissue International 69, 373-378.

Zuckerman, J. D., 1996. Hip fracture. The New England Journal of Medicine 334, 1519-1525.

Chapter 2 – Hip Fractures and Femoral Loading

Prevalence and impact of hip fractures

Hip fractures are a widespread and increasing health problem for older populations in the United States and around the world. In the United States, the annual number of hip fractures was about 281,000 in 1990 (OTA 1994), which will increase to an estimated 512,000 in 2040 (Cummings et al. 1990). Worldwide, the projected increase will be from 1.66 million in 1990 to around 6.26 million in 2050 (Cooper et al. 1992). Incidence in most western countries is about twice as high for women as for men, although the female to male ratio varies between countries and regions (Cooper et al. 1992; Gullberg et al. 1997; Schwartz et al. 1999; Sugarman et al. 2002). The incidence of hip fractures increases dramatically with age (Melton 1996; Schwartz et al. 1999; Sugarman et al. 2002), more than doubling for each decade after age 65 (Figure 2.1). Age-adjusted incidence rates increased through much of the 20th century, and while there are indications that they have plateaued or are declining in certain developed countries, they continue to increase in other parts of the world (Cooper et al. 1992; Gullberg et al. 1997; Melton et al. 1996). Nonetheless, the tremendous growth of the elderly population will continue to increase the total number of hip fractures that occur.

Hip fractures are associated with heightened mortality rates over the 6 to 12 months following the injury (Zuckerman 1996). Estimates of the one-year mortality rate for hip fracture patients range from 14-36% (Zuckerman 1996), up to 5 times higher than age and gender-matched controls (OTA 1994). The risk of dying in the year after a hip fracture increases with age and male gender (Cree et al. 2000; Marks et al. 2003; OTA 1994), reaching 48% for men over 85 (OTA 1994). Mortality following a hip fracture is also increased by co-existing illnesses

(Marks et al. 2003; OTA 1994) and living in a nursing home at the time of the fracture (Cree et al. 2000; OTA 1994).

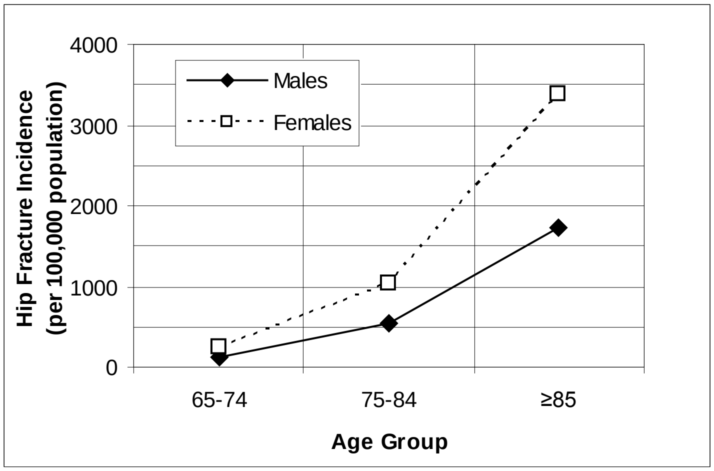

Figure 2.1: Example showing increase in hip fracture incidence with age, based on data for Medicare beneficiaries aged 65 and older in Washington State (data from Sugarman et al. 2002).

In addition to increased mortality, hip fractures can negatively impact health and quality of life for survivors. The majority of survivors do not regain their pre-fracture level of functionality in activities of daily living (Magaziner et al. 2000; OTA 1994; Wehren and Magaziner 2003). Specifically, at 1 year post-fracture, 50% or more of previously independent patients had not recovered their independence in lower extremity physical activities such as walking, climbing stairs and rising from a chair (Magaziner et al. 2000). Nearly half of patients spend some time in a nursing home or other institution following hospital discharge, and more than one third were rehospitalized in the year following their fracture (Magaziner et al. 1990).

Hip fractures incur a substantial and rising economic toll. The total US expenditure for hip fractures in 1990 was $5.4 billion (OTA 1994), or about $19,335 per patient, although this is conservative compared to other estimates (Cummings et al. 1990; Youm et al. 1999). Accounting for growing numbers of hip fractures and 5% inflation, the annual cost of hip fractures was projected to be reach $62 billion by 2020 (Cummings et al. 1990; Youm et al. 1999). This estimate is based on costs only in the first year following a hip fracture. Braithwaite et al. (2003) estimated that 56% of the cost of a hip fracture is incurred after the first year, with lifetime costs estimated as $81,300 in 2001 dollars. Accounting for the lifetime cost of hip fracture, as well as the rising costs of healthcare (Youm et al. 1999), the annual cost of hip fractures in 2020 may well exceed $62 billion.

Risk factors and etiology of hip fractures

Hip fracture is a general term for a fracture of the proximal femur. These fractures are classified based on the anatomical location in which they occur (Figure 2.2). Fractures may occur in the femoral neck region, the intertrochanteric region or the subtrochanteric region (Marks et al. 2003; Thorngren et al. 2002; Zuckerman 1996). They are further classified in various ways, depending on the degree of displacement for femoral neck fractures or the amount of fragmentation for intertrochanteric fractures (Thorngren et al. 2002). Femoral neck fractures are also called cervical fractures (e.g. Thorngren et al. 2002), or intracapsular fractures (e.g. Michelson et al. 1995), as they occur within the joint capsule of the hip. Displaced femoral neck fractures can disrupt the vascular supply to the femoral head, leading to osteonecrosis of the femoral head and nonunion of the fracture (Marks et al. 2003; Zuckerman 1996). Femoral neck and intertrochanteric fractures occur in approximately equal proportions, each accounting for between 37 and 50% of all hip fractures, with the remaining 5-14% being subtrochanteric (Michelson et al. 1995; Thorngren et al. 2002; Zuckerman 1996).

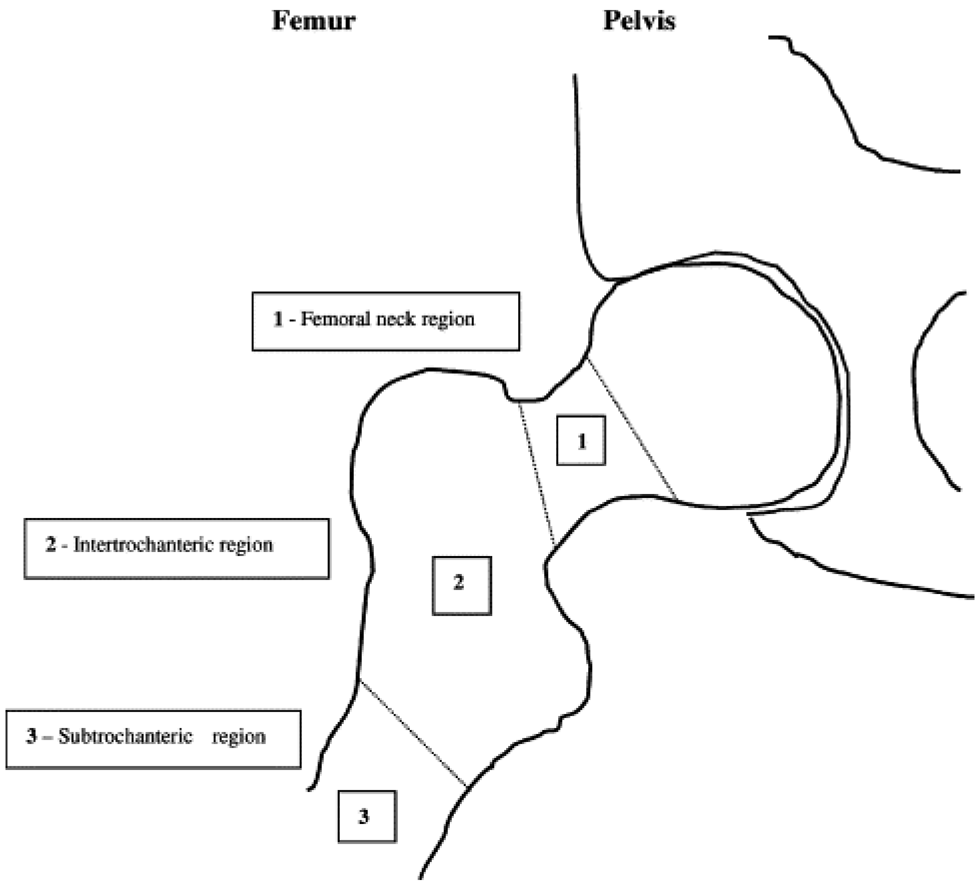

Figure 2.2: Anatomical regions for classification of hip fractures. (Reprinted from Ageing Research Reviews, 2, Marks, R., Allegrante, J. P., Ronald MacKenzie, C., and Lane, J. M., Hip fractures among the elderly: causes, consequences and control, Page 59, Copyright 2003, with permission from Elsevier).

The risk of hip fracture is related to many factors (Table 2.1) which fall into three major classifications: clinical factors, factors affecting the risk of falling, and factors that affect bone strength (Wehren and Magaziner 2003). The various risk factors may overlap and interact. For example, increased age will tend to increase the risk of falling and reduce bone strength. It has been hypothesized that a high percentage of hip fractures are due to a combination of neuromuscular mechanisms and their interactions with bone mass and fall mechanisms (Marks et al. 2003). For the purpose of this work, we are interested in a neuromuscular mechanism, specifically muscle loading of the femur, and its variation with age and effect on strains in the bone.

Table 2.1: Factors affecting the risk of hip fracture (from Wehren & Magaziner, 2003).

Bone Strength	Cigarette smoking
Bone mineral density	Height
Bone architecture and geometry	Weight and weight loss
Bone turnover	Functional impairments
Microdamage accumulation in bone	Vision impairments
Degree of mineralization of bone	Cognitive impairments
Genetics	Socioeconomic status
Gender	Season
Race	Physical activity level
Falls	Certain medications
Age	Long-acting benzodiazepines
Estrogen exposures	Other psychotropic drugs
Prior fragility fractures	Anticonvulsants
Nutrition	Corticosteriods

A hip fracture occurs when the load applied to the femur exceeds the strength of the bone, and reduced bone strength is perhaps the single most important risk factor for hip fractures. Because bone strength cannot be directly tested *in vivo*, bone mineral density (BMD), which accounts for about 70 % of bone strength (NIH 2001), is often used as a surrogate measure of strength. Dual energy x-ray absorptiometry (DXA) allows easy and non-invasive measurement of BMD (Cummings et al. 1993; NIH 2001; Wehren and Magaziner 2003). DXA is used in the diagnosis of osteoporosis, which is defined as a BMD more than 2.5 standard deviations below the mean for young adult white women (WHO 1994). Beginning at mid-life, BMD declines with increasing age for both men and women (NIH 2001). Thus, the elderly are prone to develop osteoporosis, and by definition osteoporosis implies a reduction in bone strength.

Because of its correlation with bone strength, BMD is useful as a predictor of hip fracture risk (NIH 2001). Low BMD measurements at the wrist, calcaneus, lumbar spine and proximal femur are all significant predictors of hip fracture risk, although not surprisingly the proximal femur is a better predictor than other sites (Cummings et al. 1993). However, decreases in BMD do not fully account for the increase in hip fracture risk with age (Marks et al. 2003). Because the BMD of fracture patients overlaps that of age-matched individuals without hip fracture (Marks et al., 2003, WHO, 1994), additional factors should be considered in evaluating the risk of hip fracture.

Falls are of considerable importance as a cause of hip fractures, so it is important to understand the relation between falls and hip fractures. Because more than 90% of hip fractures in the elderly are associated with a fall (Marks et al. 2003), risk of falling can strongly affect the risk of hip fracture. Dargent-Molina et al. (1996) found that fall-related risk factors, specifically reduced gait speed, difficulty performing a tandem walk and visual impairment, were significant predictors of hip fracture independent of age and BMD. The energy available in a fall far exceeds that required to fracture the proximal femur (Hayes 1994). However, only about 1% of falls in the elderly are associated with a hip fracture (Cummings et al. 1994; Hayes et al. 1996). This indicates that the mechanics of the fall itself can influence the likelihood of a fracture.

Once a fall is initiated, the likelihood of a hip fracture depends on the impact load applied to the femur and strength of the bone. Several characteristics of fall descent and impact can affect the risk of fracture, which Cummings and Nevitt (1994) broadly categorize as impact location, energy of the fall and energy absorption. Impact location is very important, as hip fracture risk is increased 3 - 6 times by falling to the side or straight down, and 20 - 30 times by impact at or near the hip (Cummings and Nevitt 1994; Hayes et al. 1996). The energy in a fall depends primarily on fall height and body weight (Cummings and Nevitt 1994). Increased body height increases impact velocity, while greater body weight increases impact load (Hayes et al. 1996). However, greater body weight may also have a protective effect, as it tends to increase bone density and soft tissue coverage of bone at the hip (Cummings and Nevitt 1994; Hayes et al. 1996). Energy absorption refers to mechanisms that help absorb the energy of the fall, reducing the energy transferred to the femur. Soft tissue coverage of the hip may contribute to energy absorption, and as can the surface impacted. Individuals falling on a hard surface are about 3 times more likely to suffer a hip fracture (Cummings and Nevitt 1994). Protective responses, such as using the arms to break the fall, reduce the risk of hip fracture, but there is little data about their importance (Cummings and Nevitt 1994). Muscle contraction during descent may help in absorbing energy and allow the faller to adjust the body to a better impact configuration, but muscle contraction during impact increases the impact load by 25-100% (Hayes et al. 1996). This supports the idea that falling in a relaxed condition reduces the risk of injury.

In medical terminology "stress fractures", or "insufficiency fractures" in the case of bone deficiency (Pentecost et al. 1964), refer to fractures in bone due to material fatigue. Fatigue refers to damage and failure in a material that is subjected to cyclic loads well below its ultimate strength. Since the load need not exceed the strength of the material, stress fractures may develop in the absence a traumatic event like a fall. In bone under cyclic loading, microcracks form and propagate, eventually becoming macrocracks unless bone remodeling occurs soon enough to counter the progression of damage (Bennell et al. 1999). Stress fractures have been reported in the femoral neck in both military recruits (Egol et al. 1998; Fullerton and Snowdy 1988) and in the elderly (Dorne and Lander 1985; Egol et al. 1998; Tountas 1993). Non-displaced stress fractures of the femoral neck are easily missed in clinical diagnosis, but usually present with pain in the hip region (Dorne and Lander 1985; Tountas 1993). If not identified and treated, a stress fracture can propagate and lead to a complete fracture (Tountas 1993).

A significant minority of hip fractures in the elderly are “spontaneous”, meaning they are not caused by an external trauma such as fall impact. In two studies that interviewed hip fracture patients about pre-fracture symptoms and circumstances surrounding the fracture, spontaneous fractures probably occurred in 22-24% of cases (Maugars et al. 1996; Sloan and Holloway 1981). Furthermore, 16-45% of patients reported hip pain in the weeks and months prior to the injury, which indicates that a spontaneous fracture often represents the full displacement of an existing stress fracture. In some cases, extreme or uncontrolled muscle contractions may ultimately overload the bone weakened by fatigue, causing a spontaneous fracture (Smith 1953; Yang et al. 1996). Some spontaneous fractures have no associated trauma (Horiuchi et al. 1988; Maugars et al. 1996; Tountas 1993), but others may cause a fall when the hip “gives out” (Maugars et al. 1996; Sloan and Holloway 1981; Smith 1953; Tountas 1993). A completely displaced stress fracture cannot be clinically distinguished from a traumatic fracture (Tountas 1993), so it remains difficult to separate spontaneous fractures that cause falls from fractures caused by fall trauma.

In vivo loading of the femur

Because *in vivo* muscular loading stimulates the remodeling and adaptation of the skeletal system, loading of the femur may play a role in maintaining femoral strength to prevent hip fractures in the elderly. For example, artificial axial compressive loading *in vivo* was found to greatly increase the resistance of rat ulnas to fatigue, which has implications for the prevention of stress fractures (Warden et al. 2005). Femoral neck BMD is weakly but significantly correlated with hip abductor and flexor strength in postmenopausal women (Bayramoglu et al. 2005; Zimmermann et al. 1990). Additionally, resistance training is associated with high BMD in both younger and older adults, and is relatively site-specific in its effect (Layne and Nelson 1999).

Bone remodeling involves the resorption of old bone and formation of new bone, with possible purposes including removal of dead bone and repair of microcracks (Currey 2002). Bone remodeling occurs at least in part due to mechanical stimulus, such as dynamic strain, experienced by the bone (Turner 1998). The result of this process is that bone adapts to changing loading conditions. Bed rest and weightlessness lead to reductions in bone mass, while increased loading leads to increased mass (Currey 2002).

In addition to stimulating bone remodeling, muscular loading can also have a prophylactic effect on bone damage. For example, muscular contraction significantly increases the load and energy required to fracture the tibia in rats (Nordsletten and Ekeland 1993). There is evidence that muscle loading reduces shear and bending loads in the femur, helping to protect it from damage (Duda et al. 1998; Polgar et al. 2003; Taylor et al. 1996). Bone is weaker in shear and tension than in compression (Reilly and Burstein 1975; Turner et al. 2001), and experiments indicate that shear plays an important role in the fatiguing of bone (Taylor et al. 2003; Turner et al. 2001). Furthermore, the fatigue life of cortical bone is significantly reduced under combined axial and torsional loading, and is lower for aged bone than for younger bone (George and Vashishth 2006). Muscle fatigue may increase bone stresses during athletic activities (Benazzo et al. 1992; Clement 1974) and significantly increases measured tibial shear strain during walking in dogs (Yoshikawa et al. 1994), although a similar experiment in humans did not reach significance (Fyhrie et al. 1998). Thus, changes in normal muscle loading could reduce the protective effect and increase the risks of fatigue damage.

Age-related changes in neuromuscular function

Aging is associated with decreases in neuromuscular function (Doherty 2003; Hurley 1995). Muscle strength tends to decline by about 12-15% for each decade after 50 years of age

(Hurley 1995), resulting in a 20-40% reduction in strength in the seventh and eighth decades of life (Doherty 2003). Multiple factors contribute to this decline, including loss of muscle mass, decreased innervation of motor units, and decreased activity levels (Doherty 2003; Hurley 1995). However, various studies have shown that resistance exercise in the elderly increases muscular strength by 17-76% (Doherty 2003; Layne and Nelson 1999; Narici et al. 2004). Thus, properly designed training interventions may be useful in preventing or reversing neuromuscular declines in the elderly.

Age-related declines in neuromuscular function are at least in part responsible for changes in the performance of daily activities. For example, healthy older adults show reduced self-selected gait velocity and step length compared to younger adults (Kerrigan et al. 1998; Winter et al. 1990). Because of strength reductions, older adults require greater effort to perform activities such as ascending and descending stairs and rising from a chair (Hortobagyi et al. 2003). Reduced strength may also affect gait, as hip extensor strength is correlated with freely selected gait velocity and step length in elderly men (Burnfield et al. 2000). When compared at identical walking velocities, older adults show a redistribution of joint torques and powers during gait compared to young adults, with more propulsive power coming from hip torques and less from ankle torques (DeVita and Hortobagyi 2000). Because strength declines at different rates in different muscle groups (Christ et al. 1992), this may represent compensation for non-uniform reductions in muscle strength (DeVita and Hortobagyi 2000; Goldberg and Neptune 2007). It may also indicate that muscle loading of the femur is altered in older adults, which could lead to reductions in femoral strength.

References

Bayramoglu, M., Sozay, S., Karatas, M., and Kilinc, S., 2005. Relationships between muscle strength and bone mineral density of three body regions in sedentary postmenopausal women. Rheumatology International 25, 513-517.

Benazzo, F., Barnabei, G., Ferrario, A., Castelli, C., and Fishchetto, G., 1992. Stress fractures in track and field athletics. Journal of Sports Traumatology and Related Research 14, 51-65.

Bennell, K., Matheson, G., Meeuwisse, W., and Brukner, P., 1999. Risk factors for stress fractures. Sports Medicine 28, 91-122.

Braithwaite, R. S., Col, N. F., and Wong, J. B., 2003. Estimating Hip Fracture Morbidity, Mortality and Costs. Journal of the American Geriatrics Society 51, 364-370.

Burnfield, J. M., Josephson, K. R., Powers, C. M., and Rubenstein, L. Z., 2000. The influence of lower extremity joint torque on gait characteristics in elderly men. Archives of Physical Medicine and Rehabilitation 81, 1153-1157.

Christ, C. B., Boileau, R. A., Slaughter, M. H., Stillman, R. J., Cameron, J. A., and Massey, B. H., 1992. Maximal Voluntary Isometric Force Production Characteristics of 6 Muscle Groups in Women Aged 25 to 74 Years. American Journal of Human Biology 4, 537-545.

Clement, D. B., 1974. Tibial stress syndrome in athletes. The Journal of Sports Medicine 2, 81-85.

Cooper, C., Campion, G., and Melton, L. J., 3rd, 1992. Hip fractures in the elderly: a world-wide projection. Osteoporosis International 2, 285-289.

Cree, M., Soskolne, C. L., Belseck, E., Hornig, J., McElhaney, J. E., Brant, R., and Suarez-Almazor, M., 2000. Mortality and institutionalization following hip fracture. Journal of the American Geriatrics Society 48, 283-288.

Cummings, S. R., Black, D. M., Nevitt, M. C., Browner, W., Cauley, J., Ensrud, K., Genant, H. K., Palermo, L., Scott, J., and Vogt, T. M., 1993. Bone density at various sites for prediction of hip fractures. The Study of Osteoporotic Fractures Research Group. Lancet 341, 72-75.

Cummings, S. R., Marcus, R., Palermo, L., Ensrud, K. E., and Genant, H. K., 1994. Does estimating volumetric bone density of the femoral neck improve the prediction of hip fracture? A prospective study. Study of Osteoporotic Fractures Research Group. Journal of Bone and Mineral Research 9, 1429-1432.

Cummings, S. R., and Nevitt, M. C., 1994. Non-skeletal determinants of fractures: the potential importance of the mechanics of falls. Study of Osteoporotic Fractures Research Group. Osteoporosis International 4 Suppl 1, 67-70.

Cummings, S. R., Rubin, S. M., and Black, D., 1990. The future of hip fractures in the United States. Numbers, costs, and potential effects of postmenopausal estrogen. Clinical Orthopaedics and Related Research, 163-166.

Currey, J. D. 2002. Bones : structure and mechanics. Princeton University Press, Princeton, NJ.

Dargent-Molina, P., Favier, F., Grandjean, H., Baudoin, C., Schott, A. M., Hausherr, E., Meunier, P. J., and Breart, G., 1996. Fall-related factors and risk of hip fracture: the EPIDOS prospective study. Lancet 348, 145-149.

DeVita, P., and Hortobagyi, T., 2000. Age causes a redistribution of joint torques and powers during gait. Journal of Applied Physiology 88, 1804-1811.

Doherty, T. J., 2003. Invited review: Aging and sarcopenia. Journal of Applied Physiology 95, 1717-1727.

Dorne, H. L., and Lander, P. H., 1985. Spontaneous stress fractures of the femoral neck. AJR Am J Roentgenol 144, 343-347.

Duda, G. N., Heller, M., Albinger, J., Schulz, O., Schneider, E., and Claes, L., 1998. Influence of muscle forces on femoral strain distribution. Journal of Biomechanics 31, 841-846.

Egol, K. A., Koval, K. J., Kummer, F., and Frankel, V. H., 1998. Stress fractures of the femoral neck. Clinical Orthopaedics and Related Research, 72-78.

Fullerton, L. R., Jr., and Snowdy, H. A., 1988. Femoral neck stress fractures. The American Journal of Sports Medicine 16, 365-377.

Fyhrie, D. P., Milgrom, C., Hoshaw, S. J., Simkin, A., Dar, S., Drumb, D., and Burr, D. B., 1998. Effect of fatiguing exercise on longitudinal bone strain as related to stress fracture in humans. Annals of Biomedical Engineering 26, 660-665.

George, W. T., and Vashishth, D., 2006. Susceptibility of aging human bone to mixed-mode fracture increases bone fragility. Bone 38, 105-111.

Goldberg, E. J., and Neptune, R. R., 2007. Compensatory strategies during normal walking in response to muscle weakness and increased hip joint stiffness. Gait & Posture 25, 360-367.

Gullberg, B., Johnell, O., and Kanis, J. A., 1997. World-wide projections for hip fracture. Osteoporosis International 7, 407-413.

Hayes, W. C. 1994. Biomechanics of Falls and Hip Fractures in the Elderly. In: Apple, D. F. and W. C. Hayes (Ed.), Prevention of Falls and Hip Fractures in the Elderly. American Academy of Orthopaedic Surgeons, Rosemont, IL, pp. 41-65.

Hayes, W. C., Myers, E. R., Robinovitch, S. N., Van Den Kroonenberg, A., Courtney, A. C., and McMahon, T. A., 1996. Etiology and prevention of age-related hip fractures. Bone 18, 77S-86S.

Horiuchi, T., Igarashi, M., Karube, S., Oda, H., Tokuyama, H., Huang, T., and Inoue, S., 1988. Spontaneous fractures of the hip in the elderly. Orthopedics 11, 1277-1280.

Hortobagyi, T., Mizelle, C., Beam, S., and DeVita, P., 2003. Old adults perform activities of daily living near their maximal capabilities. The Journals of Gerontology. Series A, Biological Sciences and Medical Sciences 58, M453-460.

Hurley, B. F., 1995. Age, gender, and muscular strength. The Journals of Gerontology. Series A, Biological Sciences and Medical Sciences 50 Spec No, 41-44.

Kerrigan, D. C., Todd, M. K., Della Croce, U., Lipsitz, L. A., and Collins, J. J., 1998. Biomechanical gait alterations independent of speed in the healthy elderly: evidence for specific limiting impairments. Archives of Physical Medicine and Rehabilitation 79, 317-322.

Layne, J. E., and Nelson, M. E., 1999. The effects of progressive resistance training on bone density: a review. Medicine and Science in Sports and Exercise 31, 25-30.

Magaziner, J., Hawkes, W., Hebel, J. R., Zimmerman, S. I., Fox, K. M., Dolan, M., Felsenthal, G., and Kenzora, J., 2000. Recovery from hip fracture in eight areas of function. The Journals of Gerontology. Series A, Biological Sciences and Medical Sciences 55, M498-507.

Magaziner, J., Simonsick, E. M., Kashner, T. M., Hebel, J. R., and Kenzora, J. E., 1990. Predictors of functional recovery one year following hospital discharge for hip fracture: a prospective study. Journal of Gerontology 45, M101-107.

Marks, R., Allegrante, J. P., Ronald MacKenzie, C., and Lane, J. M., 2003. Hip fractures among the elderly: causes, consequences and control. Ageing Research Reviews 2, 57-93.

Maugars, Y., Dubois, F., Berthelot, J. M., Dubois, C., and Prost, A., 1996. Pain due to bone insufficiency as a symptom heralding femoral neck fracture. Revue du Rhumatisme (English Ed.) 63, 30-35.

Melton, L. J., 3rd, 1996. Epidemiology of hip fractures: implications of the exponential increase with age. Bone 18, 121S-125S.

Melton, L. J., 3rd, Atkinson, E. J., and Madhok, R., 1996. Downturn in hip fracture incidence. Public Health Reports 111, 146-150; discussion 151.

Michelson, J. D., Myers, A., Jinnah, R., Cox, Q., and Van Natta, M., 1995. Epidemiology of hip fractures among the elderly. Risk factors for fracture type. Clinical Orthopaedics and Related Research, 129-135.

Narici, M. V., Reeves, N. D., Morse, C. I., and Maganaris, C. N., 2004. Muscular adaptations to resistance exercise in the elderly. Journal of Musculoskeletal & Neuronal Interactions 4, 161-164.

NIH, 2001. Osteoporosis prevention, diagnosis, and therapy. JAMA 285, 785-795.

Nordsletten, L., and Ekeland, A., 1993. Muscle contraction increases the structural capacity of the lower leg: an in vivo study in the rat. Journal of Orthoaedic Research 11, 299-304.

Office of Technology Assessment, 1994. Hip Fracture Outcomes in People Age 50 and Over-Background Paper. U.S. Government Printing Office, Washington, DC, OTA-BP-H- 120.

Pentecost, R. L., Murray, R. A., and Brindley, H. H., 1964. Fatigue, Insufficiency, and Pathologic Fractures. JAMA 187, 1001-1004.

Polgar, K., Gill, H. S., Viceconti, M., Murray, D. W., and O'Connor, J. J., 2003. Strain distribution within the human femur due to physiological and simplified loading: finite element analysis using the muscle standardized femur model. Proceedings of the Institution of Mechanical Engineers. Part H, Journal of Engineering in Medicine 217, 173-189.

Reilly, D. T., and Burstein, A. H., 1975. The elastic and ultimate properties of compact bone tissue. Journal of Biomechanics 8, 393-405.

Schwartz, A. V., Kelsey, J. L., Maggi, S., Tuttleman, M., Ho, S. C., Jonsson, P. V., Poor, G., Sisson de Castro, J. A., Xu, L., Matkin, C. C., Nelson, L. M., and Heyse, S. P., 1999. International variation in the incidence of hip fractures: cross-national project on osteoporosis for the World Health Organization Program for Research on Aging. Osteoporosis International 9, 242-253.

Sloan, J., and Holloway, G., 1981. Fractured neck of the femur: the cause of the fall? Injury 13, 230-232.

Smith, L. D., 1953. Hip fractures; the role of muscle contraction or intrinsic forces in the causation of fractures of the femoral neck. The Journal of Bone & Joint Surgery (American Volume) 35-A, 367-383.

Sugarman, J. R., Connell, F. A., Hansen, A., Helgerson, S. D., Jessup, M. C., and Lee, H., 2002. Hip fracture incidence in nursing home residents and community-dwelling older people, Washington State, 1993-1995. Journal of the American Geriatrics Society 50, 1638-1643.

Taylor, D., O'Reilly, P., Vallet, L., and Lee, T. C., 2003. The fatigue strength of compact bone in torsion. Journal of Biomechanics 36, 1103-1109.

Taylor, M. E., Tanner, K. E., Freeman, M. A., and Yettram, A. L., 1996. Stress and strain distribution within the intact femur: compression or bending? Medical Engineering & Physics 18, 122-131.

Thorngren, K. G., Hommel, A., Norrman, P. O., Thorngren, J., and Wingstrand, H., 2002. Epidemiology of femoral neck fractures. Injury 33 Suppl 3, C1-7.

Tountas, A. A., 1993. Insufficiency stress fractures of the femoral neck in elderly women. Clinical Orthopaedics and Related Research 292, 202-209.

Turner, C. H., 1998. Three rules for bone adaptation to mechanical stimuli. Bone 23, 399-407.

Turner, C. H., Wang, T., and Burr, D. B., 2001. Shear strength and fatigue properties of human cortical bone determined from pure shear tests. Calcified Tissue International 69, 373-378.

Warden, S. J., Hurst, J. A., Sanders, M. S., Turner, C. H., Burr, D. B., and Li, J., 2005. Bone adaptation to a mechanical loading program significantly increases skeletal fatigue resistance. Journal of Bone and Mineral Research 20, 809-816.

Wehren, L. E., and Magaziner, J., 2003. Hip fracture: risk factors and outcomes. Current Osteoporosis Reports 1, 78-85.

WHO, 1994. Assessment of fracture risk and its application to screening for postmenopausal osteoporosis. Report of a WHO Study Group. World Health Organization Technical Report Series 843, 1-129.

Winter, D. A., Patla, A. E., Frank, J. S., and Walt, S. E., 1990. Biomechanical walking pattern changes in the fit and healthy elderly. Physical Therapy 70, 340-347.

Yang, K. H., Shen, K. L., Demetropoulos, C. K., King, A. I., Kolodziej, P., Levine, R. S., and Fitzgerald, R. H., Jr., 1996. The relationship between loading conditions and fracture patterns of the proximal femur. Journal of biomechanical engineering 118, 575-578.

Yoshikawa, T., Mori, S., Santiesteban, A. J., Sun, T. C., Hafstad, E., Chen, J., and Burr, D. B., 1994. The effects of muscle fatigue on bone strain. The Journal of Experimental Biology 188, 217-233.

Youm, T., Koval, K. J., and Zuckerman, J. D., 1999. The economic impact of geriatric hip fractures. The American Journal of Orthopedics 28, 423-428.

Zimmermann, C. L., Smidt, G. L., Brooks, J. S., Kinsey, W. J., and Eekhoff, T. L., 1990. Relationship of extremity muscle torque and bone mineral density in postmenopausal women. Physical Therapy 70, 302-309.

Zuckerman, J. D., 1996. Hip fracture. The New England Journal of Medicine 334, 1519-1525.

Chapter 3 – Age differences in lower extremity joint torques during walking with controlled speed and step length

Abstract

Older adults exhibit differences in the kinetics of self-selected gait compared to young adults, such as reduced torque at the ankle and increased work at the hip. Older adults also exhibit reduced speed and step length. Because gait kinetics depend on these spatio-temporal characteristics, it is possible that kinetic changes with aging are the result of older adults selecting different characteristics of gait than young adults. The purpose of this study was to investigate this possibility by examining age differences in gait while controlling both speed and step length. Ten healthy young and ten healthy older adults took part in walking trials in our laboratory. Data was collected for three gait conditions: self-selected, slow controlled and fast controlled. Inverse dynamics analyses were performed to determine lower extremity joint torques during gait and peak joint torques were compared between age groups. The results indicate the importance of controlling spatio-temporal characteristics when comparing gait kinetics. However, age differences in peak joint torques were still present when speed and step length were controlled, including reduced plantar flexor torque and increased hip extensor torque. Furthermore, interactions between age and speed indicate that older adults used different neuromuscular strategies than young adults to vary the speed of their gait. This supports the idea that age-related differences in joint kinetics are adaptations to age-related changes in neuromuscular function.

Keywords: aging, walking, joint torque, gait speed, step length

Introduction

Healthy older adults exhibit differences in self-selected gait kinematics and kinetics when compared to young adults. Kinematic differences include reduced gait speed, less joint range of motion, and shorter step length in older adults (Crowinshield et al. 1978; DeVita and Hortobagyi 2000; Judge et al. 1996; Kerrigan et al. 1998; Laufer 2005; Waters et al. 1983; Winter et al. 1990), while kinetic differences include reduced ankle torque and power (DeVita and Hortobagyi 2000; Judge et al. 1996; Kerrigan et al. 1998) as well as increased work at the hip (DeVita and Hortobagyi 2000; Silder et al. 2008). The reasons for these age differences in gait are not entirely clear. While it is possible that these differences represent adaptations to provide a safer, more stable gait (Winter et al. 1990), research suggests that there is a physiological basis for these differences (McGibbon 2003). For example, aerobic capacity declines significantly with age (Astrand et al. 1973) such that walking at self-selected speed requires about 30% of aerobic capacity in young adults but about 50% of aerobic capacity in older adults, despite older adults adopting slower self-selected gait speeds (Waters et al. 1983). Age-related differences in gait may also be the result of neuromuscular changes such as reduced muscle strength (Doherty 2003; Hurley 1995). As evidence for this, hip extensor strength is correlated with gait speed and step length in older men (Burnfield et al. 2000).

One difficulty in investigating age differences in gait kinetics is that they are heavily dependent upon spatio-temporal characteristics such as speed, step length and cadence. For example, peak hip extension torque increases with gait speed (Crowinshield et al. 1978; Kerrigan et al. 1998), and peak knee extension torque increases with speed (Crowinshield et al. 1978; Kerrigan et al. 1998; Kirtley et al. 1985) and cadence and stride length (Kirtley et al. 1985). Joint powers at the hip, knee, and ankle also increase with increased speed (Graf et al. 2005; Kerrigan et al. 1998) and cadence (Winter 1983, 1983). The work done by the hip and knee joints also increases with speed in children, but the work done by the ankle does not (Chen et al. 1997). The level of effort during gait, quantified as joint torque normalized by strength, increases with cadence at the hip and ankle (Nadeau et al. 1996; Requiao et al. 2005).

As a result of these relationships between gait kinetics and spatio-temporal characteristics, previously reported age differences in gait kinetics may be confounded by age differences in self-selected gait. A few studies have compared age differences in gait kinetics while controlling speed. Larish et al. (1988) showed that older adults have lower ground reaction force (GRF) peaks than young adults when walking at identical speeds. With controlled gait speed, DeVita and Hortobagyi (2000) found age differences in gait kinetics, including more work at the hip and less at the ankle in older adults compared to young adults. However, step length was not controlled, and was reported to be significantly smaller in older adults. Silder et al. (2008) found similar age differences in work at the hip and ankle, while reporting no significant age differences in speed or step length. However, controlling spatio-temporal characteristics between age groups was not a stated objective of the study, and speed was based on preferred walking speed. To eliminate any confounding effects due to spatio-temporal characteristics, studies of age-related differences in gait kinetics should control speed, step length and cadence.

The purpose of this study was to examine age differences in lower extremity joint torques during gait while controlling speed and step length. By controlling these variables, the effects of age on joint torques can be separated from those of speed and step length. This will be a useful step in understanding the nature and causes of age-related changes in gait.

Methods

Twenty healthy adult volunteers participated in the study including ten young adults (mean±SD age of 23.9±3.3 years) and ten older adults (80.3±4.0 years). There were no significant age differences in height (young: 1.65±0.09 m, older: 1.63±0.08 m, $p = 0.639$) or body mass (young: 61.7±7.3 kg, older: 65.2±10.5 kg, $p = 0.394$), and each age group contained equal numbers of males and females. Participation was limited to individuals who could ambulate independently and who had no self-reported musculoskeletal, neurological, cardiovascular, or cognitive disorders, or previous fragility fractures that might affect gait. The project was approved by the Virginia Tech Institutional Review Board, and all participants provided written informed consent prior to participation.

Each participant performed gait trials on an 8 m long walkway in our laboratory under various experimental conditions. The gait conditions included self-selected gait and controlled gait at slow and fast speeds. In the self-selected gait condition, each participant was asked to walk normally down the walkway with no instruction given as to what speed or step length to adopt. These trials were included to examine how age differences in uncontrolled conditions differed with controlled conditions. In the controlled gait conditions, both speed and step length were controlled. Target speeds were 1.1 m/s for the slow controlled condition and 1.5 m/s for the fast controlled condition, and were achieved by having participants match pace with a moving belt alongside the walkway. These speeds are representative of the range of speeds reported in the literature for self-selected gait in both young and older adults (DeVita and Hortobagyi 2000; Judge et al. 1996; Kerrigan et al. 1998; Larish et al. 1988; Laufer 2005; Silder et al. 2008). The target step length was 0.65 m for both slow and fast speeds, and was achieved by having participants step on markings on the walkway. This step length is a mid-range value for step lengths reported in the literature for self-selected gait in both young and older adults (Judge et al. 1996; Kerrigan et al. 1998; Larish et al. 1988; Laufer 2005; Silder et al. 2008; Winter et al. 1990). Because speed, step length, and cadence are nominally related by speed = step length × cadence, setting step length and speed defined cadence as well.

During all gait trials ground reaction force (GRF) and body position data were collected over one full gait cycle of the right lower extremity. A single trial of self-selected gait was recorded, followed by three trials at each of the controlled conditions. GRF data was sampled at 1000 Hz from a six degree-of-freedom force platform (Advanced Mechanical Technology Inc., Watertown, MA) placed in the center of the walkway. The participant stepped on the force platform with their right foot during each trial. For self-selected trials, the starting position of the participant was adjusted so they would naturally step on the force platform without altering their chosen gait. Thirty-six reflective markers were placed on each participant, and marker position data was sampled at 100 Hz using a six-camera VICON 460 motion analysis system (VICON Motion Systems Inc., Lake Forest, CA).

An individualized, three-dimensional, rigid link biomechanical model was created for each participant in OpenSim, an open-source software system for musculoskeletal modeling (Delp et al. 2007). The model contained eight segments (feet, shanks, thighs, pelvis and head-arms-trunk), which were connected by seven 3-degree-of-freedom ball joints (ankles, knees, hips, and a lumbar region joint), for a total of 27 model degrees of freedom. Segment masses and center of mass positions were estimated using the methods reported by Pavol et al. (2002), and segment mass moments of inertia were estimated using the methods reported by de Leva (1996).

Joint center positions were determined by functional methods, which determine best-fit locations of the joint (e.g. hip joint center) based on the relative motion of the markers on the adjoining segments (e.g. pelvis and thigh). Various methods for calculating functional joint centers have been introduced (e.g. Gamage and Lasenby 2002; Piazza et al. 2004). For example, fitting thigh marker motions to spheres centered in the pelvic coordinate system provides the functional center of the hip joint in the pelvic system (Hicks and Richards 2005; Piazza et al. 2004; Piazza et al. 2001). This approach provides improved results over anthropometric estimates when a special calibration trial is performed (Hicks and Richards 2005; Piazza et al. 2004). A separate trial was performed prior to gait testing in which each participant performed a series of movements in order to move each joint through its range of motion. A custom program was created in Matlab (The MathWorks Inc., Natick, Massachusetts, USA), which used the algorithm of Piazza et al. (2004) to determine joint center locations using marker data from this trial.

Joint torques during gait were estimated from the collected data using an inverse dynamics analyses in OpenSim. Force platform data and marker position data were first low pass filtered at 7 Hz (4^{th} order zero-phase-lag Butterworth), and GRF and center of pressure position was determined from force platform data (Winter 2005). Gait speed for each trial was evaluated as the average forward velocity of the marker placed on the right anterior superior iliac spine, and step length as the average forward distance between left and right heel markers during stance phase. For each participant, a single gait trial best representing the desired gait condition was selected for inclusion in the analysis. Marker motion and ground reaction force data were imported into OpenSim for these trials. Inverse dynamics was performed during a single gait cycle (right foot swing and stance phase) from each trial.

Five lower extremity peak torques during the gait cycle were analyzed for age differences. The peak torques examined were hip extension in early stance (HE), hip flexion in late stance (HF), knee extension in early stance (KE), knee flexion in midstance (KF), and plantar flexion in late stance (PF). Joint torques were normalized by body mass prior to statistical analysis.

A two-way, mixed-model multivariate analysis of variance (MANOVA) was initially performed to investigate the effects of age and gait condition on all peak torques together. In the event of significant effects, univariate analyses were performed for each dependent variable. For the self-selected gait condition, this involved independent t-tests to investigate age differences in peak torques. For the controlled gait conditions, this involved using a two-way mixed-model ANOVA to examine age and speed differences in torques. Independent t-tests were also performed ensure that there were no age differences in speed and step length under controlled gait conditions. All statistical analyses were performed using JMP (SAS Institute, Inc., Cary, NC) with a significance level of 0.05. Trends were also noted when *p*-values were between 0.10 and 0.05.

Results

There were no differences in gait speed between age groups within any of the three gait conditions (Table 3.1). However, step length was smaller for older adults within the self-selected gait condition (p = 0.010).

Table 3.1: Mean (SD) values of gait speed and step length by age group for the three gait conditions tested, self-selected (SS), slow-controlled (SC) and fast-controlled (FC).

Gait Condition	Speed (m/s)		Step length (m)	
	Older	Young	Older	Young
SS*	1.188 (0.125)	1.263 (0.104)	0.650 (0.050)	0.703 (0.042)
SC	1.185 (0.044)	1.184 (0.021)	0.648 (0.006)	0.651 (0.004)
FC	1.532 (0.054)	1.520 (0.035)	0.651 (0.011)	0.656 (0.010)

*Significant age group difference in step length (p = 0.010).

MANOVA results indicated significant age effects on one or more peak lower extremity joint torque (p = 0.003) and in one or more gait condition (p = 0.041). In addition, gait condition was found to have a significant effect on peak joint torque (p<0.001). Based on these results, univariate analyses were conducted for all dependent variables.

During self-selected gait, older adults exhibited increased peak torques in HE, but reduced peak HF torques and KF torques compared to young adults (Table 3.2, Figure 3.1). In addition, older adults showed a trend toward reduced peak PF torques. However, there was no age difference in peak KE torque.

Table 3.2: Mean (SD) peak torque values during self-selected gait normalized by body mass (N-m/kg) compared between age groups.

	Older	Young	p-values
HE	0.754 (0.151)	0.612 (0.151)	**0.049**
HF	0.565 (0.126)	0.680 (0.064)	**0.019**
KE	0.505 (0.140)	0.377 (0.239)	0.162
KF	0.297 (0.167)	0.462 (0.148)	**0.031**
PF	1.409 (0.110)	1.516 (0.141)	0.075

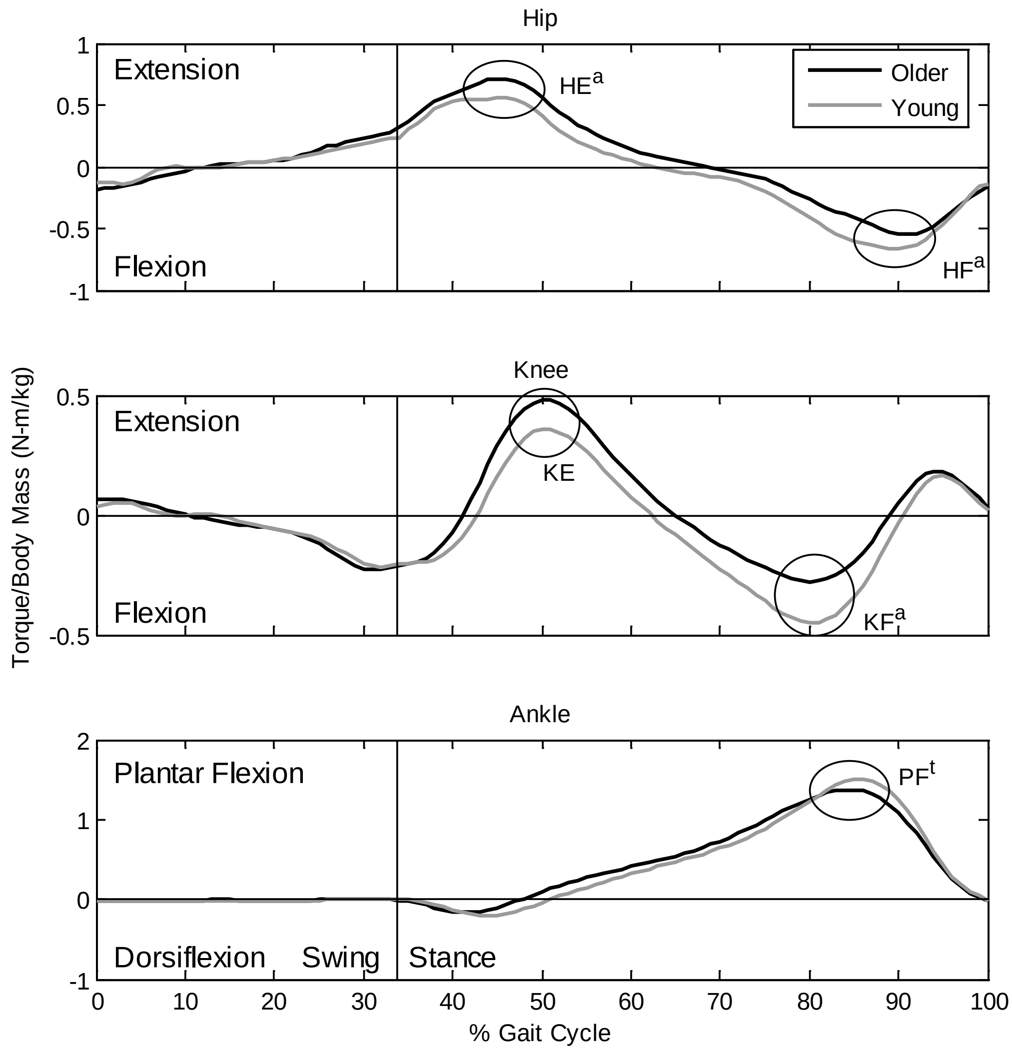

Figure 3.1: Mean joint torques normalized by body mass for young and older age groups throughout a single cycle of self-selected gait. Peak torques examined for age effects are circled. [a]Significant age difference in peak torque ($p<0.05$). [t]Trend toward significant age difference ($0.05<p<0.1$).

When speed and step length were controlled, several effects of both age and speed were found (Table 3.3, Figure 3.2). Older adults showed a trend toward increased peak HE torques, and exhibited increased peak KE torques but reduced peak KF torques and PF torques as compared to young adults. Peak HE, HF and KE torques all increased with speed. In addition to main effects, peak HE torque and peak PF torque both showed a significant age × speed interactions. A post hoc Tukey HSD test indicated that HE peak torque increased significantly with speed in young adults but not in older adults. A post hoc Tukey HSD test indicated that PF torque increased significantly with speed in young adults, but not in older adults.

Table 3.3: Mean (SD) peak torque values normalized by body mass (N-m/kg) for controlled gait conditions, compared by age group and speed.

	Slow		Fast		p-values		
	Older	Young	Older	Young	Age	Speed	Age × Speed
HE	0.787 (0.193)	0.586 (0.106)	0.902 (0.171)	0.845 (0.135)	0.056	**<0.001**	**0.023**
HF	0.563 (0.102)	0.639 (0.131)	0.788 (0.146)	0.892 (0.140)	0.116	**<0.001**	0.527
KE	0.516 (0.188)	0.328 (0.230)	0.735 (0.217)	0.482 (0.142)	**0.012**	**<0.001**	0.387
KF	0.243 (0.165)	0.459 (0.085)	0.222 (0.178)	0.461 (0.089)	**<0.001**	0.678	0.610
PF	1.403 (0.083)	1.464 (0.144)	1.345 (0.139)	1.535 (0.131)	**0.032**	0.727	**0.002**

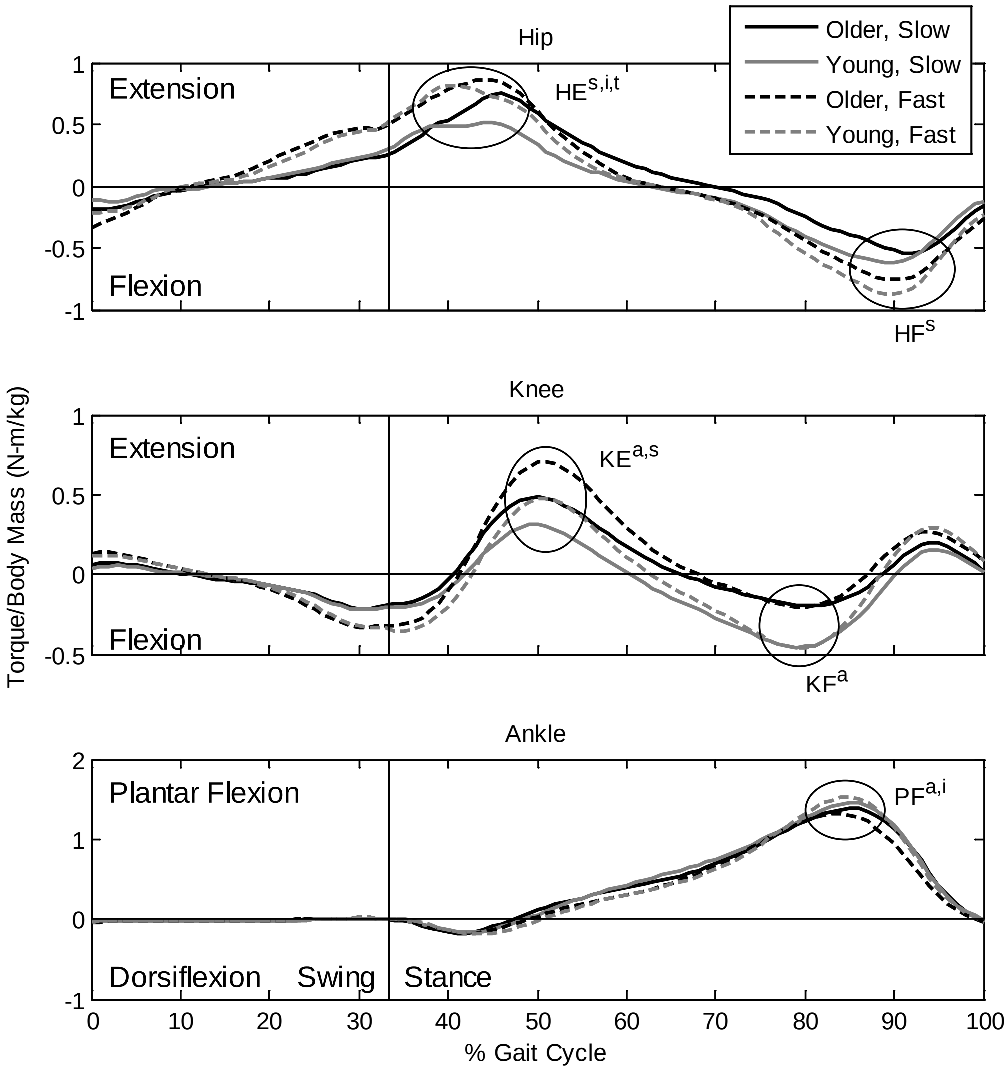

Figure 3.2: Mean joint torques normalized by body mass for young and older age groups throughout a single cycle of controlled gait (Slow and Fast). Peak torques examined for age and speed effects are circled. [a]Significant main effect of age ($p<0.05$). [s]Significant main effect of speed ($p<0.05$). [i]Significant age × speed interaction ($p<0.05$). [t]Trend toward a significant age effect ($0.05<p<0.1$).

Discussion

The purpose of this study was to examine age differences in lower extremity joint torques during gait while controlling speed and step length. Age differences during self-selected gait were also investigated for comparison. During self-selected gait, four of the five peak joint torques examined exhibited some effect of age (HE, HF, KF and PF but not KE). When speed and step length were controlled experimentally, four of the five peak joint torques exhibited some effect of age (HE, KE, KF and PF but not HF). Thus, these four measures have significant age-related effects that are separate from the effects of speed and step length. The effects of age were not fully consistent between self-selected and controlled gait conditions. Thus, controlling speed and step length is important in examining age differences in joint kinetics during gait.

Peak HE torque tended to be increased in older adults in both self-selected and controlled gait conditions. These results are similar to those of DeVita and Hortobagyi (2000), who showed increased HE angular impulse in older adults. However, the interaction between age and gait speed showed that age differences in peak HE torque are dependent on gait speed. Specifically, the Tukey HSD test indicated larger peak HE torques in older adults than young adults at slow speed, but no age difference at fast speed, and that young adults increase peak HE torque with speed, but older adults do not. The results also show that age differences occur in peak HE torque independent of step length. However, because only one step length was examined, no conclusions can be made regarding the effect of step length on peak HE torque.

Peak HF torque exhibited an age difference in the self-selected gait condition that disappeared when speed and step length were controlled. Thus, this age difference may be due solely to age differences in gait speed and step length. In the self-selected condition, older adults had reduced HF peak torque compared to young adults. This is consistent with the results of DeVita and Hortobagyi (2000), who reported decreased HF angular impulse in older adults while walking with identical speeds but shorter step lengths compared to young adults.

Peak KE torque was found to be higher in older adults during controlled gait, but not during self-selected gait. A larger sample size may have provided sufficient statistical power to reach significance in the self-selected case. Nonetheless, the results indicate a significant age effect on peak KE torque that is independent of speed and step length. Because speed had a similar effect on peak KE torque in both age groups, control of speed is important when comparing peak KE torque between age groups. It should be noted that this result is inconsistent with that reported by DeVita and Hortobagyi (2000). While they did not report a difference for peak KE torque, they did report that KE angular impulse was reduced in older adults. Although these two measures are not identical, age differences in them would most likely be in the same direction. The reason for this inconsistency is unknown.

Peak KF torque was significantly affected by age, but unlike the other joint torques examined, remained relatively constant across all gait conditions tested. While the magnitude of these torques was relatively low compared to the others examined, the relative difference between age groups was quite high, with young adults exhibiting KF peak torques about twice those of older adults. Peak KF torque was not affected by speed. While the effect of step length was not examined explicitly, the age effect was similar when step length was controlled and in self-selected gait when the age groups had significantly different step lengths. This indicates that peak KF torque is relatively insensitive to step length as well as speed. Thus, peak KF torque may represent a kinetic factor of gait that is affected by aging but not by gait speed and SL.

Peak PF torque tended to be lower in older adults during self-selected gait, and was lower during controlled gait, but also exhibited an interaction between age and speed. The Tukey HSD test indicated peak PF torque was significantly lower in older adults at fast speed, but not at slow speed. Interestingly, older adults did not appear to increase PF torque with increased gait speed, but young adults did. This behavior may be explained by a combination of reduced soleus activation and increased tibialis anterior co-contraction in older adults (Schmitz et al. 2009).

DeVita and Hortobagyi (2000) showed that older adults had significantly lower peak PF torque than young adults when both age groups were walking at a controlled target speed of 1.5 m/s (comparable to the Fast speed used here). However, step length was not controlled, and older adults took shorter steps than young adults. A similar PF age difference was found in this study when step length was controlled. Thus, peak PF torque does have an age difference independent of step length, at least at higher gait speeds. However, it should be noted that this does not preclude the possibility that step length has an effect on PF torque.

It has been proposed (DeVita and Hortobagyi 2000) that neuromuscular adaptation with age shifts the function of gait proximally, with increased contributions by the hip extensors and decreased contributions by the ankle plantar flexors. Such a shift was seen in the results of this study. Aging is associated with decreased neuromuscular function, including loss of muscle mass and decreased innervation of motor units (Doherty 2003; Hurley 1995). Thus, while the mechanism behind this shift is not fully known, the fact that older adults did not increase plantar flexor torque with speed may indicate a deficit in plantar flexor strength or neural drive. Indeed, older adults show reduced peak soleus activation than young adults (Schmitz et al. 2009), which could be a result of decreased soleus innervation. A loss in plantar flexor strength could also produce such a shift, as a forward dynamic simulation of gait indicated that a moderate strength deficit in the ankle plantar flexors may be compensated for by the hip flexors and extensors (Goldberg and Neptune 2007). An examination of the level of effort during gait for young and older adults during gait could improve our understanding of the reason for age related changes in gait.

This study controlled both speed and step length, but two speeds were tested while only a single step length was examined. As the literature (Crowinshield et al. 1978; Kerrigan et al.

1998; Kirtley et al. 1985) and these results suggest, gait speed has a significant effect on peak torques in the lower extremity. It is likely that step length also has significant effects on peak joint torques. It is also possible that older adults may adopt different neuromuscular strategies than young adults to vary step length. Future studies could examine step length effects by testing gait at multiple controlled step lengths while controlling gait speed.

In conclusion, this study examined age differences in lower extremity peak joint torques while controlling speed and step length. Older adults displayed multiple differences with young adults, including a shift in function from the plantar flexors to the hip extensors, with both speed and step length controlled. Thus, previously reported gait differences cannot be explained as the result of older adults selecting different speed and step length than young adults. Additionally, interactions between age and speed were found for HE and PF torques, indicating that older adults adopt different neuromuscular strategies than young adults to vary the speed of their gait. These results support the idea that age-related changes in joint torques are adaptations to changes in neuromuscular function that occur with aging.

Acknowledgement

This work was supported by Award Number F31AG030904 from the National Institute on Aging. The content is solely the responsibility of the author and does not necessarily represent the official views of the National Institute on Aging or the National Institutes of Health.

References

Astrand, I., Astrand, P. O., Hallback, I., and Kilbom, A., 1973. Reduction in maximal oxygen uptake with age. Journal of Applied Physiology 35, 649-654.

Burnfield, J. M., Josephson, K. R., Powers, C. M., and Rubenstein, L. Z., 2000. The influence of lower extremity joint torque on gait characteristics in elderly men. Archives of Physical Medicine and Rehabilitation 81, 1153-1157.

Chen, I. H., Kuo, K. N., and Andriacchi, T. P., 1997. The influence of walking speed on mechanical joint power during gait. Gait & Posture 6, 171-176.

Crowinshield, R. D., Brand, R. A., and Johnston, R. C., 1978. The effects of walking velocity and age on hip kinematics and kinetics. Clinical Orthopaedics and Related Research 132, 140-144.

de Leva, P., 1996. Adjustments to Zatsiorsky-Seluyanov's segment inertia parameters. Journal of Biomechanics 29, 1223-1230.

Delp, S. L., Anderson, F. C., Arnold, A. S., Loan, P., Habib, A., John, C. T., Guendelman, E., and Thelen, D. G., 2007. OpenSim: open-source software to create and analyze dynamic simulations of movement. IEEE Transactions on Biomedical Engineering 54, 1940-1950.

DeVita, P., and Hortobagyi, T., 2000. Age causes a redistribution of joint torques and powers during gait. Journal of Applied Physiology 88, 1804-1811.

Doherty, T. J., 2003. Invited review: Aging and sarcopenia. Journal of Applied Physiology 95, 1717-1727.

Gamage, S. S., and Lasenby, J., 2002. New least squares solutions for estimating the average centre of rotation and the axis of rotation. Journal of Biomechanics 35, 87-93.

Goldberg, E. J., and Neptune, R. R., 2007. Compensatory strategies during normal walking in response to muscle weakness and increased hip joint stiffness. Gait & Posture 25, 360-367.

Graf, A., Judge, J. O., Ounpuu, S., and Thelen, D. G., 2005. The effect of walking speed on lower-extremity joint powers among elderly adults who exhibit low physical performance. Archives of Physical Medicine and Rehabilitation 86, 2177-2183.

Hicks, J. L., and Richards, J. G., 2005. Clinical applicability of using spherical fitting to find hip joint centers. Gait & Posture 22, 138-145.

Hurley, B. F., 1995. Age, gender, and muscular strength. The Journals of Gerontology. Series A, Biological Sciences and Medical Sciences 50 Spec No, 41-44.

Judge, J. O., Davis, R. B., 3rd, and Ounpuu, S., 1996. Step length reductions in advanced age: the role of ankle and hip kinetics. The Journals of Gerontology. Series A, Biological Sciences and Medical Sciences 51A, M303-M312.

Kerrigan, D. C., Todd, M. K., Della Croce, U., Lipsitz, L. A., and Collins, J. J., 1998. Biomechanical gait alterations independent of speed in the healthy elderly: evidence for specific limiting impairments. Archives of Physical Medicine and Rehabilitation 79, 317-322.

Kirtley, C., Whittle, M. W., and Jefferson, R. J., 1985. Influence of walking speed on gait parameters. Journal of Biomedical Engineering 7, 282-288.

Larish, D. D., Martin, P. E., and Mungiole, M., 1988. Characteristic patterns of gait in the healthy old. Annals of the New York Academy of Sciences 515, 18-32.

Laufer, Y., 2005. Effect of age on characteristics of forward and backward gait at preferred and accelerated walking speed. The Journals of Gerontology. Series A, Biological Sciences and Medical Sciences 60, 627-632.

McGibbon, C. A., 2003. Toward a better understanding of gait changes with age and disablement: neuromuscular adaptation. Exercise and Sport Sciences Reviews 31, 102-108.

Nadeau, S., Gravel, D., Arsenault, A. B., and Bourbonnais, D., 1996. A mechanical model to study the relationship between gait speed and muscular strength. IEEE Transactions on Rehabilitation Engineering 4, 386-394.

Pavol, M. J., Owings, T. M., and Grabiner, M. D., 2002. Body segment inertial parameter estimation for the general population of older adults. Journal of Biomechanics 35, 707-712.

Piazza, S. J., Erdemir, A., Okita, N., and Cavanagh, P. R., 2004. Assessment of the functional method of hip joint center location subject to reduced range of hip motion. Journal of Biomechanics 37, 349-356.

Piazza, S. J., Okita, N., and Cavanagh, P. R., 2001. Accuracy of the functional method of hip joint center location: effects of limited motion and varied implementation. Journal of Biomechanics 34, 967-973.

Requiao, L. F., Nadeau, S., Milot, M. H., Gravel, D., Bourbonnais, D., and Gagnon, D., 2005. Quantification of level of effort at the plantarflexors and hip extensors and flexor muscles in healthy subjects walking at different cadences. Journal of Electromyography & Kinesiology 15, 393-405.

Schmitz, A., Silder, A., Heiderscheit, B., Mahoney, J., and Thelen, D. G., 2009. Differences in lower-extremity muscular activation during walking between healthy older and young adults. Journal of Electromyography & Kinesiology 19, 1085-1091.

Silder, A., Heiderscheit, B., and Thelen, D. G., 2008. Active and passive contributions to joint kinetics during walking in older adults. Journal of Biomechanics 41, 1520-1527.

Waters, R. L., Hislop, H. J., Perry, J., Thomas, L., and Campbell, J., 1983. Comparative cost of walking in young and old adults. Journal of Orthoaedic Research 1, 73-76.

Winter, D. A., 1983. Biomechanical motor patterns in normal walking. Journal of Motor Behavior 15, 302-330.

Winter, D. A. 2005. Biomechanics and Motor Control of Human Movement. Third ed. John Wiley & Sons, Hoboken, NJ.

Winter, D. A., 1983. Energy generation and absorption at the ankle and knee during fast, natural, and slow cadences. Clinical Orthopaedics and Related Research, 147-154.

Winter, D. A., Patla, A. E., Frank, J. S., and Walt, S. E., 1990. Biomechanical walking pattern changes in the fit and healthy elderly. Physical Therapy 70, 340-347.

Chapter 4– Finite element modeling of the femur

Introduction

Hip fractures, or fractures of the proximal femur, are a serious health problem in older populations. Worldwide, approximately 1.66 million hip fractures occurred in 1990, and this is projected to increase to 6.26 million hip fractures annually by 2050 (Cooper et al. 1992). Hip fractures are associated with high rates of mortality and morbidity. Mortality rates in the six months following a hip fracture are about 20% overall (NIH 2001), and the majority of survivors do not regain their pre-fracture level of functionality in activities of daily living (Magaziner et al. 2000; NIH 2001). Due to the magnitude and importance of the problem, many studies investigating hip fractures have been performed. Modeling studies are an important part of this research because they allow the investigation of factors such as *in vivo* stresses and strains that are difficult or impossible to measure experimentally (Villarraga and Ford 2001). The purpose of this chapter is to provide an overview of finite element modeling of the femur, specifically the development of femur geometry, material properties and loading conditions.

The finite element method lends itself to the analysis of skeletal structures such as the femur because it can account for complex geometry, material properties, and loading conditions, (Villarraga and Ford 2001). Two-dimensional finite element models of the femur appear in the literature as early as 1972 (Brekelmans et al. 1972; Rybicki et al. 1972). In spite of their limitations, these models improved on earlier analyses based on beam theory because they could account for portions of the bone geometry that did not resemble a slender beam. A three-dimensional model of the proximal femur, representing the next logical extension of this work, showed significant differences in stress predictions to the previous two-dimensional models

(Valliappan et al. 1977). Since that time, numerous finite element studies of the femur have been reported with increasing refinement and complexity in model geometry, material properties, and loading conditions.

Model development from computed tomography (CT) images represents the current method of choice for creating skeletal finite element models (Taddei, Martelli et al. 2006). In a CT scan, x-ray transmission measurements are made at multiple angles around an object. These may be reconstructed into a 3D image which shows the variation in x-ray attenuation throughout the object. Because of this, CT images provide accurate information on bone geometry, can be interpreted to provide mechanical properties, and allow the modeling of bones *in vivo* (Marom and Linden 1990).

Many studies using finite element models of the femur can be found in the literature addressing a variety of questions. Many estimate stresses and/or strains within the femur, for purposes including prediction of hip fracture risk (Testi et al. 2002) and comparison of different loading conditions (e.g. Duda et al. 1998). Other studies have used finite element models to estimate fracture load and location (e.g. Keyak et al. 2001). Simulations of bone remodeling processes have been performed, specifically related to bone resorption around hip implants following hip replacement (Bitsakos et al. 2005). Finite element models of the hip have also been used to simulate intertrochanteric osteotomies (surgical sectioning and realignment of the proximal femur), which may be useful for operative planning (Schmitt et al. 2001). Another study examined femoral failure with a simulated metastatic bone defect, demonstrating the possibility of predicting impending pathological fractures using finite element models (Spruijt et al. 2006).

Femoral geometry in finite element models

Accurately modeling femoral geometry is crucial in creating a finite element model that can produce realistic results. The femur consists of a central shaft region (diaphysis) with enlarged articular regions (epiphyses) at each end. The proximal end includes the head and neck, which articulate with the pelvis at the hip joint, and the greater and lesser trochanters, which serve as muscle attachment sites (Figure 4.1). A sensitivity analysis of the effects of geometric scaling and material property definitions on the results of a finite element model of the femur found that geometric errors had a significant effect on model displacements, stresses and strains (Taddei, Martelli et al. 2006).

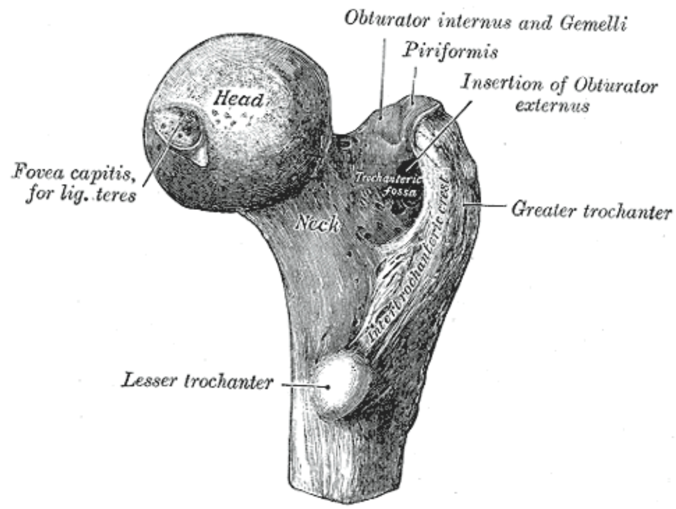

Figure 4.1: Proximal end of right femur viewed from behind and above showing femoral head and neck, greater trochanter and lesser trochanter. Image from Gray (1918), fair use.

Many femoral models create 3D geometry from CT scans of excised femurs (Bessho et al. 2007; Cody et al. 1999; Duchemin et al. 2008; Gomez-Benito et al. 2005; Keyak and Falkinstein 2003; Keyak et al. 2001; Keyak et al. 1998; Lotz et al. 1991, 1991; Merz et al. 1996; Ota et al. 1999; Schileo et al. 2007; Spruijt et al. 2006; Taylor et al. 1996). Others have used CT scans taken *in situ* (Keyak and Falkinstein 2003) or *in vivo* (Keyak et al. 1990; Schmitt et al. 2001). It should be noted that CT images of the femur taken *in situ* and *in vitro* show differences in geometry and bone density, such that finite element estimations of fracture load are different, because additional bone and soft tissue in the image field increase noise, beam hardening and streak artifacts in the *in situ* scans (Keyak and Falkinstein 2003). Other approaches to modeling femur geometry include developing 2D geometry using frontal plane radiographs (Rudman et al. 2006) or DXA scans (Testi et al. 2002), or using CAD data of the Standardized Femur, the geometry model of a femoral bone analogue, to develop a 3D finite element model (Duda et al. 1998; Polgar et al. 2003).

The time required to create a finite element model of bone from a CT image has led to the exploration of methods to automate the process (Keyak et al. 1990; Merz et al. 1996; Taddei, Cristofolini et al. 2006). Keyak et al. (1990) developed an approach where the bone is represented using cubic 8-node brick elements (Figure 4.2), with an admittedly imprecise representation of the bone surface. This method has been used in various studies (Cody et al. 1999; Keyak et al. 2001; Keyak et al. 1998; Spruijt et al. 2006), and provides good results within the bone, but is limited in dealing with surface effects. Merz et al. (1996) presented a semi-automated method that predetermines bone contours and mesh volumes in the bone, better representing bone geometry. Taddei, Cristofolini et al. (2006) used a similar semi-automated

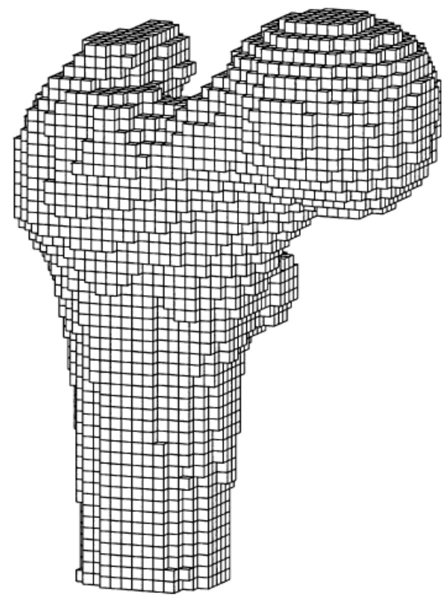

Figure 4.2: Finite element model of the proximal femur composed of 11,604 cube elements 3 mm on a side. (Reprinted from Journal of Biomechanics 31, Keyak, J. H., Rossi, S. A., Jones, K. A., and Skinner, H. B., Prediction of femoral fracture load using automated finite element modeling. Page 128, Copyright 1998, with permission from Elsevier).

approach, first determining the surface geometry of the bone, followed by automatic meshing of the volume.

Modeling of material properties

The material properties of the femur (and other bones) are non-homogeneous due to variations in the density and porosity of bone. The femur consists of a shell of cortical bone of varying thickness, with internal structures of cancellous bone inside the proximal and distal ends (Figure 4.3). Cancellous bone, also called trabecular or spongy bone, is a lattice-work of interconnected plates and rods called trabeculae. By comparison cortical, or compact, bone is relatively solid. In general, the porosity of cortical bone is 5 – 30%, while that of cancellous bone ranges from 30 – 90% (Carter and Hayes 1977). The strength and elastic modulus of bone depends on bone density (Carter and Hayes 1977; Goldstein 1987), which varies throughout the bone.

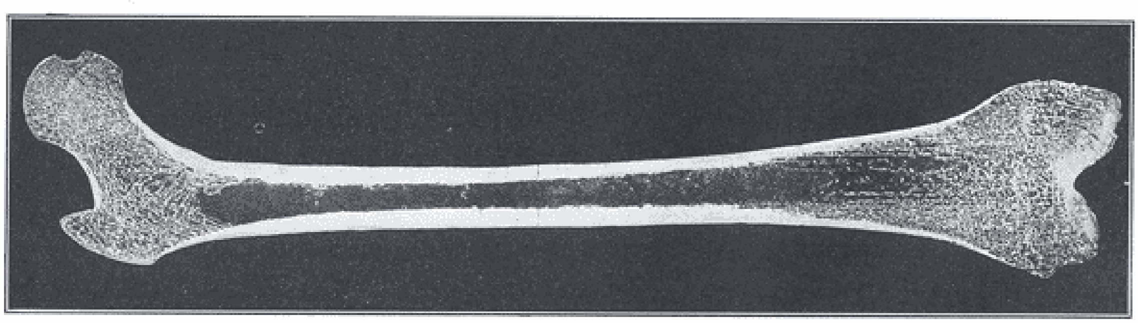

Figure 4.3: A frontal longitudinal midsection of a left femur showing cancellous bone within the proximal and distal femur, and the varying thickness of the cortical shell. Image from Gray (1918), fair use.

The material properties of the femur in some models have only accounted for bone non-homogeneity in a limited way. Valliapan et al. (1977) used a single isotropic elastic modulus for all cancellous bone (324.6 MPa), another for cortical bone (17.26 GPa) and a Poisson's ratio of

0.29. Duda et al. (1998) and Polgar et al. (2003) also used a single modulus for cancellous bone (1500 MPa), while Rudman et al. (2006) used two (100 and 400 MPa) and Taylor et al. (1996) used five separate cancellous moduli ranging from 250 to 1250 MPa. All four of these studies used a modulus of 17 GPa for cortical bone and a Poisson's ratio of 0.33.

The inclusion non-homogeneous material properties in finite element models of the femur has a significant effect on the results. For example, in a comparison between a non-homogeneous model and the corresponding homogeneous model with "averaged" material properties, peak stress was larger in the homogeneous model (Merz et al. 1996). By using a CT image as a source of information, an estimation of material non-homogeneity can be made. In experimental tests, linear relations between CT brightness numbers and cancellous bone density have proved to be statistically significant. Ciarrelli (1991) gives a coefficient of determination of $R^2 = 0.82$, while McBroom (1985) gives a value of $R^2 = 0.89$. A variety of empirical relations have been developed that relate bone density to elastic modulus. According to a review of this work by Martin (1991), the elastic modulus of cancellous bone is roughly proportional to the density squared, and to density cubed for cortical bone. Thus, CT brightness can be converted to bone density, and bone density to elastic modulus, providing an estimate of material properties throughout the bone.

To model bone non-homogeneity more accurately, some models have included many elastic modulus values based on evaluations of CT image data. Various empirical equations have been used to estimate elastic moduli from CT brightness or bone density, with some studies using multiple relationships. This includes using separate linear CT-modulus relationships for different ranges of CT brightness (Schmitt et al. 2001) or multiple non-linear density-modulus relationships for different density ranges (Bessho et al. 2007; Keyak et al. 2001; Keyak et al.

1998; Merz et al. 1996). Others have used a single density-modulus relationship for all levels of bone density (Cody et al. 1999; Duchemin et al. 2008; Keyak et al. 1990; Ota et al. 1999; Spruijt et al. 2006). Schileo et al. (2007) compared the performance of three density-modulus relationships suitable for use over the entire range of bone density. Strains predicted by the model were compared to strains measured during *in vitro* mechanical testing. For one of the relationships tested the model predicted measured strains quite well (R^2 = 0.91).

The most common strategy for modeling non-homogeneous properties in bone has been to assume that material variation within each element is negligible, and calculate an average value at each element (Taddei et al. 2004). This is typically done by averaging the CT brightness within the element volume and then converting the average value to elastic modulus using CT-density and density-modulus relations. Thus each element is homogeneous, but the material properties vary among the elements. Several different methods of calculating average CT brightness in an element can be found in the literature. Merz et al. (1996) averaged the values nearest to each element node. Zannoni et al. (1998) used an average of all values within the element. Cattaneo et al. (2001) used a geometrically weighted average of the eight CT grid values nearest the element centroid. Finally, Taddei et al. (2004) used a numerical integration over the volume of the element, providing the best estimation of the element average, though with increased computational effort. Rather than averaging CT brightness, Keyak et al. (1990) first calculated the average modulus for each CT pixel, and then averaged the moduli of pixels within an element. This approach was used because averaging the density and then converting to modulus may underestimate modulus in elements with variable density due to the non-linear density-modulus relationship.

In addition to non-homogeneity, some models have introduced additional material complexities, namely anisotropy and non-linear elasticity. Lotz et al. (1991; 1991) used isotropic elastic moduli for cancellous bone, but three different transversely-isotropic descriptions for cortical bone. Gomez-Benito et al. (2005) created anisotropic material properties by applying a bone remodeling analysis to a femoral model. While most models use a linear elastic material model, using a non-linear material description to include yielding in the simulation improves the prediction of fracture load (Keyak 2001; Lotz et al. 1991). Bessho (2007) and Lotz et al. (1991) used bi-linear elasticity models, with a reduced modulus behavior following yield. Keyak (2001) and Keyak and Falkinstein (2003) used multi-linear models featuring post-yield behavior with a perfectly plastic region, strain softening and a second perfectly plastic region (Figure 4.4).

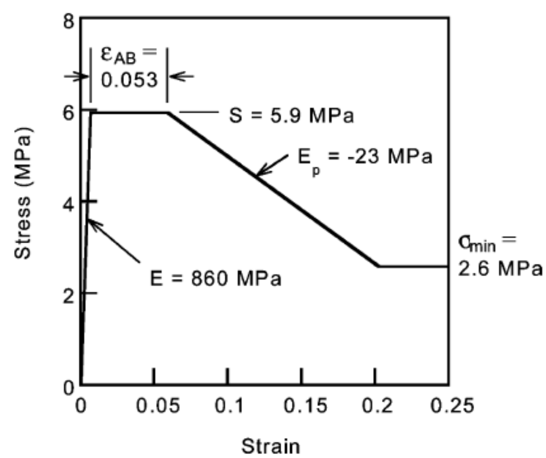

Figure 4.4: Non-linear material model of bone used by Keyak and Falkinstein. (Reprinted from Medical Engineering & Physics, 25, Keyak, J. H., and Falkinstein, Y., Comparison of in situ and in vitro CT scan-based finite element model predictions of proximal femoral fracture load, Page 783, Copyright 2003, with permission from Elsevier).

In finite element models of whole bone, cancellous bone is typically modeled as an isotropic continuum material rather than as a structure of individual trabeculae. While the trabecular architecture has definite effects on material properties (Goldstein 1987), creating a finite element model including actual trabeculae presents difficulties. Defining the geometry of the trabeculae, although possible, requires a high-resolution CT scan (Augat et al. 1998). Additionally, modeling individual trabeculae on a whole-bone scale would result in very large models, limiting the utility of such an approach. Cancellous bone also exhibits anisotropic behavior, largely due to directional differences in the trabecular structure. For example, cancellous samples from the proximal and distal femur were found to have greater stiffness in the superior- inferior direction than anterior-posterior or medial-lateral (Augat et al. 1998).

Cortical bone may or may not be modeled as distinct from cancellous bone. In some models, no real distinction is made, with variations in calculated modulus accounting for differences in bone (Cody et al. 1999; Keyak et al. 1990; Ota et al. 1999; Spruijt et al. 2006). However, with this approach the effect of cortical bone may be reduced in calculating element material properties, as the elements containing cortical bone may also contain a significant proportion of cancellous bone. Thus, some models (Bessho et al. 2007; Lotz et al. 1991, 1991, 1995) create elements specifically to represent the cortical shell. Lotz et al. (1991; 1991) used 20-node isoparametric solid elements with a minimum thickness of 1 mm, and applied a reduced modulus to elements where the shell thickness was less than 1 mm. Bessho (2007) modeled the cortex using triangular shell elements of 0.4 mm thickness added to the surface of a mesh of linear tetrahedral elements.

Loading applied to femur models

The loads and boundary conditions used in finite element models of the femur have varied widely, but are generally stated to approximate stance or gait loading or fall impact loading. Simple representations of stance or gait loads have been modeled by applying a single load to the femoral head (Bessho et al. 2007; Cody et al. 1999; Duchemin et al. 2008; Keyak 2001; Keyak and Falkinstein 2003; Keyak et al. 2001; Keyak et al. 1998; Lotz et al. 1991, 1991; Ota et al. 1999; Schileo et al. 2007; Taddei, Cristofolini et al. 2006). Other studies have modeled stance using a load on the femoral head plus an abductor load applied at the greater trochanter

(Gomez-Benito et al. 2005; Merz et al. 1996; Schmitt et al. 2001). Fall loading has been modeled with loads applied to the greater trochanter (Keyak et al. 2001; Keyak et al. 1998; Lotz et al. 1991, 1991, 1995; Testi et al. 2002). Such simplified loading conditions are often used to replicate *in vitro* mechanical testing (Bessho et al. 2007; Cody et al. 1999; Gomez-Benito et al. 2005; Keyak 2001; Keyak and Falkinstein 2003; Keyak et al. 2001; Keyak et al. 1998; Lotz et al. 1991, 1991; Ota et al. 1999; Schileo et al. 2007; Taddei, Cristofolini et al. 2006), which is important as it allows validation of the finite element models. However the loads applied to the femur *in vivo* are considerable more complex due to the many muscle attachments on the femur.

Several studies have used more realistic loading conditions when modeling stance or gait conditions by including multiple muscle forces (Bitsakos et al. 2005; Duda et al. 1998; Lotz et al. 1995; Polgar et al. 2003; Taylor et al. 1996). Polgar et al. (2003) used a model with extensive muscle attachment areas defined and tested nine different loading conditions including various numbers of muscles. More realistic muscular loading decreases strain magnitudes in the femoral shaft (Duda et al. 1998; Polgar et al. 2003) and act to keep the bone in compression rather than bending (Taylor et al. 1996). Rudman et al. (2006) also note that including tension in the hip joint capsular ligaments helps keep the femoral neck in compression. Localized muscle forces are also important in stimulating the remodeling of bone (Bitsakos et al. 2005). Thus, muscle loading has an important effect on bone *in vivo,* and models representing *in vivo* activity should include as many muscles as possible.

Summary of finite element modeling of the femur

In summary, finite element models of the femur can be used to provide reasonable estimates of stresses and strains in the femur. However the accuracy of these estimates depends on careful model development and sufficient model complexity. In particular:

- Models should accurately represent femoral geometry, as geometry errors have a significant effect on model results (Taddei, Martelli et al. 2006).
- Non-homogeneous material properties should be included, as they effect the model results (Merz et al. 1996).
- When modeling *in vivo* loading conditions, all muscle forces on the femur should be included in the analysis (Duda et al. 1998; Polgar et al. 2003).

References

Augat, P., Link, T., Lang, T. F., Lin, J. C., Majumdar, S., and Genant, H. K., 1998. Anisotropy of the elastic modulus of trabecular bone specimens from different anatomical locations. Medical Engineering & Physics 20, 124-131.

Bessho, M., Ohnishi, I., Matsuyama, J., Matsumoto, T., Imai, K., and Nakamura, K., 2007. Prediction of strength and strain of the proximal femur by a CT-based finite element method. Journal of Biomechanics 40, 1745-1753.

Bitsakos, C., Kerner, J., Fisher, I., and Amis, A. A., 2005. The effect of muscle loading on the simulation of bone remodelling in the proximal femur. Journal of Biomechanics 38, 133-139.

Brekelmans, W. A., Poort, H. W., and Slooff, T. J., 1972. A new method to analyse the mechanical behaviour of skeletal parts. Acta Orthopaedica Scandinavica 43, 301-317.

Carter, D. R., and Hayes, W. C., 1977. The compressive behavior of bone as a two-phase porous structure. The Journal of Bone & Joint Surgery (American Volume) 59, 954-962.

Cattaneo, P. M., Dalstra, M., and Frich, L. H., 2001. A three-dimensional finite element model from computed tomography data: a semi-automated method. Proceedings of the

Institution of Mechanical Engineers. Part H, Journal of Engineering in Medicine 215, 203-213.

Ciarelli, M. J., Goldstein, S. A., Kuhn, J. L., Cody, D. D., and Brown, M. B., 1991. Evaluation of orthogonal mechanical properties and density of human trabecular bone from the major metaphyseal regions with materials testing and computed tomography. Journal of Orthoaedic Research 9, 674-682.

Cody, D. D., Gross, G. J., Hou, F. J., Spencer, H. J., Goldstein, S. A., and Fyhrie, D. P., 1999. Femoral strength is better predicted by finite element models than QCT and DXA. Journal of Biomechanics 32, 1013-1020.

Cooper, C., Campion, G., and Melton, L. J., 3rd, 1992. Hip fractures in the elderly: a world-wide projection. Osteoporosis International 2, 285-289.

Duchemin, L., Mitton, D., Jolivet, E., Bousson, V., Laredo, J. D., and Skalli, W., 2008. An anatomical subject-specific FE-model for hip fracture load prediction. Computer Methods in Biomechanics and Biomedical Engineering 11, 105-111.

Duda, G. N., Heller, M., Albinger, J., Schulz, O., Schneider, E., and Claes, L., 1998. Influence of muscle forces on femoral strain distribution. Journal of Biomechanics 31, 841-846.

Goldstein, S. A., 1987. The mechanical properties of trabecular bone: dependence on anatomic location and function. Journal of Biomechanics 20, 1055-1061.

Gomez-Benito, M. J., Garcia-Aznar, J. M., and Doblare, M., 2005. Finite element prediction of proximal femoral fracture patterns under different loads. Journal of biomechanical engineering 127, 9-14.

Gray, H. 1918. Anatomy of the Human Body, 20th Edition. Place Published: Philadelphia: Lea & Febiger. www.bartleby.com/107/ (accessed 2008).

Keyak, J. H., 2001. Improved prediction of proximal femoral fracture load using nonlinear finite element models. Medical Engineering & Physics 23, 165-173.

Keyak, J. H., and Falkinstein, Y., 2003. Comparison of in situ and in vitro CT scan-based finite element model predictions of proximal femoral fracture load. Medical Engineering & Physics 25, 781-787.

Keyak, J. H., Meagher, J. M., Skinner, H. B., and Mote, C. D., Jr., 1990. Automated three-dimensional finite element modelling of bone: a new method. Journal of Biomedical Engineering 12, 389-397.

Keyak, J. H., Rossi, S. A., Jones, K. A., Les, C. M., and Skinner, H. B., 2001. Prediction of fracture location in the proximal femur using finite element models. Medical Engineering & Physics 23, 657-664.

Keyak, J. H., Rossi, S. A., Jones, K. A., and Skinner, H. B., 1998. Prediction of femoral fracture load using automated finite element modeling. Journal of Biomechanics 31, 125-133.

Lotz, J. C., Cheal, E. J., and Hayes, W. C., 1991. Fracture prediction for the proximal femur using finite element models: Part I--Linear analysis. Journal of biomechanical engineering 113, 353-360.

Lotz, J. C., Cheal, E. J., and Hayes, W. C., 1991. Fracture prediction for the proximal femur using finite element models: Part II--Nonlinear analysis. Journal of biomechanical engineering 113, 361-365.

Lotz, J. C., Cheal, E. J., and Hayes, W. C., 1995. Stress distributions within the proximal femur during gait and falls: implications for osteoporotic fracture. Osteoporosis International 5, 252-261.

Magaziner, J., Hawkes, W., Hebel, J. R., Zimmerman, S. I., Fox, K. M., Dolan, M., Felsenthal, G., and Kenzora, J., 2000. Recovery from hip fracture in eight areas of function. The Journals of Gerontology. Series A, Biological Sciences and Medical Sciences 55, M498-507.

Marom, S. A., and Linden, M. J., 1990. Computer aided stress analysis of long bones utilizing computed tomography. Journal of Biomechanics 23, 399-404.

Martin, R. B., 1991. Determinants of the mechanical properties of bones. Journal of Biomechanics 24 Suppl 1, 79-88.

McBroom, R. J., Hayes, W. C., Edwards, W. T., Goldberg, R. P., and White, A. A., 3rd, 1985. Prediction of vertebral body compressive fracture using quantitative computed tomography. The Journal of Bone & Joint Surgery (American Volume) 67, 1206-1214.

Merz, B., Niederer, P., Muller, R., and Ruegsegger, P., 1996. Automated finite element analysis of excised human femora based on precision -QCT. Journal of biomechanical engineering 118, 387-390.

NIH, 2001. Osteoporosis prevention, diagnosis, and therapy. JAMA 285, 785-795.

Ota, T., Yamamoto, I., and Morita, R., 1999. Fracture simulation of the femoral bone using the finite-element method: how a fracture initiates and proceeds. Journal of Bone and Mineral Metabolism 17, 108-112.

Polgar, K., Gill, H. S., Viceconti, M., Murray, D. W., and O'Connor, J. J., 2003. Strain distribution within the human femur due to physiological and simplified loading: finite element analysis using the muscle standardized femur model. Proceedings of the Institution of Mechanical Engineers. Part H, Journal of Engineering in Medicine 217, 173-189.

Rudman, K. E., Aspden, R. M., and Meakin, J. R., 2006. Compression or tension? The stress distribution in the proximal femur. BioMedical Engineering Online 5, 12.

Rybicki, E. F., Simonen, F. A., and Weis, E. B., Jr., 1972. On the mathematical analysis of stress in the human femur. Journal of Biomechanics 5, 203-215.

Schileo, E., Taddei, F., Malandrino, A., Cristofolini, L., and Viceconti, M., 2007. Subject-specific finite element models can accurately predict strain levels in long bones. Journal of Biomechanics 40, 2982-2989.

Schmitt, J., Meiforth, J., and Lengsfeld, M., 2001. Development of a hybrid finite element model for individual simulation of intertrochanteric osteotomies. Medical Engineering & Physics 23, 529-539.

Spruijt, S., van der Linden, J. C., Dijkstra, P. D., Wiggers, T., Oudkerk, M., Snijders, C. J., van Keulen, F., Verhaar, J. A., Weinans, H., and Swierstra, B. A., 2006. Prediction of torsional failure in 22 cadaver femora with and without simulated subtrochanteric metastatic defects: a CT scan-based finite element analysis. Acta Orthopaedica 77, 474-481.

Taddei, F., Cristofolini, L., Martelli, S., Gill, H. S., and Viceconti, M., 2006. Subject-specific finite element models of long bones: An in vitro evaluation of the overall accuracy. Journal of Biomechanics 39, 2457-2467.

Taddei, F., Martelli, S., Reggiani, B., Cristofolini, L., and Viceconti, M., 2006. Finite-element modeling of bones from CT data: sensitivity to geometry and material uncertainties. IEEE Transactions on Biomedical Engineering 53, 2194-2200.

Taddei, F., Pancanti, A., and Viceconti, M., 2004. An improved method for the automatic mapping of computed tomography numbers onto finite element models. Medical Engineering & Physics 26, 61-69.

Taylor, M. E., Tanner, K. E., Freeman, M. A., and Yettram, A. L., 1996. Stress and strain distribution within the intact femur: compression or bending? Medical Engineering & Physics 18, 122-131.

Testi, D., Viceconti, M., Cappello, A., and Gnudi, S., 2002. Prediction of hip fracture can be significantly improved by a single biomedical indicator. Annals of Biomedical Engineering 30, 801-807.

Valliappan, S., Svensson, N. L., and Wood, R. D., 1977. Three dimensional stress analysis of the human femur. Computers in Biology and Medicine 7, 253-264.

Villarraga, M. L., and Ford, C. M. 2001. Applications of Bone Mechanics. In: Cowin, S. C. (Ed.), Bone Mechanics Handbook, Second Edition. CRC Press, Boca Raton, pp.

Zannoni, C., Mantovani, R., and Viceconti, M., 1998. Material properties assignment to finite element models of bone structures: a new method. Medical Engineering & Physics 20, 735-740.

Chapter 5 – The effect of age differences in femoral loading during controlled walking on strains in the proximal femur

Abstract

Dynamic loading *in vivo* plays a role in the health and strength of the skeletal structure, as it can stimulate remodeling (which can strengthen or weaken bone) or lead to mechanical fatigue. Older adults are known to exhibit differences in gait kinetics as compared to young adults. This may indicate age differences in dynamic loading that could affect the strains in the proximal femur, and thus bone strength and risk of hip fracture. This study examined age differences in strains in the proximal femur. Femoral loading was estimated during walking for younger and older adults using static optimization. The loads were applied to finite element models of the femur, and strains in the femoral neck and sub-trochanteric region examined. Minor age differences in strain were found, particularly reduced peak strain in the posterior femoral neck in older adults in late stance, although strain magnitudes were relatively low at this location. No age differences were found for the largest magnitude shear or tensile strains. Interestingly, while peak hip joint contact forces were 18% lower in older adults, there was not a corresponding reduction the largest magnitude strains. It cannot be concluded that older adults are generally at greater risk of hip fracture due to age differences in loading conditions. However, it remains possible that some individuals apply loading conditions that increase the risk of hip fracture over time.

Keywords: aging, static optimization, finite element modeling, hip fractures

Introduction

Hip fractures are serious injuries that are associated with high rates of morbidity and mortality in older adults. The incidence of hip fractures increases dramatically with age (Melton 1996; Schwartz et al. 1999; Sugarman et al. 2002), more than doubling for each decade after age 65. Because of its correlation with bone strength, bone mineral density (BMD) is useful as a predictor of hip fracture risk (NIH 2001). However, because the BMD of fracture patients overlaps that of age-matched individuals without hip fracture (Marks et al., 2003, WHO, 1994), understanding additional factors that may contribute to hip fractures would be useful in risk evaluation and prevention. One such factor is the loading experienced by the femur over extended period of time. This can stimulate remodeling and adaption of the bone as well as play a role in the development of mechanical fatigue.

The dynamic loading experienced by bone stimulates remodeling and adaptation, and can lead to the increase, maintenance, or loss of bone mass (Turner 1998). As such, loading is important in maintaining bone health. For example, regular axial compressive loading *in vivo* over a period of weeks was found to dramatically increase the resistance of rat ulnas to mechanical fatigue, which has implications for the prevention of stress fractures (Warden et al. 2005). Muscle forces are an important component in the loading of bone, and as such can have beneficial effects on bone strength. Femoral neck BMD is weakly but significantly correlated with hip abductor and flexor strength in postmenopausal women (Bayramoglu et al. 2005; Zimmermann et al. 1990). Additionally, resistance strength training is associated with high BMD in both younger and older adults, and is relatively site-specific in its effect (Layne and Nelson 1999).

In addition to stimulating bone remodeling, muscle forces may also have a direct protective effect on bone. For example, muscular contraction significantly increases the load and energy required to fracture the tibia in rats (Nordsletten and Ekeland 1993). There is also evidence that muscle forces can protect bone from damage by reducing shear and bending loads in the femur (Duda et al. 1998; Polgar et al. 2003; Taylor et al. 1996). Bone is weaker in shear and tension than in compression (Reilly and Burstein 1975; Turner et al. 2001), and shear plays an important role in the fatiguing of bone (Taylor et al. 2003; Turner et al. 2001). Furthermore, the fatigue life of cortical bone is significantly reduced under combined axial and torsional loading (George and Vashishth 2006). Related to this, changes in muscle forces due to neuromuscular fatigue may increase bone stresses during athletic activities (Benazzo et al. 1992; Clement 1974). Neuromuscular fatigue of the quadriceps has been shown to increase measured tibial shear strains during walking in dogs (Yoshikawa et al. 1994). Thus, changes in normal muscle loading could mitigate the prophylactic effect of muscles on bone, leading to greater shear and tensile loads that increase the risks of mechanical fatigue damage.

Aging may cause changes in muscle forces during gait, as older adults are known to exhibit differences in gait kinetics as compared to young adults (Anderson 2010; DeVita and Hortobagyi 2000; Judge et al. 1996; Kerrigan et al. 1998; Silder et al. 2008). The effect of these differences on femoral loading is not known, but could be significant for the maintenance of skeletal health and prevention of hip fractures. Changes in tensile or shear strains in the proximal femur due to changes in muscle forces with aging could contribute to a decrease in fatigue life and increased risk of hip fracture.

The purpose of this study was to examine the effect of age differences in femoral loading during gait on strains in the proximal femur. As gait represents a routinely performed activity, loading during gait can be expected to occur repeatedly over an extended period of time. Muscle forces during walking were estimated by static optimization in older and younger individuals. Relevant muscle forces were applied to finite element models of the femur, and strains in the proximal femur were investigated throughout the entire gait cycle. Specifically, maximum principal and maximum shear strains in the femoral neck and sub-trochanteric region were investigated. It was hypothesized that older adults would exhibit greater strains during gait than young adults as a result of age differences in femoral loading.

Methods

Ten participants, including five older (mean±standard deviation (SD) age 79.4±4.6 years) and five young (25.0±4.3 years), were selected for this study from the participants in a previous study investigating age differences in joint torques during gait (Anderson 2010). These individuals were representative of the gait patterns seen in older and young adults, respectively. The age groups were similar in that each contained two males and three females, and there were no statistically significant differences in height or mass between groups. The project was approved by the Virginia Tech Institutional Review Board, and the participants provided written informed consent prior to participation. Each participant took part in gait testing, strength testing and a dual energy x-ray absorptiometry (DXA) scan.

Gait testing consisted of participants walking down an 8 m walkway at a controlled speed of 1.1 m/s and step length of 0.65 m. Gait was controlled in order to avoid differences in femur loading due to age differences in self-selected gait. Ground reaction force (GRF) and body position data were collected over one full gait cycle of the right lower extremity. GRF data was sampled at 1000 Hz from a six degree-of-freedom force platform (Advanced Mechanical Technology Inc., Watertown, MA) placed in the center of the walkway. Thirty-six reflective markers were placed on each participant, and marker position data was sampled at 100 Hz using a six-camera VICON 460 motion analysis system (VICON Motion Systems Inc., Lake Forest, CA).

For determination of muscle forces, a musculoskeletal model of the right lower limb (Figure 5.1) was developed for each participant. These models were created in OpenSim, an open-source software system for musculoskeletal modeling (Delp et al. 2007), and based on a model of the legs and torso developed by Delp et al. (1990). Each model consisted of the pelvis, thigh, shank and foot segments connected by hip, knee and ankle joints. Segment sizes were based on anthropometry measurements and the distance between joint centers, which was calculated by functional methods (Piazza et al. 2004). Segment masses, center of mass positions, and mass moments of inertia were estimated from anthropometric data (de Leva 1996; Pavol et al. 2002). All joints were modeled as three-degree-of-freedom ball joints, but the knee and ankle were constrained to a single axis of rotation when calculating muscle forces. Thirty-five muscles were modeled as Hill-type musculotendon actuators, detailed in Delp et al. (1990).

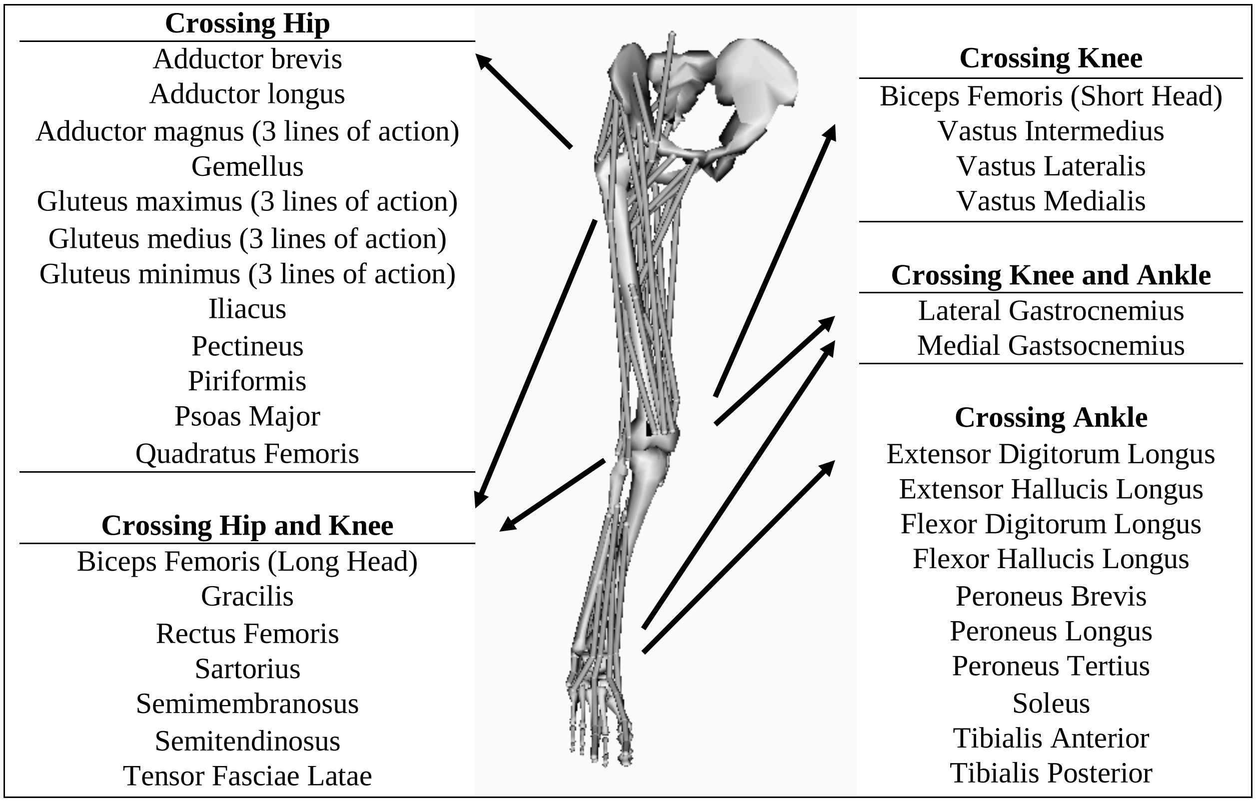

Figure 5.1: Musculoskeletal model used to estimate muscle forces during gait. The model included 35 muscles crossing the hip, knee and ankle joints as shown.

To individualize the muscle models for each participant, peak isometric forces for muscles in the model were adjusted based on torque data collected using a Biodex System 3 dynamometer. Strengths of the muscles in the model were initially based on physiological cross-sectional area information taken from the literature (Brand et al. 1986; Klein Horsman et al. 2007). Participants performed isometric maximum voluntary exertions for ankle plantar flexion and dorsiflexion, knee flexion and extension, and hip flexion, extension, abduction and adduction at joint angles approximately matching the angle of maximum isometric joint torque (Anderson et al. 2007). Corresponding maximum torques were determined from the model, compared to experimental data, and the peak isometric muscle forces were adjusted using an iterative process. The process allowed for sufficient strength in the model such that the muscles could stabilize the hip joint while producing maximum torque about a particular axis.

Muscle forces during gait were estimated using a static optimization approach. The cost function used was minimizing the sum of muscle activation squared, $\sum_{m=1}^{M} a_m{}^2$. As muscle activation is proportional to muscle stress, this is equivalent to the sum of muscle stress squared. Using muscle stress squared provides a reasonably good correlation between calculated muscle forces and EMG measurements (Glitsch and Baumann 1997; Heintz and Gutierrez-Farewik 2007).

A finite element model of the femur (Figure 5.2) was obtained from the public dataset of the VAKHUM project (Van Sint Jan 2008) and scaled to match the femur size of each participant. The VAKHUM model was created from a high resolution segmentation of a computed tomography (CT) scan and had material properties based on the CT image, providing an approximation of material non-homogeneity in the femur. The model consisted of 17696 linear hexahedral elements, and had 217 isotropic materials with Young's modulus ranging from 0.66 to 27.07 GPa. A Poisson's ratio of 0.3 was used for all materials. The model was geometrically scaled based on each participant's thigh length (hip to knee joint distance) and femoral neck axis length. A non-homogeneous scaling approach based on that described by Lewis et al (1980) was used. Femoral neck axis length was determined from a DXA scan of the hip performed using a GE Lunar Prodigy scanner (GE Healthcare, Chalfont St. Giles, UK).

Loading and boundary conditions applied to the model consisted of hip joint contact forces, forces from muscles attaching directly to the femur, and fixed boundary conditions at the distal end of the femur. Hip contact forces were applied via a hemispherical representation of the acetabulum, distributing the forces across the surface of the head of the femur. Forces for sixteen muscles muscles attaching directly to the femur were included: gluteus maximus, gluteus medius, gluteus minimus, pectineus, adductor magnus, adductor longus, adductor brevis, gemellus, quadratus femoris, iliopsoas (sum of iliacus and psoas major), piriformis, biceps femoris short head, vastus lateralis, vastus intermedius and vastus medialis. Muscle forces were distributed across the eight nodes determined to be geometrically closest to the muscle attachment point in the musculoskeletal model. The resulting locations were qualitatively compared to muscle attachment data in the literature (Duda et al. 1996; Viceconti et al. 2003) and found to be reasonable. Additionally, a force for the illiotibial tract was added, which is often included in models of the femur (Birnbaum et al. 2004; Duda et al. 1998; Taylor et al. 1996). It had a peak magnitude of 1500 N (Birnbaum et al. 2004), time variation during gait based on that of the tensor fasciae latae muscle, and was applied at the same location as the second gluteus maximus line of action. Loading was applied in a quasi-

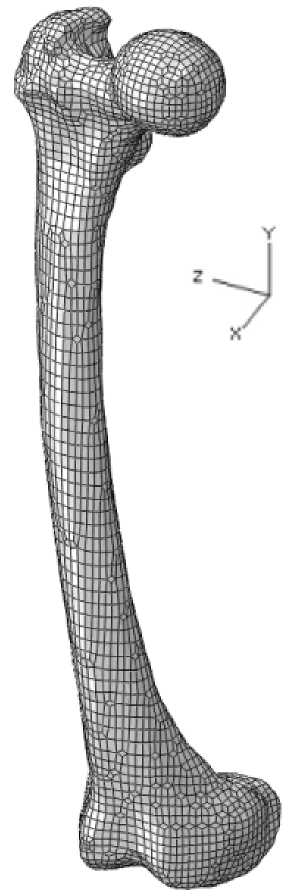

Figure 5.2: Finite element model of the femur from the VAKHUM project used in this study. In femoral coordinates, the X axis points anteriorly, Y superiorly, and Z laterally.

static manner at 1% increments of the gait cycle, and the model was solved using Abaqus (Dassault Systèmes Simulia Corp., Providence, RI, USA).

Maximum principal and maximum shear strains were examined in the proximal femur (Figure 5.3) at four locations around the femoral neck (superior, anterior, inferior and posterior) and four around a subtrochanteric cross-section (lateral, anterior, medial and posterior). These points were selected to 1) provide for a reasonable number of locations in the proximal femur that may experience differences in strain, and 2) to be sufficiently removed from the applied loads such that the results would not be directly affected them. Peak strains results and hip joint contact forces were compared between age groups using independent t-tests with significance set at $\alpha=0.05$.

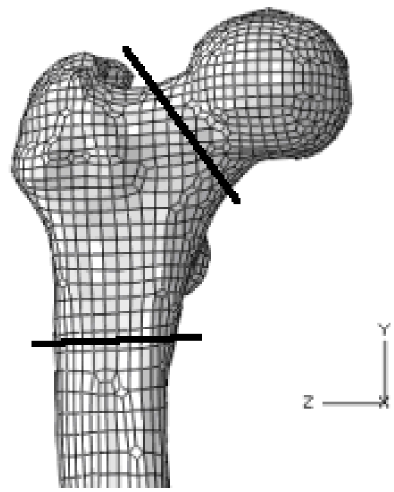

Figure 5.3: Anterior view of the proximal portion of the femur model, with heavy lines indicating sections in femoral neck and sub-trochanteric region where strains were examined.

Results

Maximum principal and maximum shear strains examined in the femoral neck were largely similar between age groups (Figure 5.4). The largest maximum principal strains occurred in the superior part of the neck in late stance, and the largest maximum shear strains occurred in the inferior part of the neck in late stance. Peak strain values at all locations in early and late stance are presented in Table 5.1. No age differences were found at any location for peak strains in early stance. The only age differences in late stance occurred at the posterior location, where peak maximum principal strain and peak maximum shear strain were greater in younger adults than older adults (p =0.037 and p=0.031, respectively).

Table 5.1: Mean (SD) values of peak strains (με) in the femoral neck during early stance and late stance.

Location	Strain	Early Stance		Late Stance	
		Older	Younger	Older	Younger
Superior	Max Principal	1738 (446)	1571 (229)	2414 (784)	2624 (340)
	Max Shear	1145 (290)	1032 (153)	1594 (518)	1728 (225)
Anterior	Max Principal	428 (189)	403 (174)	308 (110)	470 (184)
	Max Shear	426 (116)	380 (114)	385 (104)	462 (113)
Inferior	Max Principal	812 (157)	742 (116)	1057 (300)	1140 (112)
	Max Shear	1720 (330)	1573 (243)	2224 (629)	2404 (233)
Posterior	Max Principal	525 (197)	501 (150)	414 (94)	621 (154)
	Max Shear	972 (374)	934 (293)	758 (189)	1184 (297)

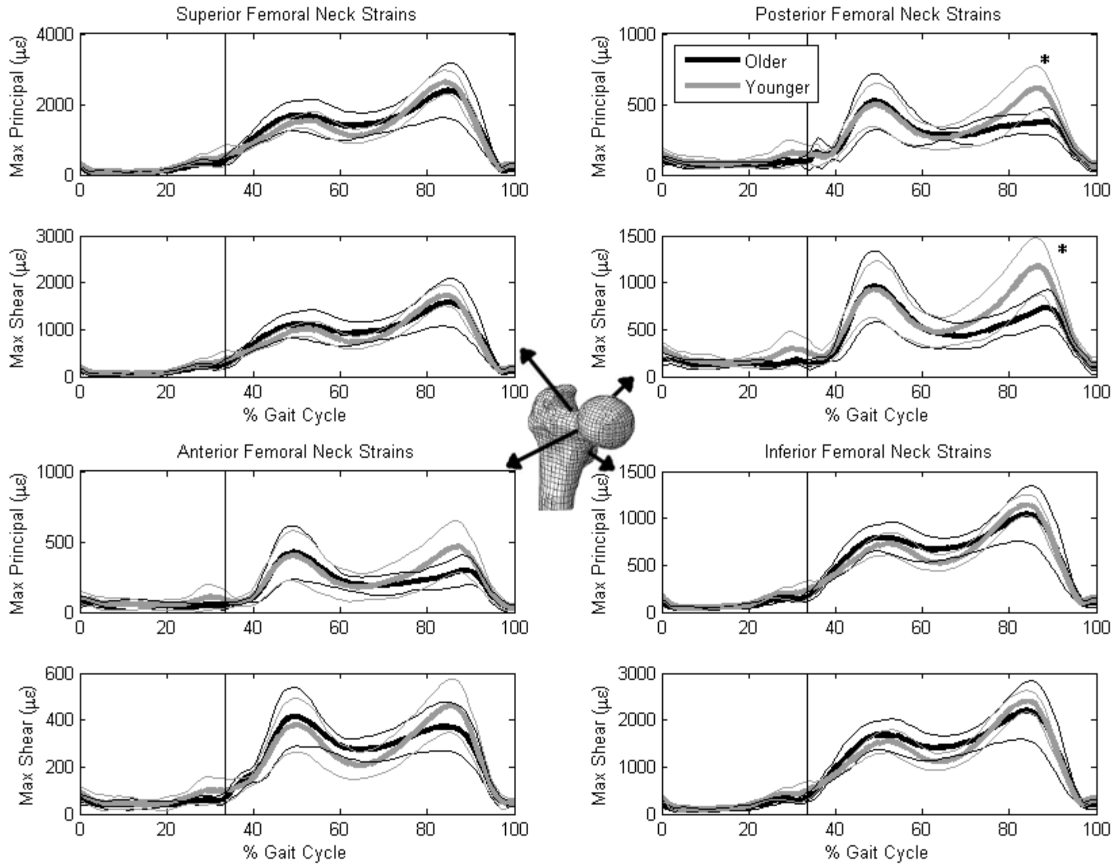

Figure 5.4: Maximum principal and maximum shear strains in the femoral neck during a full gait cycle. Thick lines indicate mean values, and the thin lines indicate ±1 SD. The vertical lines denote the beginning of stance phase. Note that strain scales are not identical. *Significant age difference in peak strain.

Maximum principal and maximum shear strains examined in the subtrochanteric region were also similar between age groups (Figure 5.5). The largest maximum principal strains occurred in the lateral location, and the largest maximum shear strains occurred in the medial location. No age differences in peak strains were found. Peak strain values at all locations in early and late stance are presented in Table 5.2. An age difference in strain, albeit not in peak strain, was seen in the posterior location occurring in mid-stance. This difference was significant in a post-hoc examination at 65% of the gait cycle, with both maximum principal ($p=0.002$) and maximum shear strains ($p=0.040$) greater in older adults.

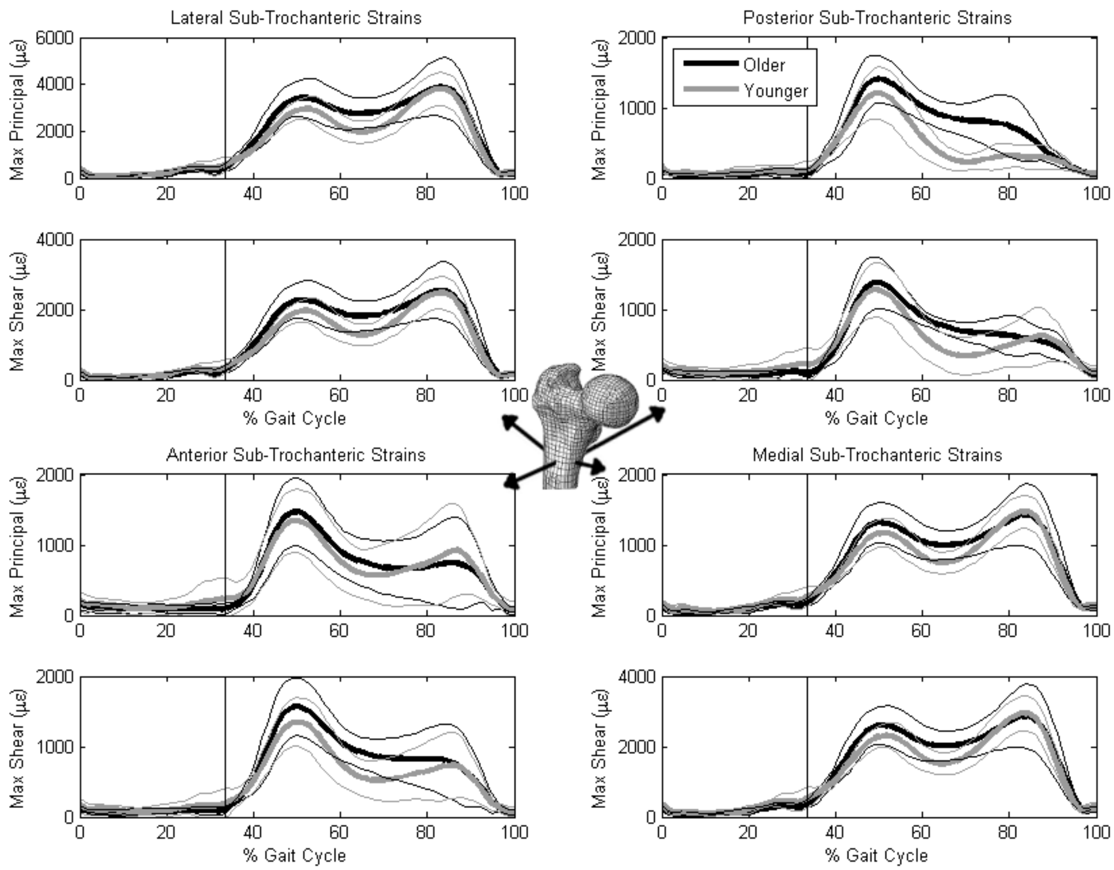

Figure 5.5: Maximum principal and maximum shear strains in sub-trochanteric locations during a full gait cycle. Thick lines indicate mean values, and the thin lines indicate ±1 SD. The vertical lines denote the beginning of stance phase. Note that strain scales are not identical.

Table 5.2: Mean (SD) values of peak strains (με) in the sub-trochanteric region during early stance and late stance. N/A indicates no peak in strain was present.

Location	Strain	Early Stance		Late Stance	
		Older	Younger	Older	Younger
Lateral	Max Principal	3485 (817)	3005 (489)	3970 (1221)	3804 (712)
	Max Shear	2312 (543)	1994 (331)	2592 (797)	2477 (464)
Anterior	Max Principal	1486 (483)	1354 (442)	803 (590)	942 (655)
	Max Shear	1586 (424)	1364 (341)	N/A	749 (461)
Medial	Max Principal	1342 (297)	1189 (210)	1453 (437)	1473 (239)
	Max Shear	2650 (564)	2353 (348)	2926 (890)	2947 (485)
Posterior	Max Principal	1433 (350)	1219 (368)	N/A	399 (175)
	Max Shear	1391 (380)	1287 (382)	N/A	704 (345)

Hip joint contact force (Figure 5.6) was the largest force applied to the femur model during gait, and thus was of particular interest in this study. Peak hip force magnitude was 18% lower in older adults, (435±51 % body weight (BW) in older adults, 529±39 %BW in young adults, p=0.011). This difference occurred in late stance phase, at which time both downward and posteriorly directed hip forces were significantly lower in older adults than young adults (p = 0.047 and 0.014, respectively).

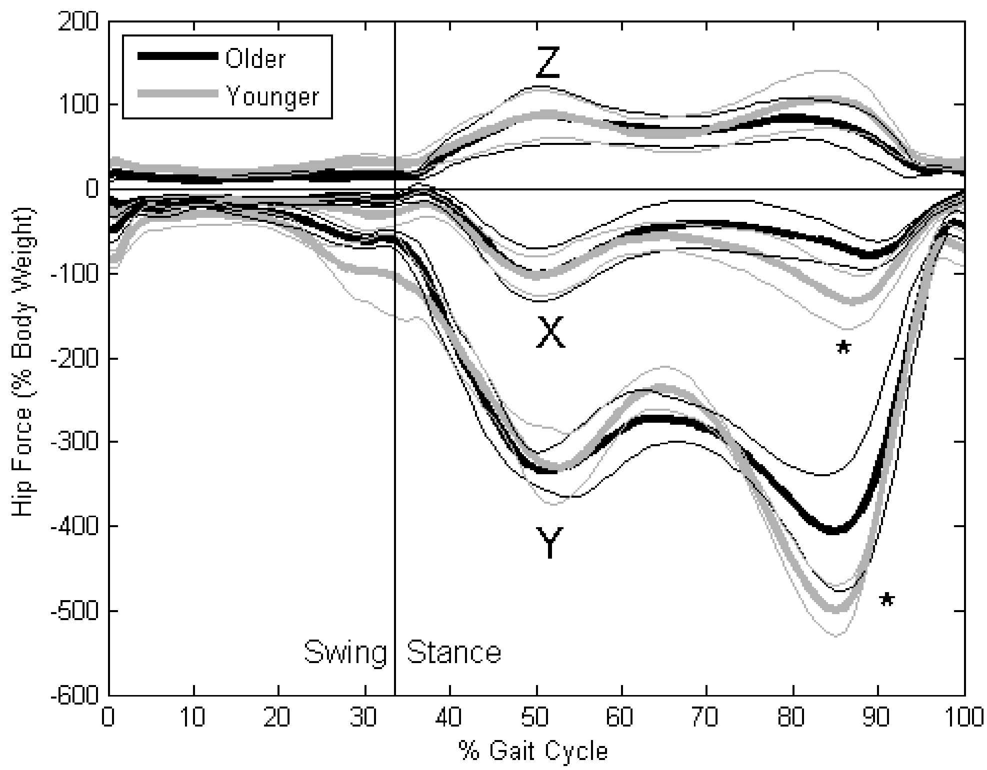

Figure 5.6: Average hip joint contact forces (%BW) in a femur-fixed coordinate frame during gait for young and older age groups. Thick lines indicate mean values, and the thin lines indicate ±1 SD. The X axis points anteriorly, Y up, and Z laterally. *Significant age difference in peak force.

Discussion

The purpose of this study was to examine age differences in strains in the proximal femur during gait due to age differences in femoral loading. In general, strains exhibited two peaks during the gait cycle, one in early stance phase and one in late stance phase. Not surprisingly, this follows the pattern seen in the hip joint reaction force and the vertical component of the typical ground reaction force. While some minor age differences in strains were found, the results do not support the hypothesis that age differences in loading of the femur lead to increased maximum principal or maximum shear strains in older adults. The largest magnitude strains examined in the femoral neck and sub-trochanteric region did not exhibit age differences. However, it is interesting to note that although peak hip joint contact force was about 18% lower in older adults, older adults did not display a corresponding reduction in the largest magnitude strains. This may indicate that young adults are better able to apply balanced loads to the femur while producing greater muscle forces during push-off in late stance.

The forces applied to the model in this study were determined using static optimization. While static optimization has been used to determine muscle forces during many different tasks, there has been little successful validation of the technique (Erdemir et al. 2007). Static optimization predicts the joint reaction forces measured by instrumented hip implants reasonably well, although it tends to overestimate peak hip contact forces during gait by an average of 12% (Heller et al. 2001). Static optimization muscle force predictions also correlate well with EMG-force predictions (Heintz and Gutierrez-Farewik 2007). This indicates that despite its limitations, static optimization can produce reasonable values for muscle forces during gait.

The hip joint contact forces found during gait were comparable in profile and magnitude to similarly determined forces in the literature (e.g. Brand et al. 1986; Duda et al. 1997). However, the magnitude of the peak hip joint contact forces was about twice that reported from patients with instrumented hip replacements (Bergmann et al. 2001). A small portion of this discrepancy may arise from over-predictions in force due to static optimization (Heller et al.

2001). In addition, direct comparisons between gait in healthy individuals and hip replacement patients should be approached with caution. For the purposes of this study, the estimated hip contact forces were determined in the same manner for all participants, and comparisons between them should be valid.

This study approximated the femur *in vivo* during gait, and was subject to a variety of modeling errors. Errors in the estimation of muscle forces would propagate into the finite element results. Simplifications were made in defining the application points of the muscle forces, and only muscles directly attaching to the femur were used. The effect of muscles crossing both the knee and hip was only included by their effect on the hip joint contact force, though in reality they could apply forces to the femur more directly through wrapping. In future studies, loads due to the ligaments of the hip joint capsule could be added. In a two-dimensional model, inclusion of capsular ligaments has been shown to change the stress in the femoral neck from tensile to compressive (Rudman et al. 2006). However, despite these simplifications, this study includes all major muscle loads on the femur, and to our knowledge provides the first examination of age differences in femoral strains.

Because the purpose of this study was to examine the effects of loading, the material properties assigned to all models were the same to reduce the effect of material properties on the results. Thus, the individual models did not represent the actual femoral material properties of the participants, and as such did not account for possible age differences in material properties. Future studies may investigate age differences in femoral strains while including both age-appropriate loading and material properties.

The data used to estimate muscle forces were collected under controlled gait conditions, with young and older adults walking at the same speed and step length. Controlled conditions were chosen because age differences in speed and step length could have confounded differences in femoral loading due to age. Older adults tend to walk with reduced speed (Judge et al. 1996; Kerrigan et al. 1998; Laufer 2005; Waters et al. 1983) and step length (Anderson 2010; Judge et al. 1996; Kerrigan et al. 1998; Laufer 2005; Winter et al. 1990) compared to young adults in self-selected conditions. It could be reasonably argued that age differences in femoral loading during self-selected gait would more realistically depict the loading regularly applied to the femur, despite or even because of differences in speed and/or step length. Thus, future work similar to this may investigate age differences in femoral strains during self-selected gait.

In conclusion, because the largest magnitude strains were not different between age groups, it cannot be stated that older adults are generally at greater risk for mechanical fatigue or loss of bone through remodeling due to age differences in loading conditions. Thus, it does not appear that age differences in femoral loading affects the risk of hip fracture. However, all participants were healthy, and their actual risk of hip fracture was unknown. The older group had larger standard deviations for a majority of the strains examined, which suggests greater loading variability in older adults. Thus, it remains possible that some older individuals apply different loading conditions that increase the risk of hip fracture over time.

Acknowledgement

This work was supported by Award Number F31AG030904 from the National Institute on Aging. The content is solely the responsibility of the author and does not necessarily represent the official views of the National Institute on Aging or the National Institutes of Health.

References

Anderson, D. E., 2010. Age differences in lower extremity joint torques during walking with controlled speed and step length. (Study 1).

Anderson, D. E., Madigan, M. L., and Nussbaum, M. A., 2007. Maximum voluntary joint torque as a function of joint angle and angular velocity: model development and application to the lower limb. Journal of Biomechanics 40, 3105-3113.

Bayramoglu, M., Sozay, S., Karatas, M., and Kilinc, S., 2005. Relationships between muscle strength and bone mineral density of three body regions in sedentary postmenopausal women. Rheumatology International 25, 513-517.

Benazzo, F., Barnabei, G., Ferrario, A., Castelli, C., and Fishchetto, G., 1992. Stress fractures in track and field athletics. Journal of Sports Traumatology and Related Research 14, 51-65.

Bergmann, G., Deuretzbacher, G., Heller, M., Graichen, F., Rohlmann, A., Strauss, J., and Duda, G. N., 2001. Hip contact forces and gait patterns from routine activities. Journal of Biomechanics 34, 859-871.

Birnbaum, K., Siebert, C. H., Pandorf, T., Schopphoff, E., Prescher, A., and Niethard, F. U., 2004. Anatomical and biomechanical investigations of the iliotibial tract. Surgical and Radiologic Anatomy 26, 433-446.

Brand, R. A., Pedersen, D. R., and Friederich, J. A., 1986. The sensitivity of muscle force predictions to changes in physiologic cross-sectional area. Journal of Biomechanics 19, 589-596.

Clement, D. B., 1974. Tibial stress syndrome in athletes. The Journal of Sports Medicine 2, 81-85.

de Leva, P., 1996. Adjustments to Zatsiorsky-Seluyanov's segment inertia parameters. Journal of Biomechanics 29, 1223-1230.

Delp, S. L., Anderson, F. C., Arnold, A. S., Loan, P., Habib, A., John, C. T., Guendelman, E., and Thelen, D. G., 2007. OpenSim: open-source software to create and analyze dynamic simulations of movement. IEEE Transactions on Biomedical Engineering 54, 1940-1950.

Delp, S. L., Loan, J. P., Hoy, M. G., Zajac, F. E., Topp, E. L., and Rosen, J. M., 1990. An interactive graphics-based model of the lower extremity to study orthopaedic surgical procedures. IEEE Transactions on Biomedical Engineering 37, 757-767.

DeVita, P., and Hortobagyi, T., 2000. Age causes a redistribution of joint torques and powers during gait. Journal of Applied Physiology 88, 1804-1811.

Duda, G. N., Brand, D., Freitag, S., Lierse, W., and Schneider, E., 1996. Variability of femoral muscle attachments. Journal of Biomechanics 29, 1185-1190.

Duda, G. N., Heller, M., Albinger, J., Schulz, O., Schneider, E., and Claes, L., 1998. Influence of muscle forces on femoral strain distribution. Journal of Biomechanics 31, 841-846.

Duda, G. N., Schneider, E., and Chao, E. Y., 1997. Internal forces and moments in the femur during walking. Journal of Biomechanics 30, 933-941.

Erdemir, A., McLean, S., Herzog, W., and van den Bogert, A. J., 2007. Model-based estimation of muscle forces exerted during movements. Clinical Biomechanics 22, 131-154.

George, W. T., and Vashishth, D., 2006. Susceptibility of aging human bone to mixed-mode fracture increases bone fragility. Bone 38, 105-111.

Glitsch, U., and Baumann, W., 1997. The three-dimensional determination of internal loads in the lower extremity. Journal of Biomechanics 30, 1123-1131.

Heintz, S., and Gutierrez-Farewik, E. M., 2007. Static optimization of muscle forces during gait in comparison to EMG-to-force processing approach. Gait & Posture 26, 279-288.

Heller, M. O., Bergmann, G., Deuretzbacher, G., Durselen, L., Pohl, M., Claes, L., Haas, N. P., and Duda, G. N., 2001. Musculo-skeletal loading conditions at the hip during walking and stair climbing. Journal of Biomechanics 34, 883-893.

Judge, J. O., Davis, R. B., 3rd, and Ounpuu, S., 1996. Step length reductions in advanced age: the role of ankle and hip kinetics. The Journals of Gerontology. Series A, Biological Sciences and Medical Sciences 51A, M303-M312.

Kerrigan, D. C., Todd, M. K., Della Croce, U., Lipsitz, L. A., and Collins, J. J., 1998. Biomechanical gait alterations independent of speed in the healthy elderly: evidence for specific limiting impairments. Archives of Physical Medicine and Rehabilitation 79, 317-322.

Klein Horsman, M. D., Koopman, H. F., van der Helm, F. C., Prose, L. P., and Veeger, H. E., 2007. Morphological muscle and joint parameters for musculoskeletal modelling of the lower extremity. Clinical Biomechanics 22, 239-247.

Laufer, Y., 2005. Effect of age on characteristics of forward and backward gait at preferred and accelerated walking speed. The Journals of Gerontology. Series A, Biological Sciences and Medical Sciences 60, 627-632.

Layne, J. E., and Nelson, M. E., 1999. The effects of progressive resistance training on bone density: a review. Medicine and Science in Sports and Exercise 31, 25-30.

Lewis, J. L., Lew, W. D., and Zimmerman, J. R., 1980. A nonhomogeneous anthropometric scaling method based on finite element principles. Journal of Biomechanics 13, 815-824.

Melton, L. J., 3rd, 1996. Epidemiology of hip fractures: implications of the exponential increase with age. Bone 18, 121S-125S.

NIH, 2001. Osteoporosis prevention, diagnosis, and therapy. JAMA 285, 785-795.

Nordsletten, L., and Ekeland, A., 1993. Muscle contraction increases the structural capacity of the lower leg: an in vivo study in the rat. Journal of Orthoaedic Research 11, 299-304.

Pavol, M. J., Owings, T. M., and Grabiner, M. D., 2002. Body segment inertial parameter estimation for the general population of older adults. Journal of Biomechanics 35, 707-712.

Piazza, S. J., Erdemir, A., Okita, N., and Cavanagh, P. R., 2004. Assessment of the functional method of hip joint center location subject to reduced range of hip motion. Journal of Biomechanics 37, 349-356.

Polgar, K., Gill, H. S., Viceconti, M., Murray, D. W., and O'Connor, J. J., 2003. Strain distribution within the human femur due to physiological and simplified loading: finite element analysis using the muscle standardized femur model. Proceedings of the Institution of Mechanical Engineers. Part H, Journal of Engineering in Medicine 217, 173-189.

Reilly, D. T., and Burstein, A. H., 1975. The elastic and ultimate properties of compact bone tissue. Journal of Biomechanics 8, 393-405.

Rudman, K. E., Aspden, R. M., and Meakin, J. R., 2006. Compression or tension? The stress distribution in the proximal femur. BioMedical Engineering Online 5, 12.

Schwartz, A. V., Kelsey, J. L., Maggi, S., Tuttleman, M., Ho, S. C., Jonsson, P. V., Poor, G., Sisson de Castro, J. A., Xu, L., Matkin, C. C., Nelson, L. M., and Heyse, S. P., 1999. International variation in the incidence of hip fractures: cross-national project on osteoporosis for the World Health Organization Program for Research on Aging. Osteoporosis International 9, 242-253.

Silder, A., Heiderscheit, B., and Thelen, D. G., 2008. Active and passive contributions to joint kinetics during walking in older adults. Journal of Biomechanics 41, 1520-1527.

Sugarman, J. R., Connell, F. A., Hansen, A., Helgerson, S. D., Jessup, M. C., and Lee, H., 2002. Hip fracture incidence in nursing home residents and community-dwelling older people, Washington State, 1993-1995. Journal of the American Geriatrics Society 50, 1638-1643.

Taylor, D., O'Reilly, P., Vallet, L., and Lee, T. C., 2003. The fatigue strength of compact bone in torsion. Journal of Biomechanics 36, 1103-1109.

Taylor, M. E., Tanner, K. E., Freeman, M. A., and Yettram, A. L., 1996. Stress and strain distribution within the intact femur: compression or bending? Medical Engineering & Physics 18, 122-131.

Turner, C. H., 1998. Three rules for bone adaptation to mechanical stimuli. Bone 23, 399-407.

Turner, C. H., Wang, T., and Burr, D. B., 2001. Shear strength and fatigue properties of human cortical bone determined from pure shear tests. Calcified Tissue International 69, 373-378.

Van Sint Jan, S. 2008. *The VAKHUM Project: Virtual Animation of the Kinematics of the Human for Industrial, Educational and Research Purposes* 2008 [cited 2008]. Available from http://www.ulb.be/project/vakhum/.

Viceconti, M., Ansaloni, M., Baleani, M., and Toni, A., 2003. The muscle standardized femur: a step forward in the replication of numerical studies in biomechanics. Proceedings of the Institution of Mechanical Engineers. Part H, Journal of Engineering in Medicine 217, 105-110.

Warden, S. J., Hurst, J. A., Sanders, M. S., Turner, C. H., Burr, D. B., and Li, J., 2005. Bone adaptation to a mechanical loading program significantly increases skeletal fatigue resistance. Journal of Bone and Mineral Research 20, 809-816.

Waters, R. L., Hislop, H. J., Perry, J., Thomas, L., and Campbell, J., 1983. Comparative cost of walking in young and old adults. Journal of Orthoaedic Research 1, 73-76.

Winter, D. A., Patla, A. E., Frank, J. S., and Walt, S. E., 1990. Biomechanical walking pattern changes in the fit and healthy elderly. Physical Therapy 70, 340-347.

Yoshikawa, T., Mori, S., Santiesteban, A. J., Sun, T. C., Hafstad, E., Chen, J., and Burr, D. B., 1994. The effects of muscle fatigue on bone strain. The Journal of Experimental Biology 188, 217-233.

Zimmermann, C. L., Smidt, G. L., Brooks, J. S., Kinsey, W. J., and Eekhoff, T. L., 1990. Relationship of extremity muscle torque and bone mineral density in postmenopausal women. Physical Therapy 70, 302-309.

Chapter 6 – Sensitivity of strains in the proximal femur to variations in muscle forces

Abstract

Muscle forces play a role in the health and strength of femur, both through stimulating remodeling processes and by protecting the bone from large tensile and shear strains that may lead to material fatigue. Aging may affect normal muscle forces during activities such as gait. Because of the high incidence of hip fractures in older adults, and the connection between muscle forces and bone strength, understanding the effect of various muscles on strains in the proximal femur is of interest. Muscle forces were estimated during walking for an older female using static optimization and applied to a finite element model of the femur. Perturbation analyses were performed at the points during gait of maximum principal strain in the femoral neck and sub-trochanteric region. Forces for muscles attaching to the femur that cross the hip joint were varied by ±10% and ±20%, and the resulting maximum principal and maximum shear strains in the femoral neck and sub-trochanteric region examined. Results indicate that strains in the femoral neck were affected by several muscles, and particularly the hip abductors. Strains in the sub-trochanteric region were less sensitive to muscle forces than in the femoral neck. Understanding the importance of various muscles to strains in the proximal femur may aid in future efforts to understand and prevent hip fractures in older adults.

Keywords: femur, finite element modeling, muscle forces, hip fractures

Introduction

Muscle forces contribute directly to loading of the femur *in vivo*, and these forces can play an important role in the health of the bone. Bone loading over time stimulates bone remodeling processes (Turner 1998), leading to increased or decreased strength. For example, increased muscle forces can lead to increased bone density, particularly near muscle areas of attachment (Bitsakos et al. 2005; Layne and Nelson 1999). In addition, muscle loading is thought to reduce shear and bending in the femur (Duda et al. 1998; Polgar et al. 2003; Taylor et al. 1996). This helps to protect it from material fatigue damage, as shear plays an important role in the fatiguing of bone (Taylor et al. 2003; Turner et al. 2001). Intrinsic factors that alter muscle loading can, therefore, influence this prophylactic effect. For example, changes in muscle forces due to neuromuscular fatigue can increase tibial shear strain during walking in dogs (Yoshikawa et al. 1994), and may increase bone stresses in humans during athletic activities (Benazzo et al. 1992; Clement 1974).

Aging is another factor that can alter muscle forces and potentially affect bone strains. For example, aging is known to cause changes in joint kinetics during gait (Anderson 2010; DeVita and Hortobagyi 2000; Judge et al. 1996; Kerrigan et al. 1998; Silder et al. 2008), which may indicate that older adults have different muscle forces than young adults during gait. Hip fractures, or fractures of the proximal femur, are common injuries in older adults that can lead to reduced quality of life (Magaziner et al. 2000; OTA 1994) and increased mortality rates (Magaziner et al. 2000; OTA 1994; Zuckerman 1996). As such, maintaining adequate strength in the proximal femur is important for maintaining good health in older adults. Age differences in muscle forces could lead to age differences in loading of the proximal femur. It is possible that these differences could ultimately alter the strength of the proximal femur through remodeling or material fatigue damage.

Because of the high incidence of hip fractures in older adults and the potential role that muscle forces have in the strength of the proximal femur, it would seem important to understand the effect of *in vivo* muscle forces on strains in the proximal femur. Such information may lead to interventions that strengthen the proximal femur by manipulating muscle forces thorough training. This study examined the sensitivity of femoral strains to variations in applied muscle forces, which has implications for remodeling processes and material fatigue in bone. Muscle forces during walking were determined by static optimization, and applied to a finite element model of the femur. At the points during gait of peak strains in the proximal femur, muscle force inputs were perturbed and the resulting changes in strain determined. It was hypothesized that for one or more of the muscles examined, increasing the muscle force would result in a decrease in strains in the proximal femur.

Methods

A finite element model of the femur with realistic loading conditions applied was used to investigate the effect of different muscle forces on strains in the proximal femur. A single participant (82 year old female, height 157.5 cm, mass 62.1 kg) was used from a previous study investigating age differences in strains in the proximal femur during gait (Anderson 2010). Methods that have been reported in Anderson (2010) are only summarized here. Body motion and ground reaction force data were collected during a single gait trial while the participant walked at 1.1 m/s with a step length of 0.65 m. These data were used in estimating muscle forces during gait with static optimization and a musculoskeletal model in OpenSim (Delp et al. 2007). The estimated forces were applied to a finite element model of the femur. The finite element model was obtained from the public dataset of the VAKHUM project (Van Sint Jan 2008) and geometrically scaled to match the size of the participant. The model had 17696 linear hexahedral elements and 217 isotropic materials with Young's modulus ranging from 0.66 to 27.07 GPa to model material non-homogeneity.

Baseline loading conditions were taken at the points in time at which peak maximum principal strains occur in the proximal femur. Peak maximum principal strains in the sub-trochanteric region and femoral neck occurred at 55% and 86% of the gait cycle, respectively (Figure 6.1), and both of these times were used as baseline conditions. A perturbation analysis was used to investigate the effect of varying muscle forces individually on the strain in the proximal femur. Perturbations were applied to forces representing 11 muscles that attach to the femur and cross the hip joint (Figure 6.2): gluteus maximus (GMAX), gluteus medius (GMED), gluteus minimus (GMIN), ilio-psoas (IP), piriformis (PIR), adductor magnus (ADM), adductor brevis (ADB), adductor longus (ADL), gemellus (GEM), quadratus femoris (QF), and pectineus (PECT). Baseline muscle forces are presented in Table 6.1. Perturbations of ±10% and ±20% of the baseline force were applied one at a time, and the model solved using Abaqus (Dassault Systèmes Simulia Corp., Providence, RI,

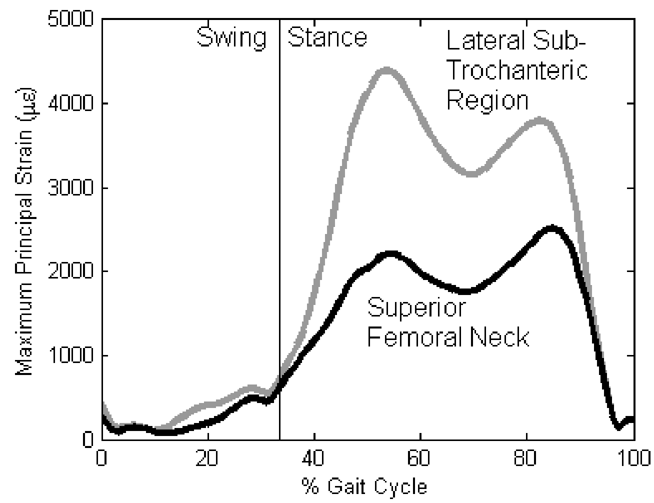

Figure 6.1: Maximum principal strains in the superior femoral neck (black) and lateral sub-trochanteric region (grey) throughout the gait cycle. These locations had the largest peak strains in the femoral neck and sub-trochanteric regions, with peaks occurring at 55% and 86% of gait.

USA). The IP force represented the combined force of the iliacus and psoas major muscles, which attached to the femur at the same location. Four of the muscles (GMAX, GMED, GMIN and ADM) were modeled with three lines of actions, and thus represented as three different forces applied to the model. For these muscles, the perturbations were applied for all lines of action together.

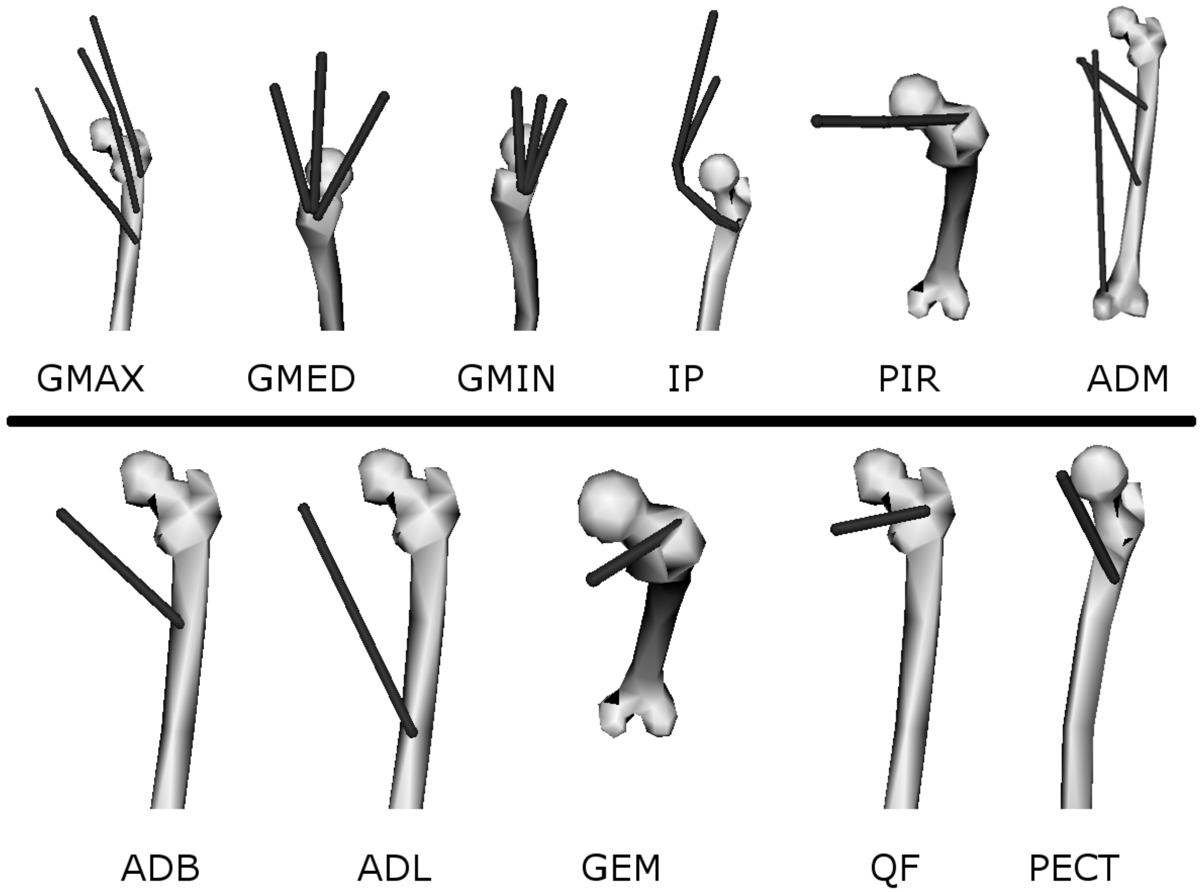

Figure 6.2: Illustrations of muscle lines of action in the musculoskeletal model for muscles attaching to the femur that cross the hip. Forces for these muscles were perturbed in the finite element model to examine their effect on strains.

Table 6.1: Baseline muscle forces (N) applied to the model, representing loading at 55% and 86% of the gait cycle

Muscle	GMAX	GMED	GMIN	IP	PIR	ADM	ADB	ADL	GEM	QF	PECT
55% Gait	344.24	1169.62	190.52	19.48	68.92	5.17	2.09	3.87	1.60	2.05	1.56
86% Gait	30.63	734.96	163.05	1132.25	20.36	7.23	2.79	6.00	1.70	3.36	2.21

Fixed boundary conditions were applied at the hip and forces were applied at the knee based on previous finite element results. In our previous study (Anderson 2010), the finite element model was fixed at the knee, and time-varying hip joint forces calculated from the musculoskeletal model were applied to the femoral head throughout the course of the gait cycle. However, in this study it was important that the femoral head be fixed in order to allow perturbations in muscle forces to cause changes in hip joint reaction forces and more realistically affect strains in the proximal femur. Thus, femoral head displacements were specified as those determined previously. Similarly, the forces applied at the knee were the reaction forces determined previously. These boundary conditions produced equivalent strains and hip joint reaction forces to the previous approach.

Strains were investigated at a total of eight locations, four in the femoral neck and four in the sub-trochanteric (Figure 6.3). Maximum principal and maximum shear strains were determined at each location of interest on the femur for each baseline and perturbed loading condition. To examine the relative importance of muscles forces to strain, percent change in strain versus percent change in muscle forces was determined. However, because muscle forces varied by several orders of magnitude, a given percent change in a larger muscle forces would logically be more likely to cause a larger change in strain than the same percent change in a smaller muscle force. Thus, the sensitivity of strain to a muscle forces in an absolute sense ($\mu\varepsilon$ /N) was also determined. The sensitivity of strain to muscle force was determined as slope of the strain versus muscle force line, using a least-squares approach to fit a line to the data.

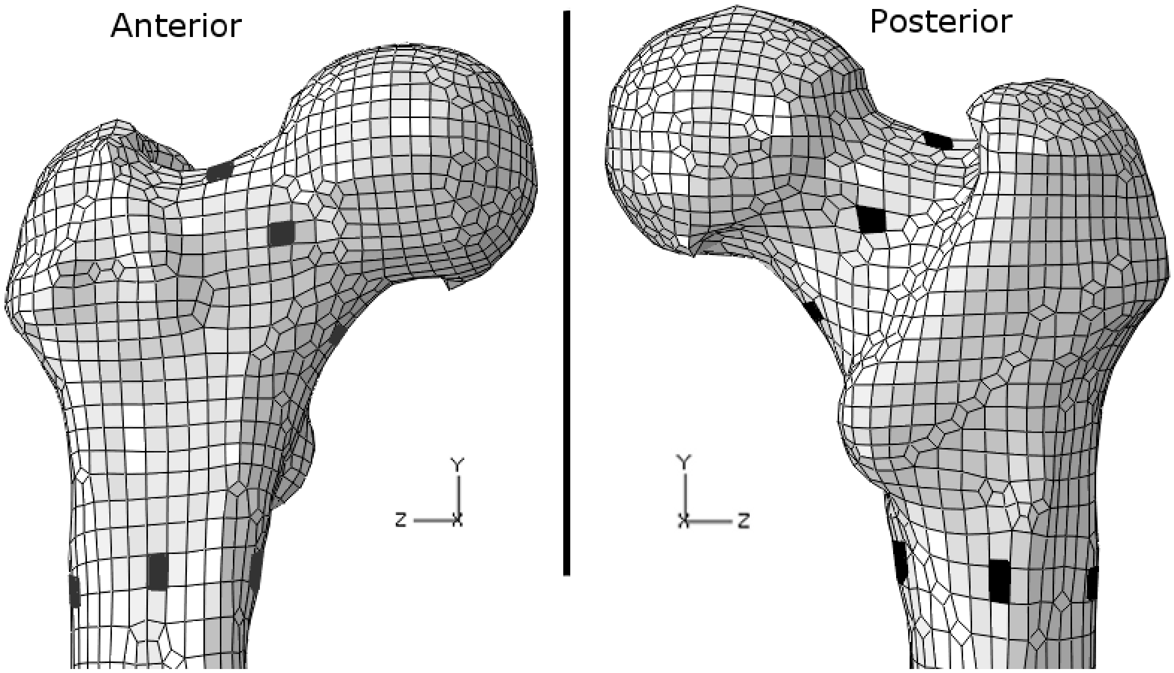

Figure 6.3: Anterior and posterior views of the proximal portion of the femur finite element model. Black areas indicate locations at which strains were examined: superior, anterior, inferior and posterior femoral neck, and lateral, anterior, medial and posterior sub-trochanteric region.

Results

In general, strains in the proximal femur when baseline muscle forces were applied were larger in the sub-trochanteric region than in the femoral neck (Table 6.2). The highest maximum principal strain among the four locations investigated in the femoral neck occurred on the superior side, and the highest maximum shear strain occurred on the inferior side, both at 86% of gait. The highest maximum principal strain among the four locations investigated in the sub-trochanteric region occurred on the lateral side, and the highest maximum shear strain occurred on the medial side, both at 55% of gait.

Table 6.2: Strain (με) in femoral neck (FN) and sub-trochanteric region (ST) of the femur when baseline muscle forces were applied.

	55% Gait Cycle		86% Gait Cycle	
Strain	Max Principal	Max Shear	Max Principal	Max Shear
FN – Superior	2202	1454	2508	1657
FN – Anterior	336	400	202	367
FN – Inferior	985	2074	1076	2258
FN – Posterior	422	768	299	517
ST – Lateral	4347	2871	3635	2373
ST – Anterior	1422	1691	186	359
ST – Medial	1575	3184	1367	2707
ST – Posterior	1537	1321	819	656

Only a subset of muscles (GMAX, GMED, GMIN, IP and PIR) produced changes in strain of more than 1% in the femoral neck with a 20% force perturbation (Figure 6.4). These muscles exhibited a near-linear relationship between muscle force and strain over the ranges investigated. Increasing GMAX force increased strains on the anterior and posterior femoral neck at 55% of gait cycle. Increasing GMED force decreased strains on the superior, anterior and inferior sides of the femoral neck, but increased strain on the posterior side. GMIN followed a similar pattern to GMED, but had a smaller effect. Increasing IP force only had an effect at 86% of gait cycle, when it decreased strains in the posterior femoral neck, but increased strains at the other locations. Increasing PIR force caused small increases in strains in the anterior and posterior femoral neck at 55% of gait cycle, but a small decrease in maximum principal strain in the posterior femoral neck at 86% of gait cycle.

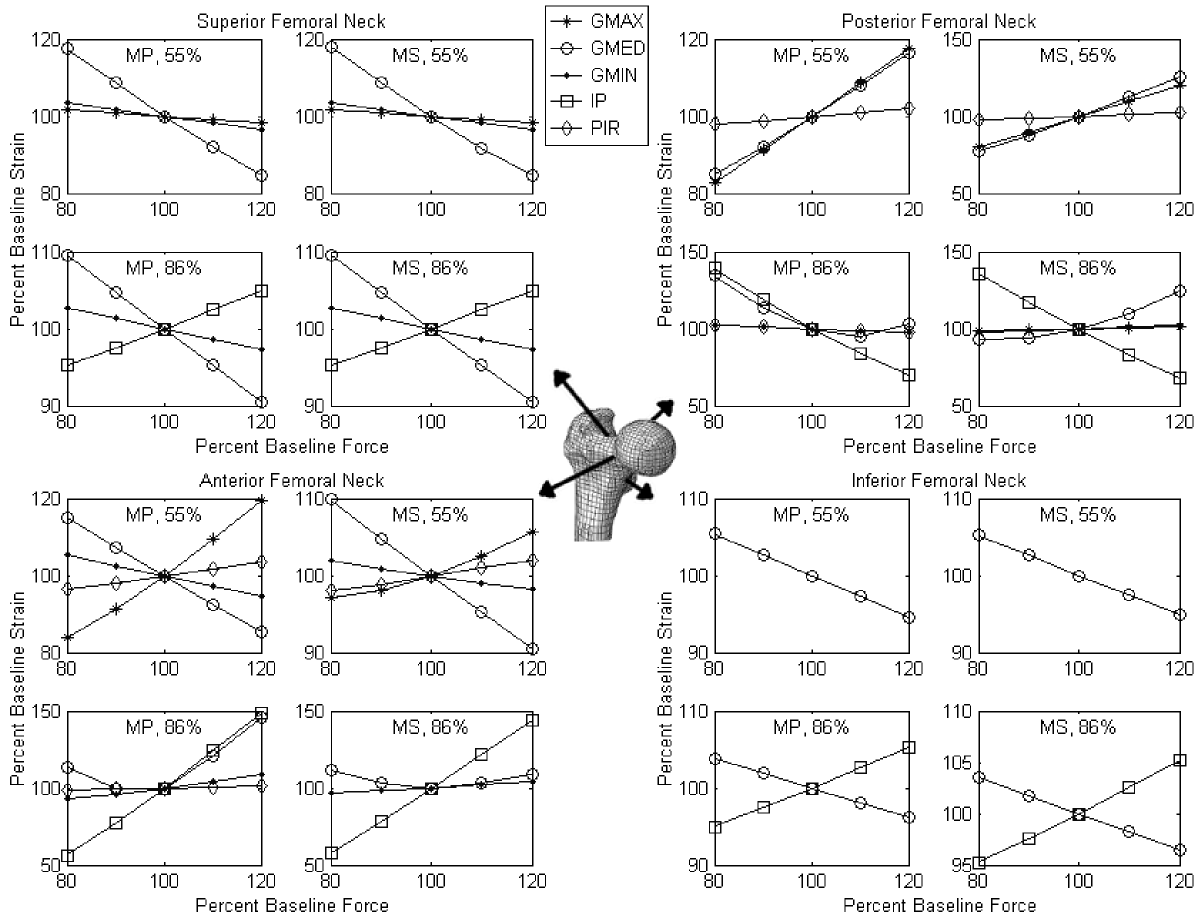

Figure 6.4: Percent change in baseline strains in the femoral neck relative to percent change in baseline muscle forces. Results are shown for both maximum principal (MP) and maximum shear (MS) strains at 55% and 86% of the gait cycle. Muscles that produced less than 1% change in strain with 20% change in muscle force have been omitted.

Similarly, only a subset of muscles (GMAX, GMED, and IP) produced changes in strain of more than 1% in the sub-trochanteric region with a 20% force perturbation (Figure 6.5). A near-linear relationship was also found here between force and strain over the ranges investigated. Increasing GMAX force increased maximum shear strain on the posterior side at 55% of gait cycle, but had no effect elsewhere. Increasing GMED force increased strain at all locations, and it was the only muscle to affect strains in the lateral and medial sub-trochanteric regions. Increasing IP force decreased strains on the anterior and posterior side at 86% of gait cycle.

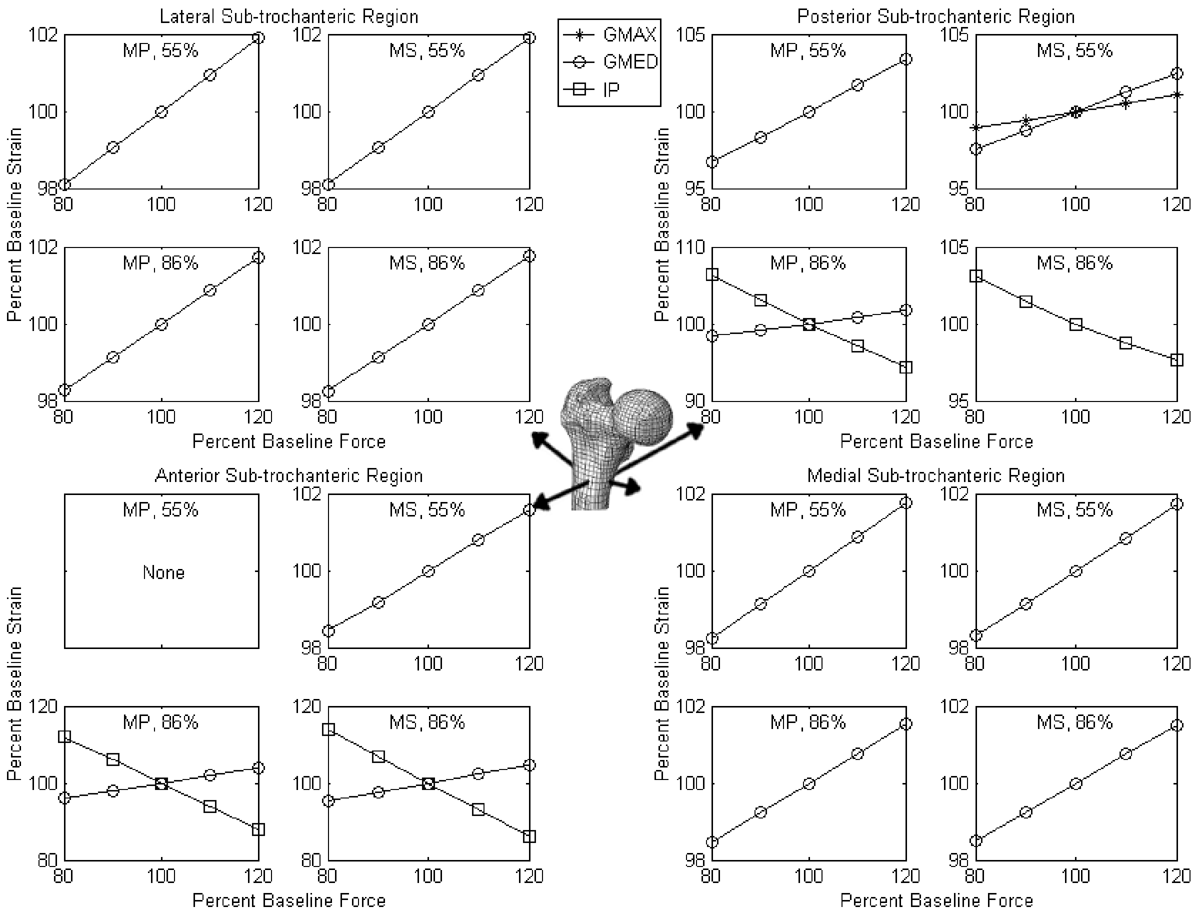

Figure 6.5: Percent change in baseline strains in the sub-trochanteric region relative to percent change in baseline muscle forces. Results are shown for both maximum principal (MP) and maximum shear (MS) strains at 55% and 86% of the gait cycle. Muscles that produced less than 1% change in strain with 20% change in muscle force have been omitted.

The sensitivities of strains to muscle forces varied from -2.06 με/N to 2.25 με/N among the four locations investigated in the femoral neck (Table 6.3). The superior femoral neck was quite sensitive to muscle forces, particularly GMED, GMIN, PIR, ADB, and GEM which all displayed sensitivities with magnitudes greater than 1 με/N. The anterior femoral neck showed more variability in strain sensitivity, and only GEM and QF had sensitivities with magnitudes greater than 1 με/N. The inferior femoral neck was most sensitive to ADB, followed by ADL and PECT. The posterior femoral neck was most sensitive to GMAX, followed by QF, GEM and PIR, all of which had sensitivities with magnitudes greater than 1 με/N.

The sensitivities of strains to muscle forces varied from -0.63 με/N to 0.68 με/N among the four locations investigated in the sub-trochanteric region (Table 6.3). The lateral sub-trochanteric region was most sensitive to ADL, followed by GMIN and GMED. The anterior sub-trochanteric region was the relatively insensitive to most muscle forces, with the largest magnitude sensitivities occurring for GEM. The medial sub-trochanteric region was most sensitive to ADL followed by ADB and ADM. The posterior sub-trochanteric region was most sensitive to PECT, followed by ADB.

Table 6.3: Sensitivities (με/N) of maximum principal (MP) and maximum shear (MS, shaded cells) strains to muscle forces at different locations in the proximal femur at 55% and 86% of gait cycle. The largest magnitude positive and negative sensitivities in each row are in bold.

Muscle	GMAX	GMED	GMIN	IP	PIR	ADM	ADB	ADL	GEM	QF	PECT
Superior Femoral Neck											
MP 55%	-0.487	-1.548	**-1.990**	0.355	-1.376	-0.060	**1.618**	0.838	-1.366	0.049	0.765
MP 86%	-0.626	-1.640	**-2.060**	0.539	-0.907	0.506	**1.607**	0.880	-0.817	0.521	0.729
MS 55%	-0.350	-1.050	**-1.347**	0.257	-0.896	-0.046	**1.065**	0.577	-0.873	0.048	0.517
MS 86%	-0.419	-1.078	**-1.354**	0.358	-0.605	0.314	**1.009**	0.558	-0.620	0.307	0.420
Anterior Femoral Neck											
MP 55%	0.856	-0.213	**-0.467**	0.237	0.869	0.398	-0.070	0.224	**1.831**	1.636	0.459
MP 86%	0.111	0.224	0.511	0.419	**0.701**	0.125	**-0.217**	0.342	0.357	0.199	0.144
MS 55%	0.245	-0.165	**-0.194**	0.533	0.576	0.310	-0.086	0.462	**1.169**	0.823	0.518
MS 86%	**-0.549**	-0.025	0.412	**0.708**	0.339	0.214	-0.046	0.589	0.085	-0.043	0.382
Inferior Femoral Neck											
MP 55%	-0.107	-0.227	-0.254	0.204	-0.177	0.064	**0.557**	0.355	**-0.263**	-0.017	0.322
MP 86%	-0.136	-0.278	**-0.319**	0.245	-0.148	0.235	**0.556**	0.328	-0.194	0.104	0.303
MS 55%	-0.191	-0.459	**-0.522**	0.416	-0.348	0.159	**1.210**	0.762	-0.480	0.025	0.720
MS 86%	-0.248	-0.553	**-0.645**	0.495	-0.281	0.522	**1.220**	0.721	-0.294	0.270	0.713
Posterior Femoral Neck											
MP 55%	1.068	0.281	-0.082	-0.264	0.623	0.252	0.215	**-0.267**	1.044	**1.343**	0.116
MP 86%	-0.289	-0.336	-0.192	-0.452	-1.465	**0.113**	-0.016	0.041	-1.719	**-1.735**	-0.149
MS 55%	**2.252**	0.789	0.093	**-0.705**	1.088	0.550	0.291	-0.633	1.553	2.204	-0.003
MS 86%	**1.126**	0.572	0.335	-0.771	-0.705	0.110	-0.178	-0.283	-1.179	**-1.231**	-0.366
Lateral Sub-trochanteric Region											
MP 55%	0.208	0.354	0.386	-0.094	0.260	0.193	0.310	**0.587**	0.113	-0.141	**-0.238**
MP 86%	0.272	0.429	0.490	-0.101	0.180	0.257	0.337	**0.597**	-0.006	**-0.265**	-0.149
MS 55%	0.150	0.233	0.252	-0.064	0.171	0.132	0.224	**0.389**	0.100	-0.068	**-0.122**
MS 86%	0.183	0.281	0.320	-0.068	0.118	0.168	0.222	**0.393**	0.003	**-0.171**	-0.093
Anterior Sub-trochanteric Region											
MP 55%	0.102	0.052	0.072	0.054	0.056	0.050	0.100	0.119	**0.457**	0.297	0.379
MP 86%	**0.129**	0.048	0.001	**-0.098**	-0.009	0.065	0.033	0.128	-0.032	-0.031	-0.068
MS 55%	0.197	0.114	0.086	**-0.094**	0.071	0.135	0.115	0.283	**0.404**	0.317	0.244
MS 86%	**0.294**	0.114	0.011	**-0.222**	-0.012	0.133	0.053	0.284	-0.051	-0.060	-0.141
Medial Sub-trochanteric Region											
MP 55%	0.126	0.118	0.128	**-0.026**	0.087	0.182	0.272	**0.344**	0.088	-0.005	0.225
MP 86%	0.104	0.144	0.173	-0.012	0.067	0.213	0.265	**0.332**	0.024	**-0.077**	0.154
MS 55%	0.258	0.232	0.262	-0.025	0.177	0.376	0.535	**0.679**	0.144	**-0.058**	0.395
MS 86%	0.193	0.277	0.340	-0.013	0.130	0.424	0.513	**0.647**	0.024	**-0.162**	0.301
Posterior Sub-trochanteric Region											
MP 55%	0.214	0.220	0.115	**-0.319**	0.100	0.083	0.372	**0.419**	0.301	0.346	0.379
MP 86%	**0.119**	0.091	-0.012	-0.219	-0.035	-0.153	-0.343	-0.012	-0.103	-0.086	**-0.632**
MS 55%	0.205	0.140	0.089	**-0.156**	0.076	0.121	0.470	0.348	0.392	0.341	**0.588**
MS 86%	-0.056	**0.011**	-0.027	-0.081	-0.028	-0.132	-0.295	-0.077	-0.065	-0.040	**-0.494**

Discussion

The purpose of this study was to examine the sensitivity of femoral strains to variation in applied muscle forces. Baseline loading conditions were estimated at two points in time corresponding to peak maximum principal strains in the proximal femur of an 82 year old female during gait. The muscle forces examined here affected strains in the femoral neck and, to a lesser extent, strains in the sub-trochanteric region. Strains in the femoral neck were highest on the superior and inferior sides. These locations were particularly sensitive to the hip abductors (GMED and GMIN) and adductors (ADM, ADB and ADL). The hip abductors tended to decrease strain with increased force, while the adductors tended to increase strain with increased force. However, adductor forces were relatively low at these points in time, and so had little overall effect on strain. Strains in the sub-trochanteric region under the same walking conditions were highest on the lateral and medial sides. These locations were less sensitive to muscle forces than the femoral neck, but most sensitive to hip adductors. However, the GMED was the only muscle examined to produce more than a 1% change in strains at these locations with a 20% change in muscle force.

While most effects were fairly linear, there were exceptions. For example, the anterior and posterior femoral neck at 86% of gait cycle showed distinctly nonlinear variation with GMED force. This was the result of the direction of maximum principal strain changing from along the length of the femoral neck (caused by bending) to along the radius of the femoral neck (caused by compression). It should be noted that maximum principal strain was quite low at these locations, indicating that there was very little bending of the femoral neck in the anterior-posterior direction. The effect of the various muscles on strain was also not always consistent between the two time points investigated. For example, the posterior femoral neck had a positive sensitivity to QF at 55% of gait cycle, but a negative sensitivity at 86%. This may be explained by differences in hip joint angles between these two time points. At 55% of gait cycle the hip was at 21.7° flexion, and at 86% of gait cycle the hip was at 14.3° extension. These differences in hip angle influence the directions of the lines of action of muscle forces applied to the femur.

It is interesting to note that our previous work (Anderson 2010) showed that young adults have greater maximum principal and maximum shear strains than older adults at the posterior femoral neck at 86% of the gait cycle. The present study indicates that these differences may result from a lower IP force, lower GMED force, or possibly a higher GMED force in young adults. Young adults also showed significantly lower strains in the posterior sub-trochanteric region at mid-stance (65% of gait cycle), although not at the time points examined here (Anderson 2010). However, strains in this location are decreased by IP force at both 55% and 86% of gait. Furthermore, IP force is small at 55% of gait, but large at 86% of gait. Thus, this age difference in strain may be in part due to an earlier onset of IP force in young adults. However, further work is needed to confirm these possible explanations of age differences in strains.

Muscle forces *in vivo* are often estimated using a static optimization approach. While this approach can provide reasonable estimates of muscle forces, it depends critically on calculated joint torques (Patriarco et al. 1981) and hence the accuracy of data collection. Muscle forces also vary depending on model parameters such as muscle attachment points (Rohrle et al. 1984), muscle cross-sectional area (Brand et al. 1986) and joint kinematics (Glitsch and Baumann 1997). Therefore, muscle force estimates vary with experimental and modeling errors. In addition to highlighting how varying muscle forces can alter strains, this study also shows that finite element results will be affected by errors in muscle inputs.

Several limitations to this study warrant discussion. Only muscles attached directly to the femur were included in the loading conditions, and the muscle attachment locations were simplified to match the musculoskeletal model. There are other muscle forces that could affect strains in the proximal femur that were not examined in the perturbation analysis. It is possible that other muscles attaching to the femur, such as the vasti, could have effects on the proximal femur, although they were excluded here because they do not cross the hip. However, of perhaps greater importance are two-joint muscles that cross both the hip and knee, such as the biceps femoris long head, semitendinosus, semimembranosus, sartorius, tensor fasciae latae and rectus femorus. The effects of these muscles were indirectly included in this model through the boundary conditions at the hip and knee. However, this approach precluded including these muscles in the perturbation analysis performed here. Forces due to muscle wrapping may also play a role and were not included. In addition to muscles, the forces produced by the ligaments of the hip joint capsule have been shown to affect stresses in the femoral neck (Rudman et al. 2006), although inclusion of these forces would not be expected to greatly affect the strain sensitivities determined here.

In conclusion, this study quantified the relationship between selected lower extremity muscle forces and strains in the proximal femur. Strains in the femoral neck during gait were influenced by several muscles, and to the largest extent by the hip abductors. Strains in the sub-trochanteric region were generally greater in magnitude than in the femoral neck, but less sensitive to changes in muscle forces. These results show the importance of muscle loading to the strain state of the femoral neck in particular. Future studies could expand on this to determine the strain sensitivity to two-joint muscles crossing both the hip and knee. In addition, these results will support future work in understanding and preventing hip fractures. Knowing the importance of different muscle forces to strains in the proximal femur may contribute to the development of exercises that purposefully apply strains to specific locations on the femur with the goal of stimulating bone remodeling to increase bone density and strength and reduce the risk of hip fracture.

Acknowledgement

This work was supported by Award Number F31AG030904 from the National Institute on Aging. The content is solely the responsibility of the author and does not necessarily represent the official views of the National Institute on Aging or the National Institutes of Health.

References

Anderson, D. E., 2010. Age differences in lower extremity joint torques during walking with controlled speed and step length. (Study 1).

Anderson, D. E., 2010. The effect of age differences in femoral loading during controlled walking on strains in the proximal femur. (Study 2).

Benazzo, F., Barnabei, G., Ferrario, A., Castelli, C., and Fishchetto, G., 1992. Stress fractures in track and field athletics. Journal of Sports Traumatology and Related Research 14, 51-65.

Bitsakos, C., Kerner, J., Fisher, I., and Amis, A. A., 2005. The effect of muscle loading on the simulation of bone remodelling in the proximal femur. Journal of Biomechanics 38, 133-139.

Brand, R. A., Pedersen, D. R., and Friederich, J. A., 1986. The sensitivity of muscle force predictions to changes in physiologic cross-sectional area. Journal of Biomechanics 19, 589-596.

Clement, D. B., 1974. Tibial stress syndrome in athletes. The Journal of Sports Medicine 2, 81-85.

Delp, S. L., Anderson, F. C., Arnold, A. S., Loan, P., Habib, A., John, C. T., Guendelman, E., and Thelen, D. G., 2007. OpenSim: open-source software to create and analyze dynamic simulations of movement. IEEE Transactions on Biomedical Engineering 54, 1940-1950.

DeVita, P., and Hortobagyi, T., 2000. Age causes a redistribution of joint torques and powers during gait. Journal of Applied Physiology 88, 1804-1811.

Duda, G. N., Heller, M., Albinger, J., Schulz, O., Schneider, E., and Claes, L., 1998. Influence of muscle forces on femoral strain distribution. Journal of Biomechanics 31, 841-846.

Glitsch, U., and Baumann, W., 1997. The three-dimensional determination of internal loads in the lower extremity. Journal of Biomechanics 30, 1123-1131.

Judge, J. O., Davis, R. B., 3rd, and Ounpuu, S., 1996. Step length reductions in advanced age: the role of ankle and hip kinetics. The Journals of Gerontology. Series A, Biological Sciences and Medical Sciences 51A, M303-M312.

Kerrigan, D. C., Todd, M. K., Della Croce, U., Lipsitz, L. A., and Collins, J. J., 1998. Biomechanical gait alterations independent of speed in the healthy elderly: evidence for specific limiting impairments. Archives of Physical Medicine and Rehabilitation 79, 317-322.

Layne, J. E., and Nelson, M. E., 1999. The effects of progressive resistance training on bone density: a review. Medicine and Science in Sports and Exercise 31, 25-30.

Magaziner, J., Hawkes, W., Hebel, J. R., Zimmerman, S. I., Fox, K. M., Dolan, M., Felsenthal, G., and Kenzora, J., 2000. Recovery from hip fracture in eight areas of function. The

Journals of Gerontology. Series A, Biological Sciences and Medical Sciences 55, M498-507.

Office of Technology Assessment, 1994. Hip Fracture Outcomes in People Age 50 and Over-Background Paper. U.S. Government Printing Office, Washington, DC, OTA-BP-H- 120.

Patriarco, A. G., Mann, R. W., Simon, S. R., and Mansour, J. M., 1981. An evaluation of the approaches of optimization models in the prediction of muscle forces during human gait. Journal of Biomechanics 14, 513-525.

Polgar, K., Gill, H. S., Viceconti, M., Murray, D. W., and O'Connor, J. J., 2003. Strain distribution within the human femur due to physiological and simplified loading: finite element analysis using the muscle standardized femur model. Proceedings of the Institution of Mechanical Engineers. Part H, Journal of Engineering in Medicine 217, 173-189.

Rohrle, H., Scholten, R., Sigolotto, C., Sollbach, W., and Kellner, H., 1984. Joint forces in the human pelvis-leg skeleton during walking. Journal of Biomechanics 17, 409-424.

Rudman, K. E., Aspden, R. M., and Meakin, J. R., 2006. Compression or tension? The stress distribution in the proximal femur. BioMedical Engineering Online 5, 12.

Silder, A., Heiderscheit, B., and Thelen, D. G., 2008. Active and passive contributions to joint kinetics during walking in older adults. Journal of Biomechanics 41, 1520-1527.

Taylor, D., O'Reilly, P., Vallet, L., and Lee, T. C., 2003. The fatigue strength of compact bone in torsion. Journal of Biomechanics 36, 1103-1109.

Taylor, M. E., Tanner, K. E., Freeman, M. A., and Yettram, A. L., 1996. Stress and strain distribution within the intact femur: compression or bending? Medical Engineering & Physics 18, 122-131.

Turner, C. H., 1998. Three rules for bone adaptation to mechanical stimuli. Bone 23, 399-407.

Turner, C. H., Wang, T., and Burr, D. B., 2001. Shear strength and fatigue properties of human cortical bone determined from pure shear tests. Calcified Tissue International 69, 373-378.

Van Sint Jan, S. 2008. *The VAKHUM Project: Virtual Animation of the Kinematics of the Human for Industrial, Educational and Research Purposes* 2008 [cited 2008]. Available from http://www.ulb.be/project/vakhum/.

Yoshikawa, T., Mori, S., Santiesteban, A. J., Sun, T. C., Hafstad, E., Chen, J., and Burr, D. B., 1994. The effects of muscle fatigue on bone strain. The Journal of Experimental Biology 188, 217-233.

Zuckerman, J. D., 1996. Hip fracture. The New England Journal of Medicine 334, 1519-1525.

Chapter 7 – Conclusions and Future Work

Conclusions

Three studies have been performed to examine age-related differences in walking, the resulting differences in strains in the proximal femur, and the effects of individual muscles forces on femoral strains. Study 1 used experimental gait analysis to evaluate age differences in peak joint torques during walking while controlling gait speed and step length. In Study 2 muscle forces during gait were determined using static optimization, and applied to finite element models of the femur to examine the effects of age differences in loading on strains in the proximal femur. Finally, Study 3 examined the effect of individual muscles on femoral strains in the proximal femur by perturbing individual muscle forces applied to a finite element model and determining the resulting change in strain.

Study 1 demonstrated that age differences in gait kinetics, specifically peak joint torques, are not fully explained by older adults selecting slower gait speed and shorter step length while walking. Furthermore, the study supports the idea put forth by DeVita and Hortobagyi (2000) that older adults shift function in gait proximally, with reduced contributions from the ankle plantar flexors, and increased contributions from the hip extensors. Interactions between age and speed in plantar flexor and hip extensor torques also indicated that older adults utilized a different neuromuscular strategy than young adults to vary the speed of their gait. This was the first study to examine age differences in gait kinetics while controlling both speed and step length. It will be submitted to the

Journals of Gerontology. Series A, Biological Sciences and Medical Sciences for publication.

Study 2 examined differences in strains in the femoral neck and sub-trochanteric region of the femur due to age differences in loading during gait. Strains were found to be lower in older adults in the posterior femoral neck during late stance phase, and lower in young adults in the posterior sub-trochanteric region in mid-stance, although strain magnitudes were relatively low in these locations. No age differences were observed for the largest magnitude strains. However, peak hip joint contact forces were 18% lower in older adults than young adults. This may indicate that young adults are better able to balance loads on the femur, and thus apply larger muscle forces during push-off without increasing strains. However, it cannot be concluded from this study that age differences in loading during gait place older adults at greater risk for hip fracture. This study is thought to be the first to examine age differences in the femur using finite element modeling. It will be submitted to the *Annals of Biomedical Engineering* for publication.

Study 3 showed that strains in the femoral neck are quite sensitive to muscle forces during gait. In particular, increasing hip abductor forces decreases the largest magnitude tensile and shear strains in the femoral neck. Strains in the sub-trochanteric region tend to be larger than those in the femoral neck, and less sensitive to muscle forces. The results of this study provide an important piece in understanding the various factors that contribute to strains in the femur, and may help future efforts in understanding the causes of and preventing hip fractures in older adults. While other studies have demonstrated the importance of applying realistic muscle loads to finite element models of the femur, this is believed to be the first study that has directly examined the effect of individual muscle forces on strains in the proximal femur. This study will be submitted to the *Journal of Biomechanics* for publication.

Future Work

The three studies presented in this dissertation represent the early results of a larger project. Thus, there is much additional work that can be done with the data collected. Generally, future work in this project will continue to examine age differences in joint kinetics, muscle forces and femoral strains during gait. This section outlines several expected future studies, as well as other possible future work.

Study 1 study examined age differences in peak joint torques while controlling speed and step length. There are several other measures of gait kinetics that have been used in the literature, particularly joint angular impulse, peak joint power, and joint work. With our data, any of these measures could be calculated and analyzed as well. As a follow-up to Study 1, we hope to complete and publish a similar study examining age differences in joint work. This will provide additional information on age differences in gait kinetics independent of speed and step length, hopefully yielding better understanding of neuromuscular changes that occur with aging.

In this dissertation, loading for the finite element models during gait was determined by static optimization from individualized musculoskeletal models. In the course of this work, it became clear that a logical supporting study would be an examination of age differences in muscle forces themselves during gait. All 20 participants from Study 1 will be included, requiring the development of musculoskeletal models for the participants not included in Study 2. This study will be the performed in the year following the completion of this dissertation. Not only will this extend examinations of age differences in gait kinetics, such as Study 1, into the area of muscle forces, it will provide support for studies such as Study 2 that utilize muscle forces from different age groups in finite element models

Another possible direction to pursue is an examination of age differences in relative effort during gait. Older adults use more of their aerobic capacity to walk than young adults (Waters et al. 1983), which may indicate that they are using more of their available strength. Using the strength measurements taken with the Biodex, and based on our previous work (Anderson et al. 2007; Bieryla et al. 2009), relative effort during gait could be assessed in terms of joint torques. Alternatively, this relative effort could be assessed in terms of muscle forces determined using OpenSim models. With either approach, this study could help us understand whether strength plays a role in the shift of function from ankle to hip during gait in older adults.

In Study 2, age differences in strains in the proximal femur were examined during gait. In the gait condition used for the study, both speed and step length were controlled. This was to make sure that age differences in strain were not the result of differences in speed and step length between participants. However, it could also be reasonably argued that strains during self-selected gait would be more representative of strains that occur in reality. Thus, age differences in strains during self-selected gait will be investigated in a study similar to Study 2. This study will be performed in the year following the completion of this dissertation.

The finite element models used in Study 2 were based on a single model of the femur from the VAKHUM project (Van Sint Jan 2008), and geometrically scaled to individualize them based on the lengths of the femoral neck axis and the total femur.

However, the scaling process could be improved by taking into account other details of femoral geometry. For example, femoral neck and shaft diameters could be determined from the DXA scans and included in the scaling process. In addition, the model material properties were left the same for all the models in this work. This was intentional, as we wanted to examine the effects of age differences in loading, and differences in material properties could have confounded this. However, more realistic individualized material property values could also be determined based on the DXA scans. Such models would more realistically represent the femurs of the participants, and could be used in an examination of actual age differences in strain, as opposed to differences due solely to age differences in loading.

While the loading and boundary conditions in Studies 2 and 3 included all major muscle forces for muscles attached to the femur, there are a variety of ways they could be improved. For example, muscle forces could possibly be distributed more realistically. The effect of muscle wrapping and two-joint muscles could be included. Forces due to capsular ligaments could be added. In addition, the boundary conditions could be made more realistic. For example, fixed boundary conditions at the distal femur, while acceptable for the purposes Study 2, did not realistically depict the interface of the femur at the knee. The possibilities for improving the realism of loading and boundary conditions could allow for a number of additional finite element studies. In particular, we hope to expand on the results of Study 3 with the inclusion of muscle wrapping and two-joint muscles in the model.

References

Anderson, D. E., Madigan, M. L., and Nussbaum, M. A., 2007. Maximum voluntary joint torque as a function of joint angle and angular velocity: model development and application to the lower limb. Journal of Biomechanics 40, 3105-3113.

Bieryla, K. A., Anderson, D. E., and Madigan, M. L., 2009. Estimations of relative effort during sit-to-stand increase when accounting for variations in maximum voluntary torque with joint angle and angular velocity. Journal of Electromyography & Kinesiology 19, 139-144.

DeVita, P., and Hortobagyi, T., 2000. Age causes a redistribution of joint torques and powers during gait. Journal of Applied Physiology 88, 1804-1811.

Van Sint Jan, S. 2008. *The VAKHUM Project: Virtual Animation of the Kinematics of the Human for Industrial, Educational and Research Purposes* 2008 [cited 2008]. Available from http://www.ulb.be/project/vakhum/.

Waters, R. L., Hislop, H. J., Perry, J., Thomas, L., and Campbell, J., 1983. Comparative cost of walking in young and old adults. Journal of Orthoaedic Research 1, 73-76.

Appendix A – IRB Approval

VirginiaTech

Office of Research Compliance
Institutional Review Board
2000 Kraft Drive, Suite 2000 (0497)
Blacksburg, Virginia 24061
540/231-4991 Fax 540/231-0959
e-mail moored@vt.edu
www.irb.vt.edu
FWA00000572(expires 1/20/2010)
IRB # is IRB00000667

DATE: May 16, 2008

MEMORANDUM

TO: Michael L. Madigan
Dennis Anderson

FROM: David M. Moore

Grant Compared 5/12/08

Approval date: 5/12/2008
Continuing Review Due Date: 3/30/2009
Expiration Date: 5/11/2009

SUBJECT: **IRB Full IRB Approval:** "Implications of In Vivo Muscle Loading for Hip Fracture Etiology" , IRB # 08-269

The above referenced protocol was submitted for full review and approval by the IRB at the May 12, 2008 meeting. The board had voted approval of this proposal contingent upon receipt of responses to questions raised during its deliberation. Following receipt and review of your responses, I, as Chair of the Virginia Tech Institutional Review Board, have, at the direction of the IRB, granted approval for this study for a period of 12 months, effective May 12, 2008.

Approval of your research by the IRB provides the appropriate review as required by federal and state laws regarding human subject research. As an investigator of human subjects, your responsibilities include the following:

1. Report promptly proposed changes in previously approved human subject research activities to the IRB, including changes to your study forms, procedures and investigators, regardless of how minor. The proposed changes must not be initiated without IRB review and approval, except where necessary to eliminate apparent immediate hazards to the subjects.
2. Report promptly to the IRB any injuries or other unanticipated or adverse events involving risks or harms to human research subjects or others.
3. Report promptly to the IRB of the study's closing (i.e., data collecting and data analysis complete at Virginia Tech). If the study is to continue past the expiration date (listed above), investigators must submit a request for continuing review prior to the continuing review due date (listed above). It is the researcher's responsibility to obtain re-approval from the IRB before the study's expiration date.
4. If re-approval is not obtained (unless the study has been reported to the IRB as closed) prior to the expiration date, all activities involving human subjects and data analysis must cease immediately, except where necessary to eliminate apparent immediate hazards to the subjects.

<u>**Important:**</u>
If you are conducting **federally funded non-exempt research**, please send the applicable OSP/grant proposal to the IRB office, once available. OSP funds may not be released until the IRB has compared and found consistent the proposal and related IRB appllication.

As indicated on the IRB application, this study is receiving federal funds. The approved IRB application has been compared to the OSP proposal listed above and found to be consistent. Funds involving procedures relating to human subjects may be released. Visit our website at www.irb.vt.edu for further information

cc: File

Invent the Future

VIRGINIA POLYTECHNIC INSTITUTE UNIVERSITY AND STATE UNIVERSITY
An equal opportunity, affirmative action institution

Appendix B – Informed Consent Form

VIRGINIA POLYTECHNIC INSTITUTE AND STATE UNIVERSITY

Informed Consent for Participants
In Research Projects Involving Human Subjects

Title of the Research Study
Implications of in vivo muscle loading for hip fracture etiology

Investigator
Michael L. Madigan, Ph.D. 231-1215
Department of Engineering Science and Mechanics

Dennis Anderson, M.S. 231-4294
Department of Engineering Science and Mechanics

I. Purpose of this Study
The purpose of this research is to investigate the influence of muscles on forces in the thigh bone during walking. Hip fractures are serious injuries that are associated with high rates of morbidity and mortality in older adults. Muscles contribute to forces in the thigh bone, and therefore may contribute to the causes of some hip fractures. Determining how muscles influence forces in the thigh bone could lead to improvements in clinical screening and preventative measures for hip fractures.

We will collect several non-invasive measurements related to body movement as you walk across our laboratory at different speeds and step frequencies. A total of 40 participants will complete the study including 18-24 year olds and individuals over 65 years in order to help understand how muscles influence forces in the thigh bone and how aging may affect these forces.

II. Procedures
The study will take place in the Musculoskeletal Biomechanics Lab of the Department of Engineering Science and Mechanics (111 Norris Hall).

The study will require 2 visits to the lab over approximately 1 week. We will work with you to schedule days/times that are convenient for you.

The first visit will involve three tasks. First, we will record several non-invasive measurements of body size including height, weight, leg circumference, etc. These data will be used during data analysis. Second, you will walk across our laboratory approximately 20 times at different speeds. These speeds will include no more than two slow walking speeds, your preferred walking speed, and two fast walking speeds. During these trials, we will record your body movements using common noninvasive motion sensors. Third, you will perform strength tests to determine the strength of selected muscle groups in the leg. This will involve you sitting in a specialized device that is designed to measure strength and exerting your muscles as much as you can. It is anticipated that this visit will take approximately 1.5 hours.

The second visit will involve two tasks. First, a dual-energy x-ray absorptiometry (DXA) scan will be collected to obtain information on the size and shape of your thigh bone. These data will

5/16/2008 1

Virginia Tech Institutional Review Board: Project No. 08-269
Approved May 16, 2008 to May 11, 2009

be used during data analysis. These DXA scans are widely used to assess bone mineral density, and provide an advantage over traditional x-ray scans in that they will only expose you to a low dosage of radiation (reported to be similar to that experienced during a long-distance airline flight). Second, you will perform additional strength tests to determine the strength of selected muscle groups in your leg. It is anticipated that this visits will also take approximately 1.5 hours.

III. Risks
The risks to involved in this study are minimal. You will be asked to simply walk across our laboratory at different speeds and stepping frequencies, and simply exert your best during strength testing. For DXA scans, you will be exposed to small levels of radiation similar to that in a long-distance airline flight.

In the unlikely event that you must seek medical services as a result of your participation, neither the investigators nor Virginia Tech has funds to pay for these services.

IV. Benefits
The scientific community will benefit through the additional information that is expected to result from the completion of this study. This information will contribute to our understanding of factors that contribute to hip fractures, and may eventually lead to improvements in clinical screening and preventative measures for hip fractures.

No promise or guarantee of benefits has been made to encourage you to participate.

V. Extent of Anonymity and Confidentiality
The results of this research study may be presented at meetings or in publications. Your identity will not be disclosed in those presentations. All subjects will be identified based only on a unique identifying number. Only the investigators will have access to these identifying numbers. We do not anticipate destroying these data in the foreseeable future.

It is possible that the Institutional Review Board (IRB) may view this study's collected data for auditing purposes. The IRB is responsible for the oversight of the protection of human subjects involved in research.

VI. Compensation
Subjects will be paid $10/hour for participation in the study. This will total an estimated $30 for each participant if they complete the entire study.

VII. Freedom to Withdraw
You are free to withdraw from the study at any time without penalty. Should you withdraw, you will be compensated for the portion of the study you complete. You are free to not answer any questions or respond to any experimental situations that you choose without penalty.

VIII. Subject Responsibilities
I voluntarily agree to participate in this study. I have the following responsibilities:

1. Arrive to my scheduled experimental sessions on time.
2. Contact the investigators if a cannot attend a scheduled session.
3. Follow instructions during testing.

IX. Subject's Permission
I have read the Consent Form and conditions of this project. I have had all my questions answered. I hereby acknowledge the above and give my voluntary consent:

____ ________________
Subject signature Date

Investigators:

Michael Madigan, PhD	231-1215	mlmadigan@vt.edu
Dennis Anderson, MS	231-4294	dennisa@vt.edu

If I should have any question about the protection of human research participants regarding this study, I may contact Dr. David Moore, Chair Virginia Tech Institutional Review Board for the Protection of Human Subjects, telephone: (540) 231-4991; email: moored@vt.edu; address: Office of Research Compliance, 2000 Kraft Drive, Suite 2000 (0497), Blacksburg, VA 24060.

Appendix C – Data Collection Sheets

Gait Data Collection Sheet

Subject #: _______________
Date: ___________________
Start Time: ______________

Gait Data Collection Session: Setup Checklist

□. Restart Vicon computer
□. Turn on: (allow 30 minutes to warm up)
- Vicon datastation
- Force plate amp (Donald)
- Treadmill for pacing

□. Open workstation software and create Vicon directory with subject number
□. Start new subsession. Set the default marker file: gait_test.mkr
□. Close blinds
□. Calibrate Vicon cameras
 Make sure calibration is adequate:
  System > Calibrate cameras
  Wand visibility > 70%
  Static reproducibility < 1.0
□. Set Up video Camera.
 Make sure it is centered on force plate & plug in Firewire cable
□. Check Vicon data collection setting
 System > Video setup
  Video sampling rate: 100Hz
 System > Analog setup
  Analog sampling rate: 1000Hz
  Collection channels 13 – 18 (Donald)
 System > Movie setup
  Device: Microsoft DV Camera and VCR
  Mode: DirectX (DV)
  Codec: Microsoft Video 1
□. Check forceplate: not in contact with platform, level
□. Check forceplate (Donald) amp settings: Excitation Voltage = 5.
 From Mz down: CCOC; CCOC; CCOC; CCOC; CCOC; CCOO.
□. Set up pacing belt across lab
□. Set up free walking carpet on walkway. Have SL carpet ready to go.
□. Once everything is warmed up:
- Collect a baseline trial with nothing on the forceplate: __________

□. Get supplies ready:
 □ Lab clothes
 □ Scale, tape, large calipers
 □ Coflex (for wrapping)
 □ Money

□ Reflective markers (36)   □ Rope

□. Randomize order for walking trials using randomize.m. Note order in collection sheet.

1.2 m/s, SL free ______
1.5 m/s, SL free ______
1.2 m/s, SL = 0.65 m ______
1.5 m/s, SL = 0.65 m ______

Gait Data Collection Session: Experimental Protocol

☐ 1. Show subject the lab and explain equipment, walkway, and background of lab

☐ 2. Give summary of study and protocol

☐ 3. Obtain informed consent. Ask subject if we may record video. Would they mind if we used video in presentations? (Y / N)

☐ 4. Give subject proper clothing in which to change (shorts, tank top) and show them to the rest room. Place signs on doors.

☐ 5. Ask subject to remove shoes

☐ 6. Collect information from subject:

Age: ______________   Gender: ____________
Height: ____________ (cm)   Weight: ___________ (kg)
Head circumference: _____________
Neck circumference: _____________
C7 height: _________
Acromion height: __________
Shoulder height: ___________
Shoulder to shoulder width (centers): __________________
Chest height: ______________
L3L4 height: ______________
Waist circumference: _____________
Hip height: _______________
Thigh length (hip to tibial plateau): ________
Hip level torso circumference: ____________
ASIS width: ______________
Mid-thigh circumference: _________
Leg length (tibial plateau to lat malleolus): ______________
Leg maximum circumference: ____________
Lateral malleolus height: __________
Axis depth at chest (back to hip-shoulder axis): ________________
Axis depth at mid-chest L3L4 (back to hip-shoulder axis): ________

Axis depth at L3L4 (back to hip-shoulder axis): _______________

Hip to shoulder angle (+ when shoulder anterior to hip): ________

Head width: ________

Head depth: ________

Shoulder level trunk depth: ______________

Chest level trunk depth: ___________

Mid-chest L3L4 trunk depth: ______

L3L4 level trunk depth: ___________

Chest level trunk width: ___________

Mid-chest L3L4 trunk width: ______

L3L4 level trunk width: ___________

Knee width (lateral to medial epicondyle): ______________

Ankle width (lateral to medial malleolus): ______________

Foot length: ______________

☐ 7. Check subject's shoes for reflection. Apply reflective markers (36).

Feet (L and R, 8 markers)

- □ R calcaneous*
- □ R 1st metatarsal head*
- □ R top of foot*
- □ R 5th metatarsal head*
- □ L calcaneous*
- □ L 1st metatarsal head*
- □ L top of foot*
- □ L 5th metatarsal head*

Shanks (L and R, 10 markers)

- □ R mid-shank† (3 markers: 2 anterior, 1 lateral) *
- □ R medial malleolus
- □ R lateral malleolus
- □ L mid-shank† (3 markers: 2 anterior, 1 lateral) *
- □ L medial malleolus
- □ L lateral malleolus

Thighs (L and R, 10 markers)

- □ R mid-thigh† (3 markers: 2 anterior, 1 lateral) *
- □ R lateral femoral epicondyle
- □ R medial femoral epicondyle
- □ L mid-thigh† (3 markers: 2 anterior, 1 lateral) *
- □ L lateral femoral epicondyle
- □ L medial femoral epicondyle

Pelvis† (4 markers)

- □ R ASIS*
- □ L ASIS*
- □ R PSIS*
- □ L PSIS*

Trunk (4 markers)

- □ T1
- □ Sternal notch
- □ R acromian
- □ L acromian

* Apply markers directly with carpet tape. †Wrap with coflex.

☐ 8. Collect static calibration trials (subject standing on Donald in anatomical position)

Trial number(s):_____________________________

Make sure markers are visible in static calibration. If necessary, redo the static calibration.

☐ 9. Hang balance rope from track. Collect functional joint center calibration trial (subject standing on force plate)

Instruct subject: *Now we will have you perform a series of motions that will help us in analyzing your movements during walking. I will demonstrate each motion, and have you mimic my movements.*

Demonstrate motions as subject moves:

Hip (L and R):	flex, extend, abduct, adduct, circumduct. (Knee remains largely extended).
Knee (L and R):	flex, extend, flex hip and knee, extend hip and knee.
Ankle (L and R):	plantar flex (raise heel), dorsiflex, invert, evert, raise foot off floor, circumduct.
Lumbar:	Lean forward, lean back (hyperextend), lean left, lean right, circumduct.

Trial number(s):______________________________

☐ 10. Self-selected gait trial

Instruct Subject: *Now we will have you walk several times down the walkway at a normal walking pace. Start with your toes at the number I indicate. When I say "go", begin walking, leading off with your right foot. When you reach the other end of the walkway, (next to treadmill), you may return to the start.*

Allow a few practice walks on the walkway; dial in starting location so that right foot is hitting force plate.

Starting point: ______ _____ _____ _____ _____ _____ _____ _____ _____

Collect self-selected gait trial
Trial number(s):______________________________

Controlled Gait trials.
Instruct subject: *In these tests, the treadmill will move this belt at a set speed. You will walk down the walkway, matching pace with the green mark on the belt. (I prefer to walk a little bit behind the mark, following it). When I tell you, walk the next time the marks go by.*

Note: Gait velocity will be checked by examining the mean velocity of a pelvis marker from the trial in Vicon (Graph, Velocity). Acceptable trials will be within 0.965 – 1.065 of the desired velocity. This is a range of ±5%, shifted up by 1.5% to account for difference between forward velocity and the total velocity of the marker seen in Vicon.

Free step length: S*tart with your toes on the line I indicate and your start off with your right foot (as before).*

Controlled step length: *Start with your left foot on the back stripe and your right foot on next, and try to step only on the white stripes while walking.*

☐ 11. Controlled Trial: Speed 1.1 m/s; step length not set. **Perform this trial ________**

Change carpets if needed.
Set treadmill to 1.1 m/s ≈ 2.5 mph.
Allow several practice trials to get subject comfortable.
Collect **3** controlled gait trials.
Check velocity of R ASIS marker. Accept if between 1.0615 – 1.1715 m/s.

Record numbers of accepted trials: ___________________________

☐ 12. Controlled Trial: Speed 1.5 m/s; step length not set. **Perform this trial ________**

Change carpets if needed.
Set treadmill to 1.5 m/s ≈ 3.4 mph.
Allow several practice trials to get subject comfortable.
Collect **3** controlled gait trials.
Check velocity of R ASIS marker. Accept if between 1.4475 – 1.5975 m/s.

Record numbers of accepted trials: ___________________________

☐ 13. Controlled Trial: Speed 1.1 m/s; step length 0.65 m. **Perform this trial ________**

Change carpets if needed.
Set treadmill to 1.1 m/s ≈ 2.5 mph.
Allow several practice trials to get subject comfortable.
Collect **3** controlled gait trials.
Check velocity of R ASIS marker. Accept if between 1.0615 – 1.1715 m/s.

Record numbers of accepted trials: ___________________________

☐ 14. Controlled Trial: Speed 1.5 m/s; step length 0.65 m. **Perform this trial ________**

Change carpets if needed.
Set treadmill to 1.5 m/s ≈ 3.4 mph.
Allow several practice trials to get subject comfortable.
Collect **3** controlled gait trials.
Check velocity of R ASIS marker. Accept if between 1.4475 – 1.5975 m/s.

Record numbers of accepted trials: ____________________________

☐ 15. Remove markers from subject.

☐ 16. Have subject change out of lab clothes.

☐ 17. Thank subject, pay them, and see them out.

☐ 18. Transfer Vicon files to network drive: Y:\Projects\Age_gait

☐ 19. Turn off equipment:
- Vicon datastation
- Force plate amp (Donald)
- Treadmill

☐ 20. Lay carpets flat on walkway

☐ 21. Wrap up pacing belt

☐ 22. Re-tape reflective markers: 24 carpet tape only, 12 carpet and transpore tape.

DXA and Strength Data Collection Sheet

Session 2: DXA Scanning and Strength Testing Setup Checklist

□. Rack position (height and backrest):

From Anthropometry: Hip height: ________cm

L3L4 depth: ________cm

Hip height	>97.0	92.2-97.0	87.5-92.2	82.7-87.5	78 – 82.7	<78
Rack Height	1	2	3	4	5	6

Rack Backrest position # = 0.903 + 0.105*L3L4 depth = ________

Set Backrest Height and Position

Measure Backrest Height, BH (floor to lower edge) ________cm

□. Stuff:

Tailor tape and tape measure
Angle Finder
Drill
Leg Brace
Money
Calculator
Rod
9/16 socket & wrench
Metal Goniometer
Jump Drive

□. Plug in cord in 111. Run cord across hall; put cable guard down. Plug in Biodex.

□. Turn on Biodex

□. Calibrate Biodex (equip_baseline_new.vi)

Position Baseline: _____ Position Coef: _____

Torque Baseline: _____ Torque Coef: _____

□. Start data collection VI (GaitAgeStudy3.vi). Set Torque and Position Baselines and Scale factors. Usual sampling rate is 200 Hz.

□. Set sampling rate and data filename in vi.

Data file name: \ankle_______.txt___

↑subject #

□. Put ankle attachment on Biodex. Put on leg support.

□. Get out hip attachment on long shoulder device.

□. Get out right knee attachment.

□. Adjust the leg brace: Mid-thigh circumference_________cm.

Leg max circumference__________cm.

AGE & GAIT STUDY
Session 2 Data Collection Sheet (Modified 10/01/2008)

Subject #: _______________
Date: ___________________

Start Time: ______________

Time for DXA scan: _____________. If there's a problem, call 1-8299

☐ 1. Greet Subject. Thank them for coming back. Describe testing session to them.

☐ 2. Take measurements for hip testing positioning (shoes on)

Trochanter Height (TR): _________ cm
ASIS Height (ASIS): _________ cm
Pelvic (ASIS) Width (PW): _________ cm

Calculations: Pelvic Height, PH = ASIS - TR = ________ cm
Hip Height, HH = TR + 0.21*PH = ________ cm

Positions for Flexion-Extension setup:
Footrest Height, FH = BH – (HH+ASIS)/2 = ________ cm
Dynamometer Height # = (HH+FH)*0.3927 – 32.739 = _______
Positions for Ab-Adduction setup:
Dynamometer Height # = HH*0.3927 – 26.849 = ________
Belt Board Position # = 0.21* ASIS – 14.832 = ________
M-L Distance from ASIS to Hip Joint Center, MLH:
0.14 * PW = ____________cm

Note Positions in spaces given (Steps 32 and 41).

Obtain DXA Scans

☐ 3. Escort subject to Human Integrative Physiology Laboratory (228 War Memorial)

☐ 4. Have subject get in appropriate apparel (if needed)

☐ 5. Perform pregnancy test for younger female subjects.

☐ 6. Explain scanning process.

☐ 7. Create patient file in system based on subject number.

☐ 9. Obtain full body scan.

☐ 11. Obtain right hip scan.

☐ 12. Return to Norris Hall.

ANKLE PROTOCOL

☐ 13. Have subject remove shoes.

☐ 14. Biodex positioning

Set Backrest Rotation to 70
Set dynamometer base at 17.5
Adjust so knee angle is about 130° and hip angle is about 100°.

☐ 15. Set and record Range of Motion: Away = Plantarflexion
Toward = Dorsiflexion

Biodex angles: PF_____ DF_____

☐ 16. Find line between lateral epicondyle and lateral malleolus. Measure angle with angle finder. Set arm of ankle attachment to identical angle.

Neutral joint angle from Biodex ______

☐ 17. Passive motion. Set Biodex to passive, 5 deg/s. and turn up torque to about 100.

Instruct subject: *Remain relaxed. Concentrate on not flexing your ankle muscles.*

Collect 2 full cycles of motion: _____

☐ 18. Isometric Dorsiflexion exertions

Set Biodex to Isometric mode. Position foot: Neutral – 15° = _________
Set baseline torque in vi.
Set tank scaling: Manual; 33 N-m.

Instruct subject: When I tell you, pull your toes up as hard as you can. Do not jerk, but increase force steadily to your maximum, hold for a couple seconds, and release. This indicator on the screen will show how hard you are pulling. Try to go as high as you can, and surpass the yellow line.

Switch to Collection Mode, collect trial.

	Trial 1	Trial 2	Trial 3	Trial 4	Trial 5
Collection #					
Max Torque					

Repeat 3 times minimum, 5 times max, with 1 minute rest breaks in between. If max > previous trials, switch back to Realtime Mode to update tank scaling and continue on to next trial.

During breaks, set up foot blocks for Hip FE.

☐ 19. Isometric Plantar flexion Exertions

Position foot: smaller of Neutral + 26° or DF end of ROM = _________
Set baseline torque in vi.
Set tank scaling: Manual; 125 N-m.

Instruct subject: When I tell you push your toes down as hard as you can. Do not jerk, but increase force steadily to your maximum, hold for a couple seconds, and release. This indicator on the screen will show how hard you are pulling. Try to go as high as you can, and surpass the yellow line.

Switch to Collection Mode, collect trial. Check if heel is coming off foot plate, and monitor straps during test.

	Trial 1	Trial 2	Trial 3	Trial 4	Trial 5
Collection #					
Max Torque					

Repeat 3 times minimum, 5 times max, with 1 minute rest breaks in between. If max > previous trials, switch back to Realtime Mode to update tank scaling and continue on to next trial.

☐ 21. **Switch to Knee setup.**

KNEE PROTOCOL

☐ 22. **Change** data filename in vi. **Reset collection number.**

Data file name: \knee_______.txt____
↑subject #

☐ 23. Biodex positioning

Set Seatback Angle to 70
Set seatback position so subject is all the way back when knee is flexed.
Align axis of rotation with lateral femoral condyle.
If pad slides down leg when extending, move seat up or forward.
If pad slides up leg when extending, move seat down or back.
Place straps across lap and chest.

☐ 24. Set and record Range of Motion: Away = Extended
Toward = Flexed

Biodex angles: KE_____ KF_____

☐ 25. Biodex angle at neutral joint position = angle at full extension: ____

☐ 26. Passive motion. Set Biodex to passive, 5 deg/s. and turn up torque to about 100.
Instruct subject: *Remain relaxed. Concentrate on not flexing your knee muscles.*
Collect 2 full cycles of motion: _____

☐ 27. Isometric Knee flexion Exertions
Set Biodex to Isometric mode. Position leg: Neutral – 30° = __________
Set baseline torque in vi.
Set tank scaling: Manual; 90 N-m.

Instruct subject: When I tell you, try to bend your leg at the knee as hard as you can. Do not jerk, but increase force steadily to your maximum, hold for a couple seconds, and release. Try to go as high as you can, and surpass the yellow line.

Switch to Collection Mode, collect trial.

	Trial 1	Trial 2	Trial 3	Trial 4	Trial 5
Collection #					
Max Torque					

Repeat 3 times minimum, 5 times max, with 1 minute rest breaks in between. If max > previous trials, switch back to Realtime Mode to update tank scaling and continue on to next trial.

☐ 28. Isometric Knee Extension Exertions

Set Biodex to Isometric mode. Position leg: Neutral – 67° = _________

Set baseline torque in vi.

Set tank scaling: Manual; 180 N-m.

Instruct subject: When I tell you, try to bend your leg at the knee as hard as you can. Do not jerk, but increase force steadily to your maximum, hold for a couple seconds, and release. Try to go as high as you can, and surpass the yellow line.

Switch to Collection Mode, collect trial.

	Trial 1	Trial 2	Trial 3	Trial 4	Trial 5
Collection #					
Max Torque					

Repeat 3 times minimum, 5 times max, with 1 minute rest breaks in between. If max > previous trials, switch back to Realtime Mode to update tank scaling and continue on to next trial.

☐ 30. **Switch to Hip Flexion/Extension Setup. Have subject put shoes back on.**

HIP FLEXION/EXTENSION PROTOCOL

☐ 31. **Change** data filename in vi. **Reset collection number.**

Data file name: \hipFE______.txt____

↑subject #

☐ 32. Set Footrest Height = ________ cm ; Dynamometer Height # = _______

Create support equivalent to footrest height.

Put knee brace on subject. Strap onto rack.

☐ 33. Set and record Range of Motion: Away = Back

Toward = Front

Biodex angles: HE_____ HF_____

☐ 34. Set right knee even with left knee; record neutral joint angle from Biodex: ______

☐ 35. Passive motion. Set Biodex to passive, 5 deg/s. and turn up torque to about 150.

Instruct subject: *Remain relaxed. Concentrate on not flexing your muscles.*

Collect 2 full cycles of motion: _____

☐ 36. Isometric Hip Flexion Exertions

Set Biodex to Isometric mode.

Position leg: Neutral – 15° or HE end of ROM = _________

Set tank scaling: Manual; 125 N-m.

Set baseline torque in vi.

Instruct subject: When I tell you, try to pull your leg forward/up as hard as you can. Do not jerk, but increase force steadily to your maximum, hold for a couple seconds, and release. Try to go as high as you can, and surpass the yellow line.

Switch to Collection Mode, collect trial.

	Trial 1	Trial 2	Trial 3	Trial 4	Trial 5
Collection #					
Max Torque					

Repeat 3 times minimum, 5 times max, with 1 minute rest breaks in between. If max > previous trials, switch back to Realtime Mode to update tank scaling and continue on to next trial.

☐ 37. Isometric Hip Extension Exertions
Position leg: Neutral + 68° or HF end of ROM = _________
Set tank scaling: Manual; 190 N-m.
Set baseline torque in vi.
Instruct subject: When I tell you, try to pull your leg down/back as hard as you can. Do not jerk, but increase force steadily to your maximum, hold for a couple seconds, and release. Try to go as high as you can, and surpass the yellow line.
Switch to Collection Mode, collect trial.

	Trial 1	Trial 2	Trial 3	Trial 4	Trial 5
Collection #					
Max Torque					

Repeat 3 times minimum, 5 times max, with 1 minute rest breaks in between. If max > previous trials, switch back to Realtime Mode to update tank scaling and continue on to next trial.

Whenever paused, place support under the right foot.

☐ 39. **Switch to Hip Abduction/Adduction.**

HIP ABDUCTION/ADDUCTION PROTOCOL

☐ 40. **Change** data filename in vi. **Reset collection number.**
Data file name: \hipAA_____.txt___________
↑subject #

☐ 41. Set Board height ________ ;
Dynamometer Height # = _______
M-L ASIS distance _______.
Strap in; adjust straps to approx M-L distance.

☐ 42. Set and record Range of Motion: Away = Out
Toward = In = Neutral
Biodex angles: ABduct_____ ADduct_____

☐ 43. Passive motion. Set Biodex to passive, 5 deg/s. and turn up torque to about 150.
Instruct subject: *Remain relaxed. Concentrate on not flexing your muscles.*
Collect 2 full cycles of motion: _____

☐ 44. Isometric Hip Abduction Exertions
Set Biodex to Isometric mode. Position leg: ADDuct end

Set tank scaling: Manual; 80 N-m.
Set baseline torque in vi.

Instruct subject: When I tell you, try to pull your leg out to the right as hard as you can. Do not jerk, but increase force steadily to your maximum, hold for a couple seconds, and release. Try to go as high as you can, and surpass the yellow line.

Switch to Collection Mode, collect trial.

	Trial 1	Trial 2	Trial 3	Trial 4	Trial 5
Collection #					
Max Torque					

Repeat 3 times minimum, 5 times max, with 1 minute rest breaks in between. If max > previous trials, switch back to Realtime Mode to update tank scaling and continue on to next trial.

☐ 45. Isometric Hip Adduction Exertions

Set Biodex to Isometric mode. Position leg: ABDuct end
Set tank scaling: Manual; 160 N-m.
Set baseline torque in vi.

Instruct subject: When I tell you, try to pull your leg in as hard as you can. Do not jerk, but increase force steadily to your maximum, hold for a couple seconds, and release. Try to go as high as you can, and surpass the yellow line.

Switch to Collection Mode, collect trial.

	Trial 1	Trial 2	Trial 3	Trial 4	Trial 5
Collection #					
Max Torque					

Repeat 3 times minimum, 5 times max, with 1 minute rest breaks in between. If max > previous trials, switch back to Realtime Mode to update tank scaling and continue on to next trial.

Whenever paused, place support under the right foot.

☐ 46. Record end time: _______________

☐ 4. Have subject change out of lab clothes.

☐ 49. Thank subject, pay them, see them out.

☐ 50. Transfer Biodex files to network drive. Save DXA files to network drive.

☐ 51. Turn off Biodex; Remove HipAA boards; unplug and stow cord and cable guard.

Appendix D - Additional Model Information

Musculoskeletal Models

Musculoskeletal models were used for inverse dynamics in Study 1, and to determine muscle and joint reaction forces in Study 2 (Figure D.1). The models for Study 2 were subsets of the Study 1 models, with individualized muscle models defined. All joints in the models were defined as ball joints, allowing three independent axes of rotation. This allowed the models to more closely follow marker position data when performing inverse kinematics. The positions of joint centers in the models were determined by functional methods. For example, fitting thigh marker motions to spheres centered in the pelvic coordinate system provides the functional center of the hip joint in the pelvic system (Hicks and Richards 2005; Piazza et al. 2004; Piazza et al. 2001). This approach provides improved results over anthropometric estimates when a special calibration trial is performed (Hicks and Richards 2005; Piazza et al. 2004). A separate trial was performed prior to gait testing in which each participant moved each joint through its range of motion. A custom program was created in Matlab (The MathWorks Inc., Natick, Massachusetts, USA), which used the algorithm of Piazza et al. (2004) to determine joint center locations using marker data from this trial.

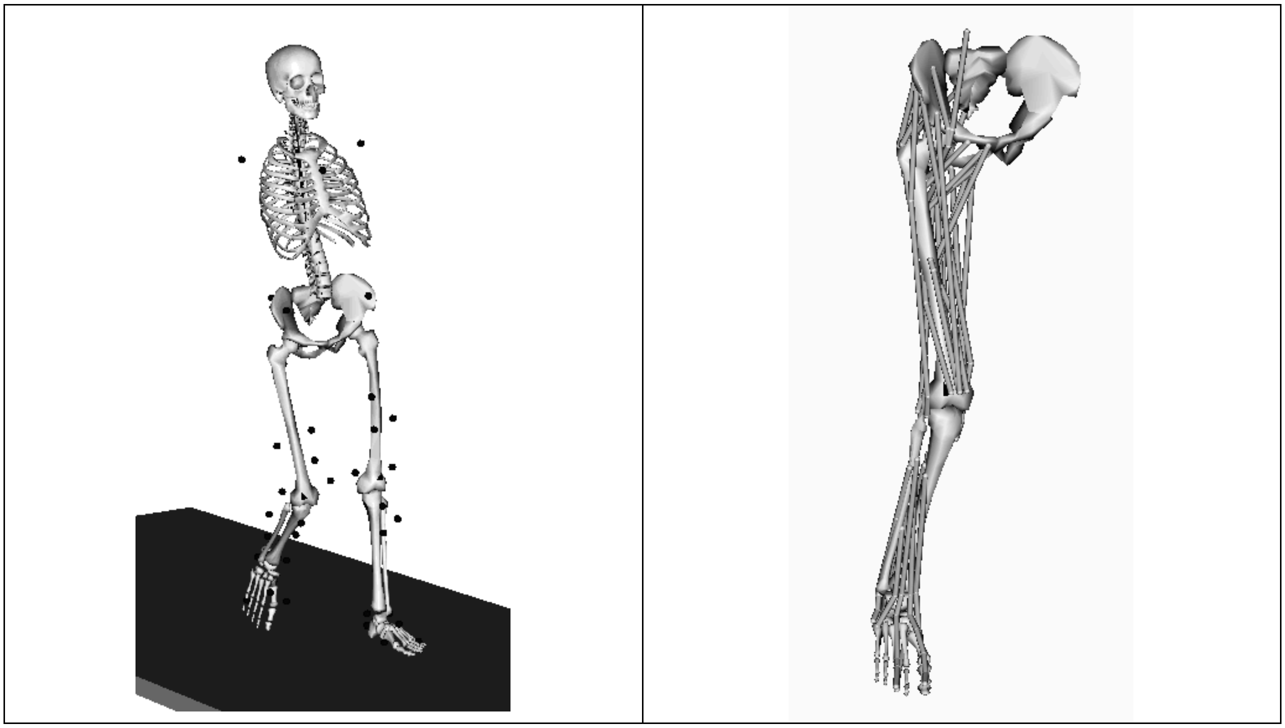

Figure D.1: Examples of the models used for inverse dynamics in Study 1 (left) and static optimization in Study 2 (right).

When performing static optimization, the muscles were not capable of stabilizing the abduction/adduction and rotation degrees of freedom in the knee, or the inversion/eversion and rotation degrees of freedom in the ankle. However, locking these degrees of freedom during static optimization sometimes resulted in undesirable errors in the kinematics, and hence errors in estimated muscle forces. To address this issue, generalized force actuators were added to the model for these degrees of freedom. In OpenSim, generalized force actuators can be created to actuate either translational or rotational degrees of freedom. Thus, these actuators applied torques to these degrees of freedom, stabilizing the model during static optimization.

To determine hip joint reaction forces during gait, additional degrees of freedom and generalized forces were added to the model. Specifically, translational degrees of freedom were added to the hip joint, thus allowing the femur to translate with respect to the pelvis. Generalized force actuators were created for these degrees of freedom. The translation of the femur relative to the pelvis was set to zero in the kinematics file, effectively constraining the hip to its three rotational degrees of freedom. The forces applied by the generalized force actuators to keep the hip in place were the hip joint reaction forces in global coordinates, and were determined during static optimization.

Maximum Isometric Muscle Force Estimates

Individualized maximum isometric muscle forces for the musculoskeletal models were based on isometric joint torques measured using a Biodex System 3 dynamometer. Participants performed maximum voluntary exertions for ankle plantar flexion and dorsiflexion, knee flexion and extension, and hip flexion, extension, abduction and adduction. For each torque measurement, the musculoskeletal model was set in the testing position, and moment arms and force-length factors determined for each muscle. From this information, the joint torque produced by the model could be estimated as:

$$Torque = \sum_{m=1}^{43} F_m MA_m FL_m$$

where F is maximum isometric torque, MA is moment arm, and FL is the force-length factor. The resulting torque values were compared to measured torques, and the maximum isometric forces adjusted based on the error. Because many muscles contributed to more than one measured torque, maximum isometric forces were adjusted iteratively. The initial values for the maximum isometric muscle forces in the process were based on physiological cross-sectional area information (Brand et al. 1986; Klein Horsman et al. 2007) multiplied by a maximum muscle stress of 1 MPa. While the magnitude of these initial forces was relatively large (Table D.1), this was not of great concern as the primary purpose of the initial values was to provide relative sizes of muscle forces, and the magnitudes would be adjusted.

Using the measured joint torques directly to estimate muscle forces in the manner described resulted in musculoskeletal models that were in some cases too weak to produce the required forces during gait. There are thought to be two primary reasons for this. First, errors in joint torque measurements may have underestimated maximum voluntary torques in some cases. Secondly, the process as described does not account for the fact that the musculoskeletal system must act to stabilize the joint as well as producing a maximum torque. This was a particular problem in the hip where, for example, muscles could be strong enough to produce a peak hip extension torque, but not simultaneously stabilize the hip in the abduction/adduction direction. To produce models that had the required strength, measured joint torques were multiplied by the following factors prior to being used in muscle force determination: 1.5 for dorsiflexion, plantar flexion, knee flexion and knee extension, 1.8 for hip flexion and hip extension, and 2.1 for hip abduction and adduction.

The individualized maximum isometric muscle forces determined for the models compared relatively well (Table D.1) with the maximum isometric muscle forces present originally in the musculoskeletal model (Delp et al. 1990). This seems indicate that the increasing the measured joint torques as described did not result in the models having excessive strength. A two-way mixed-model ANOVA examining average maximum isometric muscle forces normalized by body weight showed muscle forces were lower in older adults ($p = 0.0465$) and, not surprisingly, varied between muscles ($p < 0.001$). Individual muscles that showed significant age differences in independent t-tests are indicated in Table D.1.

Table D.1: Maximum isometric muscle forces in the musculoskeletal model. *Initial* indicates initial values for force estimation process. Mean (standard deviation) values are given for young and older adults in terms of force (N) and percent body weight (%BW). *Original* provides values from original OpenSim model for comparison. Forces that are significantly greater in young adults ($p < 0.05$) are displayed in bold.

Muscle	Initial (N)	Older (N)	Young (N)	Original (N)	Older (%BW)	Young (%BW)
Add. Brevis	968	298 (58)	508 (232)	429	**43.9 (7.3)**	**78.8 (30.0)**
Add. Longus	1647	610 (101)	999 (409)	627	**90.0 (11.6)**	**154.6 (50.6)**
Add. Magnus 1	1679.25	480 (119)	849 (412)	381	**70.8 (15.7)**	**131.9 (54.3)**
Add. Magnus 2	1469.25	387 (106)	678 (342)	343	**57.2 (14.2)**	**105.4 (45.7)**
Add. Magnus 3	1431	395 (121)	707 (367)	488	**58.3 (16.1)**	**110.1 (49.4)**
Bic. Fem. (LH)	2791.25	755 (219)	1230 (569)	896	**111.5 (29.3)**	**192.0 (75.7)**
Bic. Fem. (SH)	1099.5	217 (51)	284 (99)	804	**31.8 (5.7)**	**44.5 (12.6)**
Ext. Dig. Long.	1011.25	308 (79)	351 (61)	512	45.2 (8.8)	56.0 (10.5)
Ext. Hall. Long.	666	203 (52)	231 (40)	162	29.8 (5.8)	36.9 (6.9)
Flex. Dig. Long.	794.25	216 (68)	257 (95)	310	32.1 (10.5)	40.4 (12.7)
Flex. Hall. Long.	2127.75	580 (183)	688 (255)	322	86.1 (28.1)	108.3 (34.0)
Gemellus	525	198 (44)	373 (189)	164	**29.2 (6.1)**	**57.8 (25.1)**
Glut. Maximus 1	1636	572 (159)	968 (458)	573	**84.4 (21.3)**	**150.8 (60.6)**
Glut. Maximus 2	2345.5	847 (298)	1572 (840)	819	**125.2 (41.4)**	**245.2 (114.3)**
Glut. Maximus 3	1644.75	469 (142)	843 (439)	552	**69.2 (19.3)**	**131.3 (59.3)**
Glut. Medius 1	2311.75	763 (176)	1091 (406)	819	**112.3 (20.9)**	**169.4 (48.7)**
Glut. Medius 2	1664.75	558 (126)	831 (325)	573	**82.2 (15.3)**	**129.3 (40.1)**
Glut. Medius 3	1898.75	649 (157)	1030 (446)	653	**95.7 (20.1)**	**160.3 (57.3)**
Glut. Minimus 1	782.5	258 (60)	369 (137)	270	**38.0 (7.1)**	**57.3 (16.5)**
Glut. Minimus 2	764	252 (58)	360 (134)	285	**37.1 (6.9)**	**56.0 (16.1)**
Glut. Minimus 3	817.5	271 (62)	389 (144)	323	**39.9 (7.4)**	**60.5 (17.3)**
Gracilis	343.25	92 (23)	153 (69)	162	**13.5 (2.9)**	**23.8 (9.0)**
Iliacus	1942.75	1045 (182)	1746 (692)	1073	**154.2 (20.3)**	**270.7 (84.5)**
Lat. Gastroc.	2035	500 (127)	610 (216)	683	74.0 (18.5)	95.9 (28.3)
Med. Gastroc.	4370	1077 (276)	1313 (466)	1558	159.5 (40.2)	206.3 (61.0)
Pectineus	604.5	242 (39)	397 (162)	266	**35.7 (4.5)**	**61.5 (20.1)**
Peroneus Brevis	1599.5	436 (138)	517 (191)	435	64.7 (21.1)	81.4 (25.5)
Peroneus Longus	2402	654 (207)	777 (287)	943	97.2 (31.7)	122.3 (38.4)
Peroneus Tertius	422	129 (33)	147 (25)	180	18.9 (3.7)	23.4 (4.4)
Piriformis	1073	368 (91)	592 (262)	444	**54.3 (11.8)**	**92.1 (33.8)**
Psoas Major	1579.25	854 (150)	1426 (566)	1113	**125.9 (16.7)**	**221.2 (69.1)**
Quad. Femoris	1112.25	379 (94)	691 (336)	381	**55.9 (12.5)**	**107.4 (44.3)**
Rect. Femorus	3378.25	1576 (348)	2438 (889)	1169	**231.7 (38.0)**	**378.0 (104.3)**
Sartorius	554.5	245 (42)	369 (137)	156	**36.1 (4.7)**	**57.2 (16.3)**
Semimem.	4270	1142 (329)	1834 (837)	1288	**168.6 (43.6)**	**286.4 (111.3)**
Semitend.	1009.75	263 (73)	429 (200)	410	**38.8 (9.5)**	**67.0 (26.5)**
Soleus	15294	4166 (1316)	4948 (1830)	3549	619.0 (202.1)	778.4 (244.3)
Tens. Fasc. Latae	674.75	281 (56)	423 (158)	233	**41.5 (6.5)**	**65.7 (18.9)**
Tibialis Anterior	2287.25	697 (178)	795 (137)	905	102.3 (19.9)	126.8 (23.8)
Tibialis Posterior	3480.25	948 (299)	1126 (416)	1588	140.9 (46.0)	177.1 (55.6)
Vastus Intermed.	5630.25	1699 (688)	2599 (977)	1365	**247.1 (83.6)**	**403.1 (116.3)**
Vastus Lateralis	7458.5	2250 (912)	3443 (1294)	1871	**327.3 (110.7)**	**534.0 (154.0)**
Vastus Medialis	4700.5	1418 (575)	2170 (815)	1294	**206.3 (69.8)**	**336.6 (97.1)**

Convergence Check

The VAKHUM project (Van Sint Jan 2008) has six levels of mesh refinement (Table D.2) available for the femur model. To select the refinement to use, all six were tested under a simple loading condition, and the results compared. The loading condition was a hip joint contact force of 711 N posteriorly, 2700 N downward and 702 N laterally. Maximum deflections, which occurred at the top of the femoral head, were determined and error estimated for each mesh refinement. In order to estimate error, an estimate of the true deflection was made by comparing the calculated deflections to the characteristic element size, h, of each mesh (Cook et al. 2002). Characteristic element size was taken as the inverse of the cube root of the number of elements. Because hexahedral elements were used, this value is proportional to the average length of element edges in each mesh. A linear least-squares fit was found (Figure D.2), and the intercept of the best fit line, 76.909 mm, was taken as the true deflection.

Table D.2: Information on the different refinements of the femur model available from the VAKHUM project and results of convergence testing.

Refinement	1	2	3	4	5	6
Nodes	6941	9294	13740	20279	44502	115835
Elements	5884	7934	11842	17696	39443	104945
Materials	194	201	208	217	249	286
Maximum Deflection (mm)	79.58	79.24	79.20	77.29	78.82	77.92
Characteristic element size, *h*	0.0554	0.0501	0.0439	0.0384	0.0294	0.0212
Estimated Error (%)	3.47	3.03	2.98	0.50	2.48	1.31

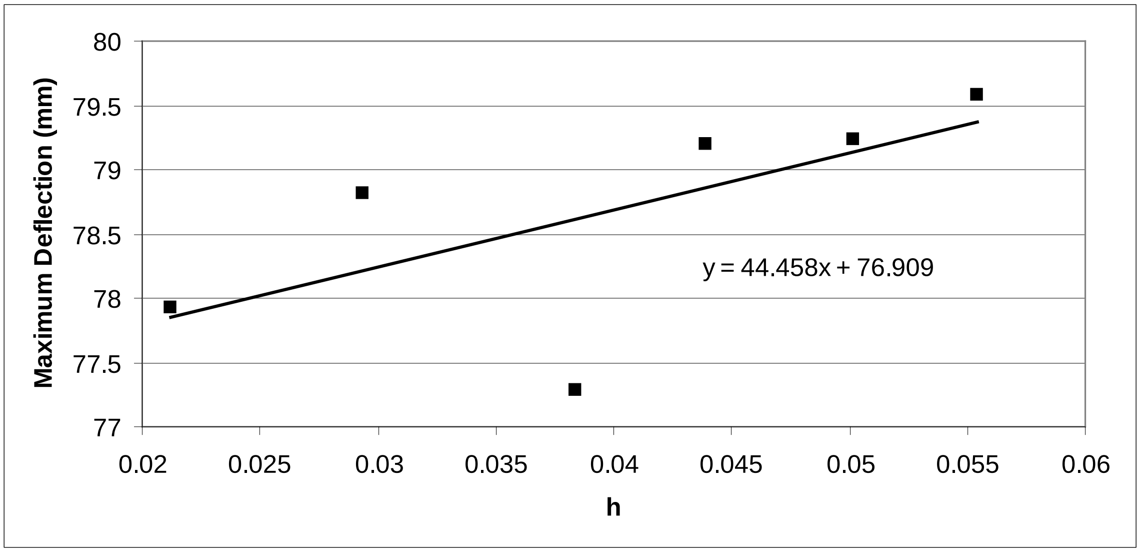

Figure D.2: Linear least-squares best fit of maximum deflection to characteristic element size. The intercept of the best fit equation was used as true deflection for error calculations.

Estimated error (Table D.2) was lowest for Refinement 4 by far, and Refinement 4 was chosen for use. In fact, Refinement 4 appeared to be somewhat of an outlier as compared to the other meshes. However, even if it was excluded from the linear fit, it still had the smallest estimated error. Increasing mesh refinement tended to stiffen the bone, reducing maximum deflection. More typically, mesh refinement "softens" a structure, leading to greater deflections. A possible explanation for this is that the more refined meshes represent the material non-homogeneity better, creating a more realistic and stiffer "cortical shell". In the course of the convergence check, it was also determined that full integration should be used, as using reduced integration "softened" the bone significantly and led to larger errors in deflection.

Finite Element Model Loading and Boundary Conditions

Loading and boundary conditions of the finite element models in Study 2 included hip contact forces applied as pressures, muscle forces applied as concentrated forces, and fixed zero-displacement boundary conditions at the knee (Figure D.3). Note that in Abaqus, a concentrated force is a linear force that is applied directly to one or more points or nodes. Pressure forces were used instead of concentrated forces at the hip because the direction of concentrated forces remained in the direction of the global coordinate system despite the deflection of the femoral head. The result of this was excessive deflection of the femoral head. Pressure loads by definition act normal to the surface they are applied to. Three “blocks” were created on the acetabulum part to create surfaces for easier application of the pressure loads. By using pressure loads and turning on nonlinear geometry in the solver, the hip contact forces followed the rotation of the femoral head. This gave more realistic results and reduced deflection of the femoral head by about 23%.

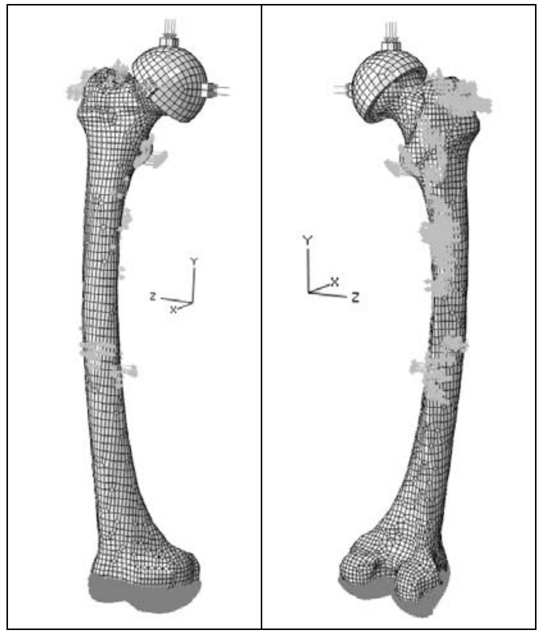

Figure D.3: Finite element model for Study 2, from antero-medial (left) and postero-lateral (right) directions. Hip joint contact forces were applied as pressure loads on the acetabulum part. Light grey arrows indicate applied muscle forces, and dark grey at the distal femur indicates fixed boundary conditions.

Muscle forces were applied as concentrated forces distributed across multiple nodes. All muscle forces were evenly distributed across eight nodes, except for the iliopsoas and gluteus maximus 2/iliotibal band forces, which were applied to 20 nodes due to their greater magnitudes. The locations of the muscle forces were determined by finding the nodes geometrically nearest to the attachment point of the muscle in the musculoskeletal model. This was felt to be appropriate, because it most accurately modeled the application of the forces as calculated by static optimization. Although this was a simplification anatomically speaking, it has been shown that the application of concentrated loads at the centroids of muscle attachment areas can provide a reasonable estimate of physiological strains in the femur (Polgar et al. 2003).

In Study 3 the boundary conditions were reversed from Study 2, with fixed boundary conditions at the hip and loading applied at the knee. It was desired to fix the femoral head to better determine the effects of muscle forces on strains in the proximal femur while maintaining an equivalent state of strain under baseline loading conditions. In order to more simply carry out this change, an additional part was added to the model at the distal femur (Figure D.4), allowing application of the knee conditions to a limited number of nodes. The model was first solved in the original way, with pressure loads at the femoral head and fixed zero-displacement boundary conditions at the knee. The displacements at the femoral head and reaction forces at the knee thus determined were then applied to the model as boundary conditions for Study 3.

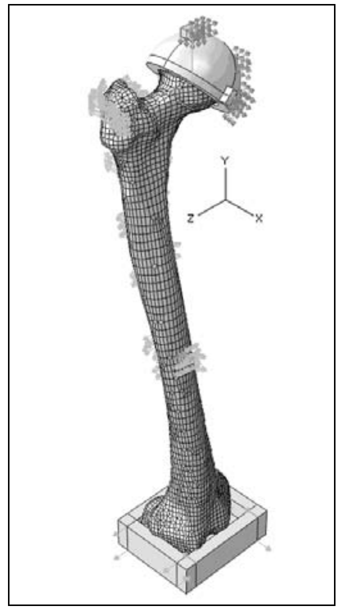

Figure D.4: The finite element model for Study 3, showing the additional part added to apply loading at the distal femur.

References

Brand, R. A., Pedersen, D. R., and Friederich, J. A., 1986. The sensitivity of muscle force predictions to changes in physiologic cross-sectional area. Journal of Biomechanics 19, 589-596.

Cook, R. D., Malkus, D. S., Plesha, M. E., and Witt, R. J. 2002. Concepts and Applications of Finite Element Analysis. Fourth ed. John Wiley & Sons, Hoboken, NJ.

Delp, S. L., Loan, J. P., Hoy, M. G., Zajac, F. E., Topp, E. L., and Rosen, J. M., 1990. An interactive graphics-based model of the lower extremity to study orthopaedic surgical procedures. IEEE Transactions on Biomedical Engineering 37, 757-767.

Hicks, J. L., and Richards, J. G., 2005. Clinical applicability of using spherical fitting to find hip joint centers. Gait & Posture 22, 138-145.

Klein Horsman, M. D., Koopman, H. F., van der Helm, F. C., Prose, L. P., and Veeger, H. E., 2007. Morphological muscle and joint parameters for musculoskeletal modelling of the lower extremity. Clinical Biomechanics 22, 239-247.

Piazza, S. J., Erdemir, A., Okita, N., and Cavanagh, P. R., 2004. Assessment of the functional method of hip joint center location subject to reduced range of hip motion. Journal of Biomechanics 37, 349-356.

Piazza, S. J., Okita, N., and Cavanagh, P. R., 2001. Accuracy of the functional method of hip joint center location: effects of limited motion and varied implementation. Journal of Biomechanics 34, 967-973.

Polgar, K., Gill, H. S., Viceconti, M., Murray, D. W., and O'Connor, J. J., 2003. Strain distribution within the human femur due to physiological and simplified loading: finite element analysis using the muscle standardized femur model. Proceedings of the Institution of Mechanical Engineers. Part H, Journal of Engineering in Medicine 217, 173-189.

Van Sint Jan, S. 2008. *The VAKHUM Project: Virtual Animation of the Kinematics of the Human for Industrial, Educational and Research Purposes* 2008 [cited 2008]. Available from http://www.ulb.be/project/vakhum/.

Appendix E – Permissions and Fair Use

Figure 2.2
Marks, R., Allegrante, J. P., Ronald MacKenzie, C., and Lane, J. M., 2003. Hip fractures among the elderly: causes, consequences and control. Ageing Research Reviews 2, 57-93. http://www.sciencedirect.com/science/journal/15681637 (Accessed March 5, 2010). Used with permission of Elsevier, letter attached.

Figure 4.1
Gray, H. 1918. Anatomy of the Human Body, 20th Edition. Place Published: Philadelphia: Lea & Febiger. http://www.bartleby.com/107/illus243.html (Accessed March 5, 2010). Fair use determination attached.

Figure 4.2
Keyak, J. H., Rossi, S. A., Jones, K. A., and Skinner, H. B., 1998. Prediction of femoral fracture load using automated finite element modeling. Journal of Biomechanics 31, 125-133. http://www.sciencedirect.com/science/journal/00219290 (Accessed March 5, 2010)
Used with permission of Elsevier, letter attached.

Figure 4.3
Gray, H. 1918. Anatomy of the Human Body, 20th Edition. Place Published: Philadelphia: Lea & Febiger. http://www.bartleby.com/107/illus249.html (Accessed March 5, 2010). Fair use determination attached.

Figure 4.4
Keyak, J. H., and Falkinstein, Y., 2003. Comparison of in situ and in vitro CT scan-based finite element model predictions of proximal femoral fracture load. Medical Engineering & Physics 25, 781-787. http://www.sciencedirect.com/science/journal/13504533 (Accessed March 5, 2010)
Used with permission of Elsevier, letter attached.

ELSEVIER LICENSE
TERMS AND CONDITIONS

Mar 02, 2010

This is a License Agreement between Dennis E Anderson ("You") and Elsevier ("Elsevier") provided by Copyright Clearance Center ("CCC"). The license consists of your order details, the terms and conditions provided by Elsevier, and the payment terms and conditions.

All payments must be made in full to CCC. For payment instructions, please see information listed at the bottom of this form.

Supplier	Elsevier Limited The Boulevard,Langford Lane Kidlington,Oxford,OX5 1GB,UK
Registered Company Number	1982084
Customer name	Dennis E Anderson
Customer address	ESM Department (0219) Blacksburg, VA 24061
License Number	2380841000564
License date	Mar 02, 2010
Licensed content publisher	Elsevier
Licensed content publication	Ageing Research Reviews
Licensed content title	Hip fractures among the elderly: causes, consequences and control
Licensed content author	Ray Marks, John P. Allegrante, C. Ronald MacKenzie, Joseph M. Lane
Licensed content date	January 2003
Volume number	2
Issue number	1
Pages	37
Type of Use	Thesis / Dissertation
Portion	Figures/tables/illustrations
Number of Figures/tables/illustrations	1
Format	Both print and electronic
You are an author of the Elsevier article	No
Are you translating?	No
Order Reference Number	
Expected publication date	May 2010
Elsevier VAT number	GB 494 6272 12
Permissions price	0.00 USD
Value added tax 0.0%	0.00 USD
Total	0.00 USD
Terms and Conditions	

INTRODUCTION

1. The publisher for this copyrighted material is Elsevier. By clicking "accept" in connection with completing this licensing transaction, you agree that the following terms and conditions apply to this transaction (along with the Billing and Payment terms and conditions

established by Copyright Clearance Center, Inc. ("CCC"), at the time that you opened your Rightslink account and that are available at any time at http://myaccount.copyright.com).

GENERAL TERMS

2. Elsevier hereby grants you permission to reproduce the aforementioned material subject to the terms and conditions indicated.

3. Acknowledgement: If any part of the material to be used (for example, figures) has appeared in our publication with credit or acknowledgement to another source, permission must also be sought from that source. If such permission is not obtained then that material may not be included in your publication/copies. Suitable acknowledgement to the source must be made, either as a footnote or in a reference list at the end of your publication, as follows:

"Reprinted from Publication title, Vol /edition number, Author(s), Title of article / title of chapter, Pages No., Copyright (Year), with permission from Elsevier [OR APPLICABLE SOCIETY COPYRIGHT OWNER]." Also Lancet special credit - "Reprinted from The Lancet, Vol. number, Author(s), Title of article, Pages No., Copyright (Year), with permission from Elsevier."

4. Reproduction of this material is confined to the purpose and/or media for which permission is hereby given.

5. Altering/Modifying Material: Not Permitted. However figures and illustrations may be altered/adapted minimally to serve your work. Any other abbreviations, additions, deletions and/or any other alterations shall be made only with prior written authorization of Elsevier Ltd. (Please contact Elsevier at permissions@elsevier.com)

6. If the permission fee for the requested use of our material is waived in this instance, please be advised that your future requests for Elsevier materials may attract a fee.

7. Reservation of Rights: Publisher reserves all rights not specifically granted in the combination of (i) the license details provided by you and accepted in the course of this licensing transaction, (ii) these terms and conditions and (iii) CCC's Billing and Payment terms and conditions.

8. License Contingent Upon Payment: While you may exercise the rights licensed immediately upon issuance of the license at the end of the licensing process for the transaction, provided that you have disclosed complete and accurate details of your proposed use, no license is finally effective unless and until full payment is received from you (either by publisher or by CCC) as provided in CCC's Billing and Payment terms and conditions. If full payment is not received on a timely basis, then any license preliminarily granted shall be deemed automatically revoked and shall be void as if never granted. Further, in the event that you breach any of these terms and conditions or any of CCC's Billing and Payment terms and conditions, the license is automatically revoked and shall be void as if never granted. Use of materials as described in a revoked license, as well as any use of the materials beyond the scope of an unrevoked license, may constitute copyright infringement and publisher reserves the right to take any and all action to protect its copyright in the materials.

9. Warranties: Publisher makes no representations or warranties with respect to the licensed material.

10. Indemnity: You hereby indemnify and agree to hold harmless publisher and CCC, and their respective officers, directors, employees and agents, from and against any and all claims arising out of your use of the licensed material other than as specifically authorized pursuant to this license.

11. No Transfer of License: This license is personal to you and may not be sublicensed, assigned, or transferred by you to any other person without publisher's written permission.

12. No Amendment Except in Writing: This license may not be amended except in a writing

signed by both parties (or, in the case of publisher, by CCC on publisher's behalf).

13. Objection to Contrary Terms: Publisher hereby objects to any terms contained in any purchase order, acknowledgment, check endorsement or other writing prepared by you, which terms are inconsistent with these terms and conditions or CCC's Billing and Payment terms and conditions. These terms and conditions, together with CCC's Billing and Payment terms and conditions (which are incorporated herein), comprise the entire agreement between you and publisher (and CCC) concerning this licensing transaction. In the event of any conflict between your obligations established by these terms and conditions and those established by CCC's Billing and Payment terms and conditions, these terms and conditions shall control.

14. Revocation: Elsevier or Copyright Clearance Center may deny the permissions described in this License at their sole discretion, for any reason or no reason, with a full refund payable to you. Notice of such denial will be made using the contact information provided by you. Failure to receive such notice will not alter or invalidate the denial. In no event will Elsevier or Copyright Clearance Center be responsible or liable for any costs, expenses or damage incurred by you as a result of a denial of your permission request, other than a refund of the amount(s) paid by you to Elsevier and/or Copyright Clearance Center for denied permissions.

LIMITED LICENSE

The following terms and conditions apply only to specific license types:

15. **Translation**: This permission is granted for non-exclusive world **English** rights only unless your license was granted for translation rights. If you licensed translation rights you may only translate this content into the languages you requested. A professional translator must perform all translations and reproduce the content word for word preserving the integrity of the article. If this license is to re-use 1 or 2 figures then permission is granted for non-exclusive world rights in all languages.

16. **Website**: The following terms and conditions apply to electronic reserve and author websites:
Electronic reserve: If licensed material is to be posted to website, the web site is to be password-protected and made available only to bona fide students registered on a relevant course if:
This license was made in connection with a course,
This permission is granted for 1 year only. You may obtain a license for future website posting,
All content posted to the web site must maintain the copyright information line on the bottom of each image,
A hyper-text must be included to the Homepage of the journal from which you are licensing at http://www.sciencedirect.com/science/journal/xxxxx or the Elsevier homepage for books at http://www.elsevier.com , and
Central Storage: This license does not include permission for a scanned version of the material to be stored in a central repository such as that provided by Heron/XanEdu.

17. **Author website** for journals with the following additional clauses:

All content posted to the web site must maintain the copyright information line on the bottom of each image, and
he permission granted is limited to the personal version of your paper. You are not allowed to download and post the published electronic version of your article (whether PDF or HTML, proof or final version), nor may you scan the printed edition to create an electronic version,
A hyper-text must be included to the Homepage of the journal from which you are licensing at http://www.sciencedirect.com/science/journal/xxxxx , As part of our normal production process, you will receive an e-mail notice when your article appears on Elsevier's online service ScienceDirect (www.sciencedirect.com). That e-mail will include the article's Digital Object Identifier (DOI). This number provides the electronic link to the published article and should be included in the posting of your personal version. We ask that you wait

until you receive this e-mail and have the DOI to do any posting.
Central Storage: This license does not include permission for a scanned version of the material to be stored in a central repository such as that provided by Heron/XanEdu.

18. **Author website** for books with the following additional clauses:
Authors are permitted to place a brief summary of their work online only.
A hyper-text must be included to the Elsevier homepage at http://www.elsevier.com

All content posted to the web site must maintain the copyright information line on the bottom of each image
You are not allowed to download and post the published electronic version of your chapter, nor may you scan the printed edition to create an electronic version.
Central Storage: This license does not include permission for a scanned version of the material to be stored in a central repository such as that provided by Heron/XanEdu.

19. **Website** (regular and for author): A hyper-text must be included to the Homepage of the journal from which you are licensing at http://www.sciencedirect.com/science/journal/xxxxx. or for books to the Elsevier homepage at http://www.elsevier.com

20. **Thesis/Dissertation**: If your license is for use in a thesis/dissertation your thesis may be submitted to your institution in either print or electronic form. Should your thesis be published commercially, please reapply for permission. These requirements include permission for the Library and Archives of Canada to supply single copies, on demand, of the complete thesis and include permission for UMI to supply single copies, on demand, of the complete thesis. Should your thesis be published commercially, please reapply for permission.

21. **Other Conditions**: None

v1.6

Gratis licenses (referencing $0 in the Total field) are free. Please retain this printable license for your reference. No payment is required.

If you would like to pay for this license now, please remit this license along with your payment made payable to "COPYRIGHT CLEARANCE CENTER" otherwise you will be invoiced within 48 hours of the license date. Payment should be in the form of a check or money order referencing your account number and this invoice number RLNK10743550.
Once you receive your invoice for this order, you may pay your invoice by credit card. Please follow instructions provided at that time.

Make Payment To:
Copyright Clearance Center
Dept 001
P.O. Box 843006
Boston, MA 02284-3006

If you find copyrighted material related to this license will not be used and wish to cancel, please contact us referencing this license number 2380841000564 and noting the reason for cancellation.

Questions? customercare@copyright.com or +1-877-622-5543 (toll free in the US) or +1-978-646-2777.

ELSEVIER LICENSE
TERMS AND CONDITIONS

Mar 02, 2010

This is a License Agreement between Dennis E Anderson ("You") and Elsevier ("Elsevier") provided by Copyright Clearance Center ("CCC"). The license consists of your order details, the terms and conditions provided by Elsevier, and the payment terms and conditions.

All payments must be made in full to CCC. For payment instructions, please see information listed at the bottom of this form.

Supplier	Elsevier Limited The Boulevard,Langford Lane Kidlington,Oxford,OX5 1GB,UK
Registered Company Number	1982084
Customer name	Dennis E Anderson
Customer address	ESM Department (0219)
	Blacksburg, VA 24061
License Number	2380850420886
License date	Mar 02, 2010
Licensed content publisher	Elsevier
Licensed content publication	Journal of Biomechanics
Licensed content title	Prediction of femoral fracture load using automated finite element modeling
Licensed content author	Joyce H. Keyak, Stephen A. Rossi, Kimberly A. Jones, Harry B. Skinner
Licensed content date	12 May 1997
Volume number	31
Issue number	2
Pages	9
Type of Use	Thesis / Dissertation
Portion	Figures/tables/illustrations
Number of Figures/tables/illustrations	1
Format	Both print and electronic
You are an author of the Elsevier article	No
Are you translating?	No
Order Reference Number	
Expected publication date	May 2010
Elsevier VAT number	GB 494 6272 12
Permissions price	0.00 USD
Value added tax 0.0%	0.00 USD
Total	0.00 USD
Terms and Conditions	

INTRODUCTION

1. The publisher for this copyrighted material is Elsevier. By clicking "accept" in connection with completing this licensing transaction, you agree that the following terms and conditions

apply to this transaction (along with the Billing and Payment terms and conditions established by Copyright Clearance Center, Inc. ("CCC"), at the time that you opened your Rightslink account and that are available at any time at http://myaccount.copyright.com).

GENERAL TERMS

2. Elsevier hereby grants you permission to reproduce the aforementioned material subject to the terms and conditions indicated.

3. Acknowledgement: If any part of the material to be used (for example, figures) has appeared in our publication with credit or acknowledgement to another source, permission must also be sought from that source. If such permission is not obtained then that material may not be included in your publication/copies. Suitable acknowledgement to the source must be made, either as a footnote or in a reference list at the end of your publication, as follows:

"Reprinted from Publication title, Vol /edition number, Author(s), Title of article / title of chapter, Pages No., Copyright (Year), with permission from Elsevier [OR APPLICABLE SOCIETY COPYRIGHT OWNER]." Also Lancet special credit - "Reprinted from The Lancet, Vol. number, Author(s), Title of article, Pages No., Copyright (Year), with permission from Elsevier."

4. Reproduction of this material is confined to the purpose and/or media for which permission is hereby given.

5. Altering/Modifying Material: Not Permitted. However figures and illustrations may be altered/adapted minimally to serve your work. Any other abbreviations, additions, deletions and/or any other alterations shall be made only with prior written authorization of Elsevier Ltd. (Please contact Elsevier at permissions@elsevier.com)

6. If the permission fee for the requested use of our material is waived in this instance, please be advised that your future requests for Elsevier materials may attract a fee.

7. Reservation of Rights: Publisher reserves all rights not specifically granted in the combination of (i) the license details provided by you and accepted in the course of this licensing transaction, (ii) these terms and conditions and (iii) CCC's Billing and Payment terms and conditions.

8. License Contingent Upon Payment: While you may exercise the rights licensed immediately upon issuance of the license at the end of the licensing process for the transaction, provided that you have disclosed complete and accurate details of your proposed use, no license is finally effective unless and until full payment is received from you (either by publisher or by CCC) as provided in CCC's Billing and Payment terms and conditions. If full payment is not received on a timely basis, then any license preliminarily granted shall be deemed automatically revoked and shall be void as if never granted. Further, in the event that you breach any of these terms and conditions or any of CCC's Billing and Payment terms and conditions, the license is automatically revoked and shall be void as if never granted. Use of materials as described in a revoked license, as well as any use of the materials beyond the scope of an unrevoked license, may constitute copyright infringement and publisher reserves the right to take any and all action to protect its copyright in the materials.

9. Warranties: Publisher makes no representations or warranties with respect to the licensed material.

10. Indemnity: You hereby indemnify and agree to hold harmless publisher and CCC, and their respective officers, directors, employees and agents, from and against any and all claims arising out of your use of the licensed material other than as specifically authorized pursuant to this license.

11. No Transfer of License: This license is personal to you and may not be sublicensed, assigned, or transferred by you to any other person without publisher's written permission.

12. No Amendment Except in Writing: This license may not be amended except in a writing signed by both parties (or, in the case of publisher, by CCC on publisher's behalf).

13. Objection to Contrary Terms: Publisher hereby objects to any terms contained in any purchase order, acknowledgment, check endorsement or other writing prepared by you, which terms are inconsistent with these terms and conditions or CCC's Billing and Payment terms and conditions. These terms and conditions, together with CCC's Billing and Payment terms and conditions (which are incorporated herein), comprise the entire agreement between you and publisher (and CCC) concerning this licensing transaction. In the event of any conflict between your obligations established by these terms and conditions and those established by CCC's Billing and Payment terms and conditions, these terms and conditions shall control.

14. Revocation: Elsevier or Copyright Clearance Center may deny the permissions described in this License at their sole discretion, for any reason or no reason, with a full refund payable to you. Notice of such denial will be made using the contact information provided by you. Failure to receive such notice will not alter or invalidate the denial. In no event will Elsevier or Copyright Clearance Center be responsible or liable for any costs, expenses or damage incurred by you as a result of a denial of your permission request, other than a refund of the amount(s) paid by you to Elsevier and/or Copyright Clearance Center for denied permissions.

LIMITED LICENSE

The following terms and conditions apply only to specific license types:

15. **Translation**: This permission is granted for non-exclusive world **English** rights only unless your license was granted for translation rights. If you licensed translation rights you may only translate this content into the languages you requested. A professional translator must perform all translations and reproduce the content word for word preserving the integrity of the article. If this license is to re-use 1 or 2 figures then permission is granted for non-exclusive world rights in all languages.

16. **Website**: The following terms and conditions apply to electronic reserve and author websites:
Electronic reserve: If licensed material is to be posted to website, the web site is to be password-protected and made available only to bona fide students registered on a relevant course if:
This license was made in connection with a course,
This permission is granted for 1 year only. You may obtain a license for future website posting,
All content posted to the web site must maintain the copyright information line on the bottom of each image,
A hyper-text must be included to the Homepage of the journal from which you are licensing at http://www.sciencedirect.com/science/journal/xxxxx or the Elsevier homepage for books at http://www.elsevier.com , and
Central Storage: This license does not include permission for a scanned version of the material to be stored in a central repository such as that provided by Heron/XanEdu.

17. **Author website** for journals with the following additional clauses:

All content posted to the web site must maintain the copyright information line on the bottom of each image, and
he permission granted is limited to the personal version of your paper. You are not allowed to download and post the published electronic version of your article (whether PDF or HTML, proof or final version), nor may you scan the printed edition to create an electronic version,
A hyper-text must be included to the Homepage of the journal from which you are licensing at http://www.sciencedirect.com/science/journal/xxxxx , As part of our normal production process, you will receive an e-mail notice when your article appears on Elsevier's online service ScienceDirect (www.sciencedirect.com). That e-mail will include the article's

Digital Object Identifier (DOI). This number provides the electronic link to the published article and should be included in the posting of your personal version. We ask that you wait until you receive this e-mail and have the DOI to do any posting.
Central Storage: This license does not include permission for a scanned version of the material to be stored in a central repository such as that provided by Heron/XanEdu.

18. **Author website** for books with the following additional clauses:
Authors are permitted to place a brief summary of their work online only.
A hyper-text must be included to the Elsevier homepage at http://www.elsevier.com

All content posted to the web site must maintain the copyright information line on the bottom of each image
You are not allowed to download and post the published electronic version of your chapter, nor may you scan the printed edition to create an electronic version.
Central Storage: This license does not include permission for a scanned version of the material to be stored in a central repository such as that provided by Heron/XanEdu.

19. **Website** (regular and for author): A hyper-text must be included to the Homepage of the journal from which you are licensing at http://www.sciencedirect.com/science/journal/xxxxx. or for books to the Elsevier homepage at http://www.elsevier.com

20. **Thesis/Dissertation**: If your license is for use in a thesis/dissertation your thesis may be submitted to your institution in either print or electronic form. Should your thesis be published commercially, please reapply for permission. These requirements include permission for the Library and Archives of Canada to supply single copies, on demand, of the complete thesis and include permission for UMI to supply single copies, on demand, of the complete thesis. Should your thesis be published commercially, please reapply for permission.

21. **Other Conditions**: None

v1.6

Gratis licenses (referencing $0 in the Total field) are free. Please retain this printable license for your reference. No payment is required.

If you would like to pay for this license now, please remit this license along with your payment made payable to "COPYRIGHT CLEARANCE CENTER" otherwise you will be invoiced within 48 hours of the license date. Payment should be in the form of a check or money order referencing your account number and this invoice number RLNK10743558.
Once you receive your invoice for this order, you may pay your invoice by credit card. Please follow instructions provided at that time.

Make Payment To:
Copyright Clearance Center
Dept 001
P.O. Box 843006
Boston, MA 02284-3006

If you find copyrighted material related to this license will not be used and wish to cancel, please contact us referencing this license number 2380850420886 and noting the reason for cancellation.

Questions? customercare@copyright.com or +1-877-622-5543 (toll free in the US) or +1-978-646-2777.

Test of fair use for: Gray, H. 1918. Anatomy of the Human Body, 20th Edition. Place Published: Philadelphia: Lea & Febiger. http://www.bartleby.com/107/

Fair Use Factor		In Favor of Fair Use		In Favor of Copyright Holder (not fair use)
Purpose and Character of Use				
commercial or educational use	X	*Research*		*Commercial activity*
for profit or not	X	*Scholarship*		*Profit (monetarily) from use*
degree of transformation; value added	X	*Nonprofit university*		*Entertainment*
for criticism, commentary, news reporting, teaching, scholarship, research		*Criticism*		*Bad-faith behavior*
		Comment		*Denying credit to original author*
		Transformative: changes the original work for new purpose		
		Parody		
Nature of the Copyrighted Work				
character of the work	X	*Published work*		*Unpublished work*
for example, fact or fiction	X	*Factual or non-fiction based*		*Highly creative work (art, music, novels, films, plays)*
worthy of (extensive) protection?		*Important to favored educational objectives*		*Fiction*
Amount and Substantiality				
use only what's necessary	X	*Small quantity of the work*		*Large poprtion or whole work used*
quantity and quality in relation to the whole work	X	*Portion used is not central or significant to entire work*		*Portion used is central to work or "heart of the work"*
	X	*Amount is appropriate for favored educational purpose*		
Effect				
harm to potential market or value of a work after a portion has been used separately from the whole	X	*User has lawfully acquired copy of the original work*		*Could replace sale of copyrighted work*
		One or fewer copies made		Significantly impairs market or potential market for copyright work or derivative
	X	*No significant effect o the market or potential market of copyrighted work*		Reasonably available licensing mechanism for use of the copyrighted work
		No similar product marketed by the copyright holder		*Affordable permission available for using work*
		Lack of licensing mechanism		*Numerous copies made*
				You made it accessible on Web or in other public forum
				Repeated or long term use

All considerations weigh in favor of fair use.

Fair use checklist taken from http://scholar.lib.vt.edu/theses/copyright/FairUseChecklistVT.pdf

Rightslink Printable License https://s100.copyright.com/App/PrintableLicenseFrame.jsp?publishe...

ELSEVIER LICENSE
TERMS AND CONDITIONS

Mar 02, 2010

This is a License Agreement between Dennis E Anderson ("You") and Elsevier ("Elsevier") provided by Copyright Clearance Center ("CCC"). The license consists of your order details, the terms and conditions provided by Elsevier, and the payment terms and conditions.

All payments must be made in full to CCC. For payment instructions, please see information listed at the bottom of this form.

Supplier	Elsevier Limited The Boulevard,Langford Lane Kidlington,Oxford,OX5 1GB,UK
Registered Company Number	1982084
Customer name	Dennis E Anderson
Customer address	ESM Department (0219)
	Blacksburg, VA 24061
License Number	2380850875649
License date	Mar 02, 2010
Licensed content publisher	Elsevier
Licensed content publication	Medical Engineering & Physics
Licensed content title	Comparison of in situ and in vitro CT scan-based finite element model predictions of proximal femoral fracture load
Licensed content author	Joyce H. Keyak, Yuri Falkinstein
Licensed content date	November 2003
Volume number	25
Issue number	9
Pages	7
Type of Use	Thesis / Dissertation
Portion	Figures/tables/illustrations
Number of Figures/tables/illustrations	1
Format	Both print and electronic
You are an author of the Elsevier article	No
Are you translating?	No
Order Reference Number	
Expected publication date	May 2010
Elsevier VAT number	GB 494 6272 12
Permissions price	0.00 USD
Value added tax 0.0%	0.00 USD
Total	0.00 USD
Terms and Conditions	

INTRODUCTION

1. The publisher for this copyrighted material is Elsevier. By clicking "accept" in connection

1 of 4 3/2/2010 11:56 AM

Rightslink Printable License https://s100.copyright.com/App/PrintableLicenseFrame.jsp?publishe...

with completing this licensing transaction, you agree that the following terms and conditions apply to this transaction (along with the Billing and Payment terms and conditions established by Copyright Clearance Center, Inc. ("CCC"), at the time that you opened your Rightslink account and that are available at any time at http://myaccount.copyright.com).

GENERAL TERMS

2. Elsevier hereby grants you permission to reproduce the aforementioned material subject to the terms and conditions indicated.

3. Acknowledgement: If any part of the material to be used (for example, figures) has appeared in our publication with credit or acknowledgement to another source, permission must also be sought from that source. If such permission is not obtained then that material may not be included in your publication/copies. Suitable acknowledgement to the source must be made, either as a footnote or in a reference list at the end of your publication, as follows:

"Reprinted from Publication title, Vol /edition number, Author(s), Title of article / title of chapter, Pages No., Copyright (Year), with permission from Elsevier [OR APPLICABLE SOCIETY COPYRIGHT OWNER]." Also Lancet special credit - "Reprinted from The Lancet, Vol. number, Author(s), Title of article, Pages No., Copyright (Year), with permission from Elsevier."

4. Reproduction of this material is confined to the purpose and/or media for which permission is hereby given.

5. Altering/Modifying Material: Not Permitted. However figures and illustrations may be altered/adapted minimally to serve your work. Any other abbreviations, additions, deletions and/or any other alterations shall be made only with prior written authorization of Elsevier Ltd. (Please contact Elsevier at permissions@elsevier.com)

6. If the permission fee for the requested use of our material is waived in this instance, please be advised that your future requests for Elsevier materials may attract a fee.

7. Reservation of Rights: Publisher reserves all rights not specifically granted in the combination of (i) the license details provided by you and accepted in the course of this licensing transaction, (ii) these terms and conditions and (iii) CCC's Billing and Payment terms and conditions.

8. License Contingent Upon Payment: While you may exercise the rights licensed immediately upon issuance of the license at the end of the licensing process for the transaction, provided that you have disclosed complete and accurate details of your proposed use, no license is finally effective unless and until full payment is received from you (either by publisher or by CCC) as provided in CCC's Billing and Payment terms and conditions. If full payment is not received on a timely basis, then any license preliminarily granted shall be deemed automatically revoked and shall be void as if never granted. Further, in the event that you breach any of these terms and conditions or any of CCC's Billing and Payment terms and conditions, the license is automatically revoked and shall be void as if never granted. Use of materials as described in a revoked license, as well as any use of the materials beyond the scope of an unrevoked license, may constitute copyright infringement and publisher reserves the right to take any and all action to protect its copyright in the materials.

9. Warranties: Publisher makes no representations or warranties with respect to the licensed material.

10. Indemnity: You hereby indemnify and agree to hold harmless publisher and CCC, and their respective officers, directors, employees and agents, from and against any and all claims arising out of your use of the licensed material other than as specifically authorized pursuant to this license.

11. No Transfer of License: This license is personal to you and may not be sublicensed, assigned, or transferred by you to any other person without publisher's written permission.

2 of 4 3/2/2010 11:56 AM

Rightslink Printable License https://s100.copyright.com/App/PrintableLicenseFrame.jsp?publishe...

12. No Amendment Except in Writing: This license may not be amended except in a writing signed by both parties (or, in the case of publisher, by CCC on publisher's behalf).

13. Objection to Contrary Terms: Publisher hereby objects to any terms contained in any purchase order, acknowledgment, check endorsement or other writing prepared by you, which terms are inconsistent with these terms and conditions or CCC's Billing and Payment terms and conditions. These terms and conditions, together with CCC's Billing and Payment terms and conditions (which are incorporated herein), comprise the entire agreement between you and publisher (and CCC) concerning this licensing transaction. In the event of any conflict between your obligations established by these terms and conditions and those established by CCC's Billing and Payment terms and conditions, these terms and conditions shall control.

14. Revocation: Elsevier or Copyright Clearance Center may deny the permissions described in this License at their sole discretion, for any reason or no reason, with a full refund payable to you. Notice of such denial will be made using the contact information provided by you. Failure to receive such notice will not alter or invalidate the denial. In no event will Elsevier or Copyright Clearance Center be responsible or liable for any costs, expenses or damage incurred by you as a result of a denial of your permission request, other than a refund of the amount(s) paid by you to Elsevier and/or Copyright Clearance Center for denied permissions.

LIMITED LICENSE

The following terms and conditions apply only to specific license types:

15. **Translation**: This permission is granted for non-exclusive world **English** rights only unless your license was granted for translation rights. If you licensed translation rights you may only translate this content into the languages you requested. A professional translator must perform all translations and reproduce the content word for word preserving the integrity of the article. If this license is to re-use 1 or 2 figures then permission is granted for non-exclusive world rights in all languages.

16. **Website**: The following terms and conditions apply to electronic reserve and author websites:
Electronic reserve: If licensed material is to be posted to website, the web site is to be password-protected and made available only to bona fide students registered on a relevant course if:
This license was made in connection with a course,
This permission is granted for 1 year only. You may obtain a license for future website posting,
All content posted to the web site must maintain the copyright information line on the bottom of each image,
A hyper-text must be included to the Homepage of the journal from which you are licensing at http://www.sciencedirect.com/science/journal/xxxxx or the Elsevier homepage for books at http://www.elsevier.com , and
Central Storage: This license does not include permission for a scanned version of the material to be stored in a central repository such as that provided by Heron/XanEdu.

17. **Author website** for journals with the following additional clauses:

All content posted to the web site must maintain the copyright information line on the bottom of each image, and
he permission granted is limited to the personal version of your paper. You are not allowed to download and post the published electronic version of your article (whether PDF or HTML, proof or final version), nor may you scan the printed edition to create an electronic version,
A hyper-text must be included to the Homepage of the journal from which you are licensing at http://www.sciencedirect.com/science/journal/xxxxx , As part of our normal production process, you will receive an e-mail notice when your article appears on Elsevier's online service ScienceDirect (www.sciencedirect.com). That e-mail will include the article's

3 of 4 3/2/2010 11:56 AM

Rightslink Printable License https://s100.copyright.com/App/PrintableLicenseFrame.jsp?publishe...

Digital Object Identifier (DOI). This number provides the electronic link to the published article and should be included in the posting of your personal version. We ask that you wait until you receive this e-mail and have the DOI to do any posting.
Central Storage: This license does not include permission for a scanned version of the material to be stored in a central repository such as that provided by Heron/XanEdu.

18. **Author website** for books with the following additional clauses:
Authors are permitted to place a brief summary of their work online only.
A hyper-text must be included to the Elsevier homepage at http://www.elsevier.com

All content posted to the web site must maintain the copyright information line on the bottom of each image
You are not allowed to download and post the published electronic version of your chapter, nor may you scan the printed edition to create an electronic version.
Central Storage: This license does not include permission for a scanned version of the material to be stored in a central repository such as that provided by Heron/XanEdu.

19. **Website** (regular and for author): A hyper-text must be included to the Homepage of the journal from which you are licensing at http://www.sciencedirect.com/science/journal/xxxxx. or for books to the Elsevier homepage at http://www.elsevier.com

20. **Thesis/Dissertation**: If your license is for use in a thesis/dissertation your thesis may be submitted to your institution in either print or electronic form. Should your thesis be published commercially, please reapply for permission. These requirements include permission for the Library and Archives of Canada to supply single copies, on demand, of the complete thesis and include permission for UMI to supply single copies, on demand, of the complete thesis. Should your thesis be published commercially, please reapply for permission.

21. **Other Conditions**: None

v1.6

Gratis licenses (referencing $0 in the Total field) are free. Please retain this printable license for your reference. No payment is required.

If you would like to pay for this license now, please remit this license along with your payment made payable to "COPYRIGHT CLEARANCE CENTER" otherwise you will be invoiced within 48 hours of the license date. Payment should be in the form of a check or money order referencing your account number and this invoice number RLNK10743562.
Once you receive your invoice for this order, you may pay your invoice by credit card. Please follow instructions provided at that time.

Make Payment To:
Copyright Clearance Center
Dept 001
P.O. Box 843006
Boston, MA 02284-3006

If you find copyrighted material related to this license will not be used and wish to cancel, please contact us referencing this license number 2380850875649 and noting the reason for cancellation.

Questions? customercare@copyright.com or +1-877-622-5543 (toll free in the US) or +1-978-646-2777.

4 of 4 3/2/2010 11:56 AM